



UNIVERSITÀ DEGLI STUDI DI SALERNO



UNIVERSITÀ DEGLI STUDI DI SALERNO
Dipartimento di Farmacia

Dottorato di Ricerca
in **Scienze del Farmaco**
Ciclo XXIX — Anno accademico 2016/2017

Tesi di Dottorato in

***Design, synthesis and biological
evaluation of new anticancer and/or
anti-inflammatory agents***

Dottorando

Dott. Antonio Foglia

Tutore

Chiar.mo Prof.
Carmela Saturnino

Coordinatore: Chiar.mo Prof. *Gianluca Sbardella*

Preface

My PhD three years course in Drug Discovery & Development at the Department of Pharmacy of Salerno University was started in 2014 under the supervision of Prof. Carmela Satunino.

In the first part of my project, the research was mainly focused on the design and synthesis of new anti-cancer agents. In particular, were designed two series of compounds as new modulators of C-terminal domain of the molecular chaperone Heat Shock protein 90 (Hsp90), these compounds were designed on the base of the first synthetic inhibitor of C-terminal domain of Hsp90.

In the second part of my research activity was focused on the design and synthesis of new inhibitors of microsomal Prostaglandin E₂ synthase-1 (mPGES-1) as potential anti-inflammatory agents.

The work was performed under the direct supervision of Prof. Carmela Saturnino and in collaboration with Prof. Ines Bruno and Dr. Stefania Terracciano. Computational guided design of compounds was performed in collaboration with Prof. Giuseppe Bifulco's research group. Biological screenings were performed in collaboration with Prof. Oliver Werz of Friedrich Schiller University (Germany) in the case of mPGES-1, and with Dr. Maria Carmela Vaccaro and Fabrizio Dal Piaz of Salerno University in the case of Hsp90.

Furthermore, to improve my knowledge about the synthesis techniques, in 2016 I joined Prof. Patrick Dallemagne's research group at the Centre d'Etudes et de Recherche sur le Médicament de Normandie de l'Université de Caen Normandie (France), where I spent four months.

List of publications related to the scientific activity performed during the three years PhD course in Drug Discovery & Development

Papers:

- ✓ Terracciano S.,[‡] **Foglia A.**,[‡] Chini M.G., Vaccaro M.C., Russo A., Dal Piaz F., Saturnino C., Riccio R., Bifulco G., Bruno I. “New dihydropyrimidin-2(1*H*)-one based Hs90 C-terminal inhibitors” *RSC Adv.* (2016), **6**, 82330-82340.
- ✓ Terracciano S., Chini M.G., Vaccaro M.C., Strocchia M., **Foglia A.**, Vassallo A., Saturnino C., Riccio R., Bifulco G., Bruno I. “Identification of the key structural elements of dihydropyrimidinone core driving toward more potent Hsp90 C-terminal inhibitors” *Chem. Commun.* (2016), **52**, 12857-12860.
- ✓ Botta A., Sirignano E., Popolo A., Saturnino C., Terracciano S., **Foglia A.**, Sinicropi M.S., Longo P. and Di Micco S. “Identification of Lead Compounds as Inhibitors of STAT3: Design, Synthesis and Bioactivity”. *Mol. Inf.* (2015), **34**, 689 – 697.

[‡] These authors contributed equally to this work.

Conference proceedings:

- ✓ **Foglia A.**, Di Micco S., Terracciano S., Saturnino C., Riccio R., Bruno I., Bifulco G. “Design, Virtual Screening and Synthesis of Potential Microsomal Prostaglandine E₂ Synthase-1 (mPGES-1)”, XXV National Meeting of Italian Chemical Society, Rende (Italy), 7-12 September 2014.

- ✓ **Foglia A.**, Di Micco S., Terracciano S., Saturnino C., Riccio R., Oppermann U., Bifulco G., Bruno I. “Design and Synthesis of 4-substituted-pyridine-2,6-dicarboxylic acids as new potential JMJD3 modulators”. XL Summer School "A. Corbella" Gargnano (BS), Palazzo Feltrinelli, 14 - 18 June 2015.

- ✓ **Foglia A.**, Terracciano S., Lauro G., Saturnino C., Riccio R., Bruno I., Bifulco G. “Targeting Microsomal Prostaglandin E2 Synthase 1 For The Development Of New Potential Anti-inflammatory Drugs.” XXXVI Convegno della Divisione di Chimica Organica - CDCO 2015 Bologna, 13-17 September 2015.

- ✓ Terracciano S., Strocchia M., Dal Piaz F., Vaccaro M.C., **Foglia A.**, Chini M.G., Leone A., Riccio R., Bifulco G., Bruno I. “Discovery of innovative Hsp90 C-terminal modulators: synthesis and biological evaluation of 3,4-dihydropyrimidinone derivatives.” XXXVI Convegno della Divisione di Chimica Organica - CDCO 2015 Bologna, 13-17 September 2015.

- ✓ **Foglia A.**, Terracciano S., Lauro G., Saturnino C., Riccio R., Bruno I., Bifulco G. “Inhibition of Microsomal Prostaglandin E₂ Synthase1: Focused Design of New Anti-inflammatory and Anticancer Drugs.” XV Edizione del congresso SAYCS (Sigma Aldrich Young Chemists Symposium) Rimini 27-29 October 2015.

- ✓ **Foglia A.**, Vaccaro M.C., Saturnino C., Riccio R., Bifulco G., Chini M.G., Bruno I., Terracciano S. “Exploration of dihydropyrimidin-2(1H)-one scaffold for the discovery of new promising C-terminal Hsp 90 inhibitors” XXXVII Convegno della divisione di chimica organica CDCO 2016. Venezia 18–22 September 2016.

- ✓ S. Terracciano, **A. Foglia**, M. G. Chini, M. C. Vaccaro, M.a Strocchia, A. Russo, R. Riccio, G. Bifulco, I. Bruno “Development of C-terminal heat shock protein 90 inhibitors as therapeutic agents” XXXVII Convegno della divisione di chimica organica CDCO 2016. Venezia 18–22 September 2016.

Index

	1
Abstract.....	
CHAPTER 1	4-35
1.1 A short history of anticancer therapy	5
1.2 Inflammation	7
1.3 Why cancer and inflammation?	9
1.4 The drug discovery	11
1.5 Heat shock protein 90 (Hsp90)	13
1.6 Microsomal prostaglandin E₂ synthase-1 (mPGES-1)	22
1.7 How to proceed in the research project	31
CHAPTER 2	37-64
2.1 The need to develop Hsp90 C-terminal inhibitors	38
2.2 Where do we start?	39
2.3 Influence of the chemical functionalization on the phenyl ring at C4 position of DHPM core based Hsp90 C-terminal inhibitors	41
2.3.1 Surface Plasmon Resonance assay	43
2.3.2 Antiproliferative assay and Western Blot analysis	44
2.3.3 Molecular docking studies	47
2.4 Enhanced inhibitory activity of C-terminal Hsp90 domain through substitution of DHPM core at C2 position	51
2.4.1 Surface Plasmon Resonance assay	53
2.4.2 Antiproliferative assay, Western Blot analysis and effect on cell cycle progression	55
2.4.3 Study of Hsp90α/18 interaction	58
2.4.4 Molecular docking studies	60
CHAPTER 3	65-80
3.1 Why mPGES-1?	66
3.2 Looking for new molecular platforms	67
3.2.1 Design and synthesis of 5-Pyrazolone compound	67
3.2.2 Design and synthesis of Carbazole compounds	72
3.2.3 Design and synthesis of Biaryl compounds	76
Conclusion	83
Experimental Section	85

CHAPTER 4	86-100
4.1 General information	87
4.2 Methods and materials	88
4.2.1 General procedure for synthesis of the second generation of DHPMs derivatives by microwave-assisted Biginelli reaction	88
4.2.2 General procedure for synthesis of 14a and 14b by microwave-assisted Biginelli reaction	95
4.2.3 General procedure for microwave-assisted Liebeskind-Srogl cross coupling reaction	96
CHAPTER 5	101-123
5.1 General synthetic methods	102
5.2 General procedures for the preparation of 4-arylidene-1,3-disubstituted-5-pyrazolone compounds	102
5.2.1 General procedure for the preparation of 5-pyrazolones 23a-23h	102
5.2.2 General procedure for the preparation of 24-41	103
5.3 General procedure for the synthesis of carbazole compound .	112
5.3.1 General procedure for the preparation of 42a-42e	112
5.3.2 General procedure for synthesis of 43-47	112
5.3.3 General procedure for the synthesis of biaryl compounds	115
5.3.3.1 Synthesis of 58	122
References	123-149

Abstract

One of the main goal of modern medicinal chemistry is the development of new agents able to modulate biological targets involved in inflammation and cancer processes. In this context, my PhD project was focused on the exploration and structural optimization of various chemical moieties able to interfere with two targets involved in both processes. In particular, two biological targets were selected: Heat shock protein 90 (Hsp90) and microsomal Prostaglandin E₂ Synthase-1 (mPGES-1). The results obtained can be divided into two sections in accordance with the target of interest.

a) Exploration and structural optimization of DHPM core in order to guide the synthesis of new and more potent Hsp90 C-terminal inhibitors.

Hsp90 is a molecular chaperone involved in the maturation and stabilization of a wide range of client proteins that play a crucial role in the development, survival and proliferation of cancer cells. In the literature there are several compounds capable of inhibiting this molecular chaperone. The most part of these compounds inhibit the protein through modulation of the N-terminal domain. However, this type of modulation involves a well-known heat shock response, a cytoprotective mechanism that as a final result leads to the increase of cytosolic levels of heat shock proteins with consequent cell survival. Therefore, the modulation of C-terminal domain of Hsp90 represents a better strategy for the development of new antitumor agents, since, they do not induce heat shock response. In an attempt to discover new modulators of the C-terminal domain of Hsp90 and taking into account the structure of the first synthetic inhibitor of this domain, a 3,4-dihydropyrimidin-2(1*H*)-one (DHPM)

derivative, two more generations of DHPM derivatives have been synthesized. Relatively to the second generation of DHPM derivatives, the synthesis was focused on the influence of the chemical functionalization of aromatic ring at C4 position of DHPM core, while the third generation has been designed with the aim to functionalize the C2 position of the core. The exploration and optimization processes of DHPM core led to the identification of novel and more potent inhibitors of the C-terminal domain of Hsp90.

b) Identification of new mPGES-1 inhibitors.

mPGES-1 is an inducible enzyme that catalyzes the terminal step of the biosynthesis of PGE₂ from the PGH₂ precursor. The inhibition of this enzyme appears to be a promising strategy for the identification of novel anti-inflammatory agents, because, the use of selective inhibitors would allow to overcome the classical side effects of traditional anti-inflammatory drugs. Moreover, mPGES-1 is overexpressed in a wide variety of human cancers and for this reason it has emerged as an attractive biological target for anticancer drug discovery. In order to identify new molecular platforms able to interact with the target protein three collections of compounds (carbazoles, biaryl compounds and 5-pyrazolones) were synthesized. Biological evaluation revealed the identification of five biaryl compounds (**60-64**) as new chemical entities that inhibit mPGES-1 activity with promising IC₅₀ values (ranging 0.18-1.64 μM).

INTRODUCTION

-CHAPTER 1-

1.1 A short history of anticancer therapy

"Cancer" term includes a group of more 100 diseases in which the cells begin to grow out of control.¹ With the onset of tumorigenesis body cells begin to divide and spread into the surrounding tissue. In addition, it is possible that some tumor cells can break off from the primary tumor and through the blood stream or the lymph system create a secondary tumor far from the original in a process known as metastasis.² The processes that trigger oncogenesis are varied and are not yet well defined, to date many risk factors have been identified that could increase the chance of getting cancer, for these reason it is nearly impossible to know the development of cancer causes.^{3,4} The tumor arises from a normal cell when its DNA is damaged fact, the cancer is a disease characterized by a large genetic instability. When the DNA of cells is damaged and the repair mechanisms do not work there is an upheaval of cellular functions. In cancer cells, indeed the damaged DNA is not repaired, and the cell does not die, instead it gives rise to more such abnormal cells with abnormal DNA.⁵ In most cases surgery is the main strategy to remove the tumors, while chemotherapy and radiotherapy are used especially to remove residual cells by acting on their continued proliferation.⁶ Unfortunately, the chemotherapy and radiotherapy don't have a real specificity of action and they cause considerable side effects.⁷

The coming of the nitrogen mustards and antifolate drugs have allowed the first chemotherapy treatment only in 1940. While, radiotherapy has become a valuable resource for the control of this disease in 1960 with the invention of the linear accelerator.⁸ At that time the main strategies in cancer therapy were surgery and radiotherapy, but soon it became clear that cure rates after ever more radical local treatments had plateaued at about 33% due to the presence of heretofore unappreciated micrometastases. After these observations, it was

Introduction

decided to introduce the opportunity to apply chemotherapy drugs in conjunction with surgery and/or radiation treatments, doing so the concept of adjuvant chemotherapy was born. The purpose of the combined treatment modality was to maximize the antitumor effect of each of the three therapies with minimal toxicity to normal tissues.^{9,10} Over time, it was needed to develop an effective therapies not based only on empirical observations but increasing dependent on an understanding of human tumour biology.¹¹ With this purpose doctors, researchers, and patients worked together to improve treatment options and identify new drugs that have action on a selected biological entities, with this new concept, chemotherapy entered into the era of "*targeted therapy*". The new concept of the identification of biological targets is started in 1960 with an unrelated program, the Special Virus Cancer Program (SVCP), which wanted to clarify the association between viruses with cancer.¹² When it failed in its purpose it was transformed into a program of molecular biology to study genes that have been aggregated by tumor viruses. This work identified oncogenes, suppressor oncogenes, and signaling pathways essential for developmental biology itself.¹³ In order to understand the cellular activities such as proliferation and survival and with the aim to repair the molecular defects directly in cancer cells, researches of biotechnology firms were focused on the molecular and biological processes. Molecular targeting offers a more convenient solution for the development of potential therapeutic agents with reduced systemic toxicity, on the other hand the tumor cells, thanks to their intrinsic genetic plasticity, easily adapt to a new environment. Finally, this study led to the identification of new drug targets which currently influences the development of anticancer drugs. New targets include growth factors, signalling molecules, cell-cycle proteins, modulators of apoptosis and molecules that promoted angiogenesis.¹⁴ In the last decades, have been discovered many differences between normal cells and tumor cells,

Introduction

many of which help the proliferation of cancer cells, therefore, scientific research has accelerated the development of new anticancer drugs with the main objective to offer a real hope to all those who suffer from cancer.

1.2 Inflammation

Inflammation is defined as the immediate body's response when it feels threatened by pathogens, noxious stimuli such as chemicals, or physical injury.¹⁵ This process leads defensive cells at the site of the damage so as to neutralize and eliminate the noxious stimulus, repair the structure and restore the function of damaged tissues. Clinically inflammation is characterized by four cardinal signs which they were reported in the first century by Celsus, they are: redness (rubor), heat (Calor), swelling (tumor) and pain (dolor).¹⁶ Later Virchow has added a fifth signs: loss of function (functio laesa).¹⁷

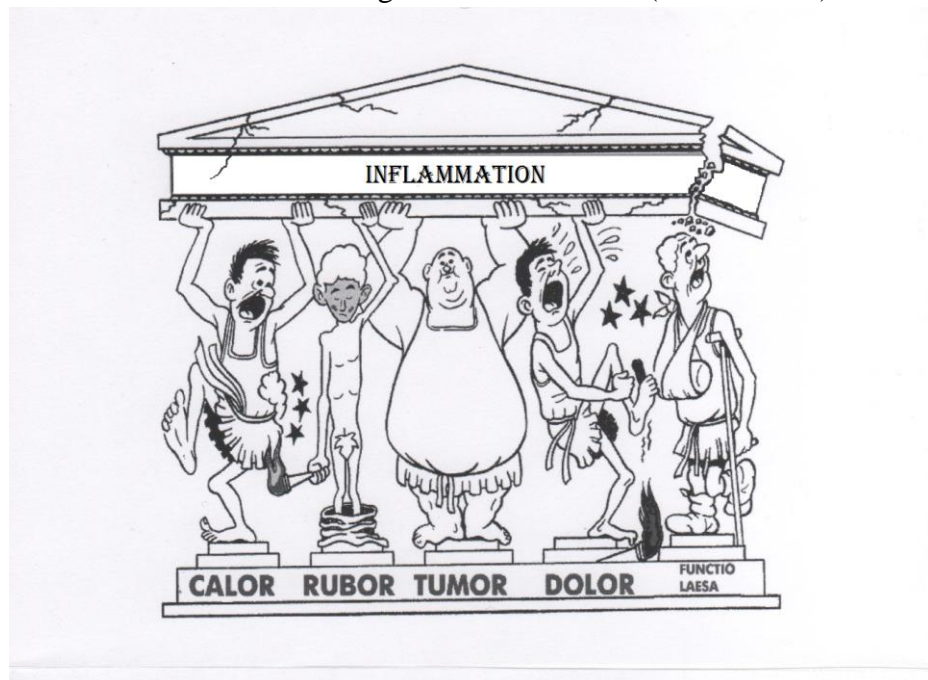


Figure 1.1 *Rappresentation of cardinal signs of inflammation*

Introduction

Inflammation is a generic response, and therefore it is considered as a mechanism of innate immunity, compared to adaptive immunity which is specific for each pathogen.¹⁸ Furthermore, the inflammation damage has substantial differences from the damage of autoimmune disease that determine a specific immune-mediated attack on the tissue that is no longer recognized as self.²⁰ Based on the time duration, the evolution of inflammation can be classified as either acute or chronic.²¹ The first response observed after a noxious stimulus is acute inflammation which as consequence increases the contribution of leukocytes (mainly granulocytes) from the blood to damaged tissue, while chronic inflammation is a more prolonged response resulting from the persistence of the mediators of inflammation of an acute inflammation not completely resolved.²² Historically the first anti-inflammatory drugs have their origin in the discovery of some plant extracts that gave relief to disorders related to inflammation. In the mid-19th century were discovered salicylates, this has allowed the development of some drugs such as acetyl-salicylic acid (Aspirin).²³ With the discovery of the mechanism of action of aspirin it is exponentially increased the interest of the development of new anti-inflammatory therapies which have as mechanism of action the inhibition of cyclooxygenase (COX).²⁴ However, many side effects, particularly related to gastrointestinal and cardiovascular toxicity, were associated with the use of these drugs.²⁵ This toxicity appears to be a serious drawback in a long-term therapy,²⁶ so today, the development of small molecules safer and clinically useful with decreased side-effect profiles is a continuous effort.

1.3 Why cancer and inflammation?

The relationship between cancer and inflammation is a concept that has been observed many years ago, however, the mechanisms underlying this interconnection are still unclear. Cancer and inflammation go hand in hand, the first triggers an inflammatory response, while the inflammatory microenvironment increases the aggressiveness of the tumor and the dissemination of metastases.²⁷ The connection between cancer and inflammation was observed in the nineteenth century, when they noticed that the tumors arose in a chronic inflammation sites and when inflammatory cells were found in biopsy samples from tumors.²⁸ It is well known that many chronic inflammatory factors increase the risk of developing cancer, this factors include autoimmune diseases (inflammatory bowel disease is associated with colon cancer), microbial infections (infection with *Helicobacter pylori* is associated with gastric cancer and gastric mucosal lymphoma) and inflammatory conditions of unknown origin (prostatitis is associated with prostate cancer).²⁹ The link between inflammation and cancer can be divided into two pathways as shown in Figure 1.2.³⁰ The intrinsic pathway is activated by genetic events as oncogenes activation, oncosuppressor inactivation and chromosomal rearrangement or amplification, in this manner cells are transformed producing an attractive environment for tumour growth, facilitating genomic instability and promoting angiogenesis.³¹ The extrinsic pathway is mediated by inflammatory cells of innate immunity, so, inflammatory or infectious conditions enhance the risk of developing cancer (for example, such as inflammatory bowel disease for colorectal cancer and prostatitis for prostate).³² The two pathways activate the transcription factors, such as nuclear factor- κ B (NF- κ B), signal transducer and activator of transcription 3 (STAT3) and hypoxia-inducible factor 1 α (HIF1 α), in tumour

Introduction

cells^{33,34} that coordinate the production of inflammatory mediators, including cytokines, chemokines and cyclooxygenase 2 (COX-2) which, in turn, synthesize the prostaglandins.³⁴

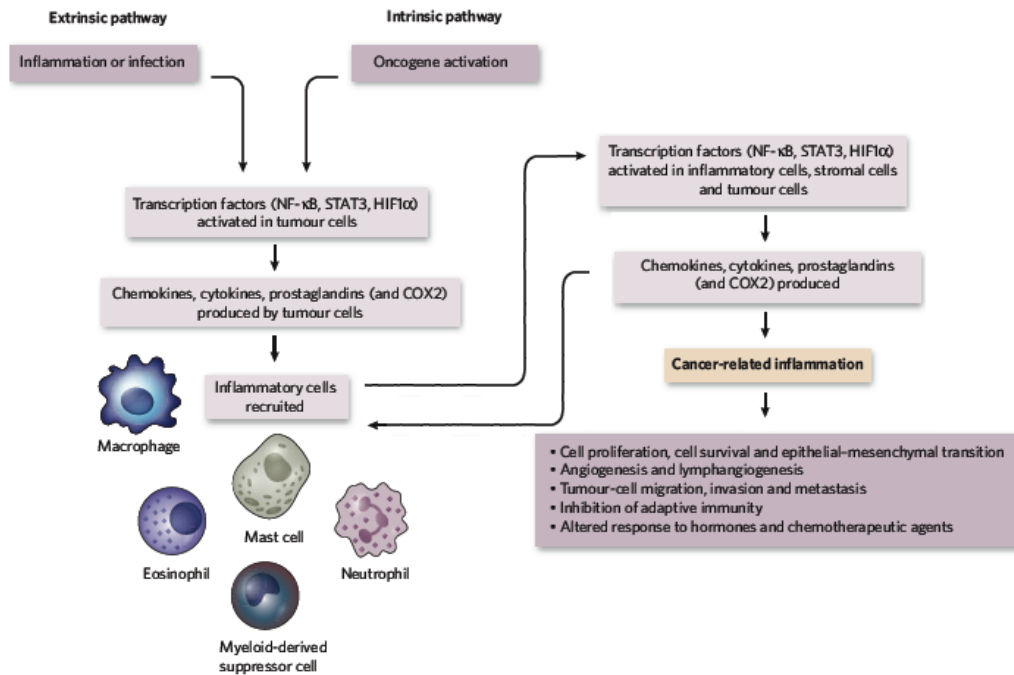


Figure 1.2 Pathways that connect inflammation and cancer

The cytokines activate the same transcription factors in inflammatory cells, stromal cells and tumour cells, resulting in more inflammatory mediators being produced and a cancer-related inflammatory microenvironment being generated. On the other hand, inflammatory mediators contribute to genomic instability resulting to the known mutations associated with tumours. Many of them act as direct mutagens or as deregulators of DNA repair mechanism and cell cycle checkpoints acquiring the ability of cancer cells to proliferate, invade and escape from host defence.^{35,36} Moreover, the relationship between cancer and inflammation is well documented by numerous studies that demonstrate how aspirin is able to prevent certain cancer such as colorectal,

lung, stomach, esophagus and prostate.³⁷⁻³⁹ Anyway, many evidences have been gathered supporting the improved therapeutic efficacy that can be achieved by blocking the two signalling networks and their pathways.^{40,41} In this way, my PhD project has worked.

1.4 The drug discovery

The development of new drugs requires a complex process involving many scientific areas, such as, biology, statistics, pharmacology, pharmaceutical chemistry, toxicology, computational chemistry, organic chemistry and proteomics.⁴² The network between the various areas of science cleared the way for what we now call the “*drug discovery process*”. The aim of drug discovery is to turn “*molecules into medicine for the public health*”, this means find new therapeutic agents with suitable pharmaceutical properties (i.e., efficacy, bioavailability, toxicity) for preclinical evaluation. The drug discovery is one of the most challenging human activities, these processes must proceed through several stages in order to produce a product that is safe, efficacious, and has passed all regulatory requirements.⁴³ This process begins with the "target identification". Any enzyme or any biochemical mechanism involved in the pathological condition may represent a potential therapeutic target. After the identification there is the step of target validation, which takes place indirectly, ie through the use of compounds that block the target thus giving the desired effect.⁴⁴ Furthermore, the process of discovery of new drugs requires the knowledge of pharmaceutical technology to make new bioavailable products without losing the pharmacological effect, for this purpose it is requires a close collaboration between a pharmaceutical and chemical pharmaceutical technologist.⁴⁵ Currently, the drug discovery process is focusing on small organic molecules, appropriately designed to act directly

Introduction

on the biological target of interest, without interacting with other biological system.⁴⁶ However, drug discovery requires simple and variable methods of synthesis to vary the lead structure extensively, which is essential for the derivation of structure–activity relationships (SARs, ligand-based design) and rapid optimization to obtain the active ingredient. The efficient optimization of drugs and the provision of sufficient amounts for further biological characterization is the central task of medicinal chemistry.⁴⁷ Today, researchers employ various techniques to overcome the difficulties in the drugs discovery process, for example, analytical and purification methods such as high-performance liquid chromatography (HPLC),⁴⁸ multicomponent and domino reactions,²⁷ microwave-assisted and flow chemistry,^{49,50} etc. In the present PhD project, thanks to combined of medicinal and pharmaceutical chemistry approaches, new chemical entities with antitumor or anti-inflammatory effects have been successfully identified. With the aim of discovering new potential anticancer agents I focused my attention on exploration and structural optimization of the first synthetic inhibitor of C-terminal domain of Heat shock protein 90. After completion of this project I had the opportunity to work on a second project aimed to identification new anti-inflammatory agents that target the microsomal Prostaglandin E₂ synthase-1 (mPGES-1), enzyme involved in the terminal step of PGE₂ synthesis.

1.5 Heat shock protein 90 (Hsp90)

Exposure of cells to stress conditions (including heat shock, oxidative stress, heavy metals), or pathologic conditions such as ischemia and reperfusion, inflammation, tissue damage, infection, usually cause protein dysfunction.⁵¹ The cell responds to environmental stress by increasing synthesis of several molecular chaperons with the aim to prevent cellular damage and to re-establish cellular homeostasis.⁵¹ These proteins help to maintain cellular cellular homeostasis (proteostasis) in cells, in fact, in accordance with the general definition, molecular chaperone are each protein that helps or stabilizes another protein to acquire its functionally active conformation⁵² and prevent the aggregation of non-native protein.⁵³ In the cells, several different classes of chaperones exist, many of these classes are often known as stress proteins or heat-shock proteins (HSPs), as they are upregulated under conditions of stress in which the concentrations of aggregation-prone folding intermediates increase. Heat Shock proteins are categorized according to their molecular weight into six classes: small Hsps, Hsp40, Hsp60, Hsp70, Hsp90 and Hsp100.⁵⁴ Family members of Hsps are localized in the nucleus, cytoplasm, and subcellular compartments, such as mitochondria and endoplasmic reticulum (ER), the high molecular weight HSPs are ATP-dependent chaperones, whereas small HSPs act in an ATP-independent manner.⁵⁵ It is important to emphasize that the expression of HSPs requires a precise balance, because, over-expression of some HSPs shows the way to certain diseases such as cancer. Tumor cells having more signal transduction pathways and a higher metabolic requirements than normal cells, so they have a greater need of chaperones to maintain cancer cells survival.⁵⁶ For these reasons, the expression of Hsps is severely elevated in cancer cells, and it is associated with enhanced tumorigenicity, metastatic potential of cancer cells

Introduction

and resistance to chemotherapy. Moreover, in association with key apoptotic factors they are strong anti-apoptotic proteins, blocking the cell death process at different levels, for these reasons they are suitable targets for modulating the streets of cell death.⁵⁷ Among the Hsps's family, heat shock protein 90 (Hsp90) has emerged as being of prime importance to the survival of cancer cells.⁵⁸ Hsp90 is constitutively expressed at 1-2% of total cytosolic proteins and its level increases up to 10-fold in tumor cells, suggesting that it may be critically important for tumor cell growth and/or survival.⁵⁹ Firstly, Hsp90 protein is involved in the maturation and stabilization of a wide range of '*client proteins*' that plays a central pathogenic role in human diseases including cerebro- and cardiovascular diseases,⁶⁰ autoimmune diseases,⁶¹ neurodegenerative diseases, viral infections and cancer.⁶² Regarding the latter, many Hsp90 client proteins are involved in critical cellular functions that promote cell growth, cell survival and proliferation as they are able to facilitate an escape from normal proteolytic turnover, thereby overall promoting an oncogenic transformation.⁶³ Hsp90 client proteins comprise proteins that contribute to all of the six hallmarks of cancer, including the ability to produce growth factors, resistance to anticancer agents, avoidance of apoptosis, unlimited replicative potential, uninterrupted angiogenesis and invasiveness and metastasis.⁶⁴⁻⁶⁶ Hsp90 play a central role in acquisition and maintenance of each of six hallmarks of cancer (**Figure 1.3**). For example, Hsp90 influences angiogenesis by folding hypoxia-inducible factor-1 α (HIF-1 α) and vascular endothelial growth factor receptor (VEGFR) in addition to governing nitric oxide synthase upregulation. Many client proteins of Hsp90 are apoptotic mediators, including Bcl-2, Apaf-1, the serine-threonine protein kinase AKT/PKB and survivin.⁶⁷ Also, Hsp90 may promote tissue invasion and metastasis through MMP-2 activation, or digesting extracellular matrix proteins.⁶⁷ Other client proteins of Hsp90 that play a role in cell signaling processes include FAK (integrin pathway), IL6R

Introduction

(JAK/STAT3 pathway), I κ B kinases (NF κ B pathway), CDK 4, 6, 9, hTERT (cell cycle), p53 (tumor suppressor genes), and the steroid hormone receptors (estrogen receptor and androgen receptor).⁶⁸

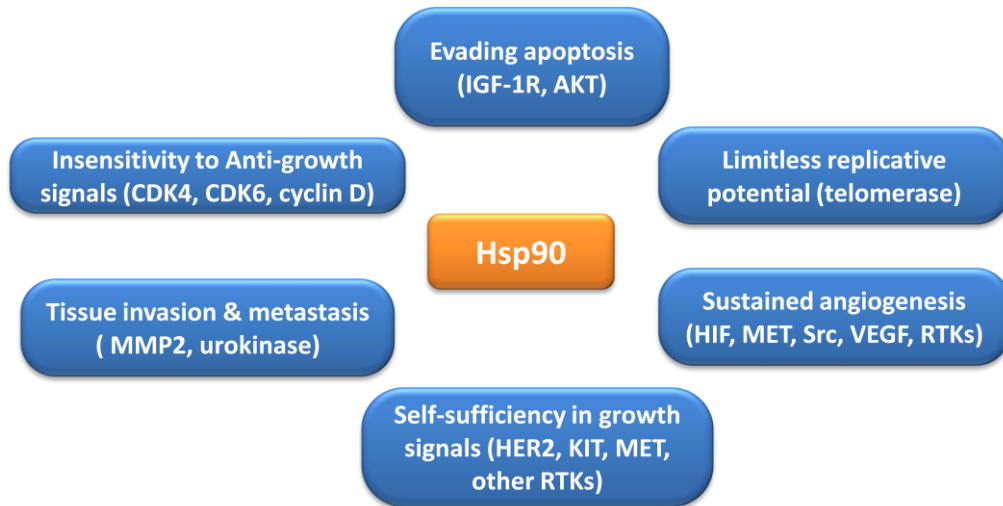


Figure 1.3 *Hsp90 functions implicated in establishment of each of the hallmarks of cancer. Importantly, Hsp90 functions may also permit the genetic instability on which acquisition of the six hallmarks depends.*

In addition, Hsp90 exists as a multi-chaperone complex with unusually high affinity for ATP and some substances in tumor cells, whereas in normal cells a latent form of Hsp90 protein is present. In the human proteome there are four isoforms of Hsp90, the two major isoforms correspond to the inducible Hsp90 α isoforms and the constitutive Hsp90 β , that are located predominantly in the cytosol, whereas two non-cytosolic forms are known, the 94 kDa glucose-regulated protein (GRP94) and the Hsp75/tumor necrosis factor receptor associated protein 1 (TRAP-1), that are expressed in the endoplasmic reticulum and in the mitochondrial matrix respectively.⁶⁹ Structurally, this enzyme exist as a homodimer and each monomer contains three flexibly linked regions.⁷⁰ The amino (N)-terminal domain consists of a α - and β -sandwich motif, it is responsible for the protein's ATPase activity, since that contains an adenosine triphosphate (ATP)-binding and hydrolyzing pocket.⁷¹

Introduction

Another intriguing characteristic of the N-terminal domain is that several conserved amino acid residues form a “lid” (residues 100–121) that closes over the nucleotide binding pocket in the ATP bound state but is open during the ADP-bound state.⁷² The middle domain consist of a large $\alpha\beta\alpha$ segment connecting to a small $\alpha\beta\alpha$ segment via several short α -helices,⁷³ it is a linker region involved in co-chaperones and client proteins recognition/binding, also participates in forming the active ATPase.⁷⁴ Finally, there is the carboxy (C)-terminal domain consist of a curved α -helix, a three-stranded β -sheet, a three-helix coil and an extended disordered arm, this region directs Hsp90 dimerization.⁷³ This region contains another ATP-binding site, without hydrolases activity, this pocket is only available when the N-terminal domain ATP binding site is occupied.⁷⁴⁻⁷⁶ In particular, the C-terminal domain is implicated into the functional switch between the closed and the open protein conformation,⁷⁷ and there is a conserved MEEVD motif involved in the binding of co-chaperones which containing a tetratricopeptide repeat (TRP) motif.^{78,79} Hsp90 helps nascent proteins to assume their biologically active conformations, corrects the conformation of misfolded proteins, and helps incorrigibly misfolded proteins to be removed and degraded by the ubiquitin-proteasome system through the presence of co-chaperones, immunophilins, and partner proteins to form multiprotein complexes, thus facilitates the maturation, stability, activity of client proteins.⁸⁰⁻⁸³

ATP hydrolysis is necessary for Hsp90 activity.⁸⁴ Structural studies showed that Hsp90 assumes several structurally distinct conformations. In the resting state, through the dimerization of its C-terminal domain, Hsp90 forms a V shape conformation which is defined as the “*open conformation*”.⁸⁵ The ATP-binding N-terminal domain of Hsp90 induces a series of conformational changes including repositioning of the N-terminal lid region.⁸⁶

Introduction

After lid closures, Hsp90 reaches a more compact conformation, termed “closed conformation” in which the N-domains are dimerized. After Hsp90 finishes its chaperoning tasks of assisting the proper folding, stabilization and activation of client proteins under the active state, the ATP molecule is hydrolyzed, so the N-domain release ADP, Pi and Hsp90 returns to the open conformation again.⁸⁷

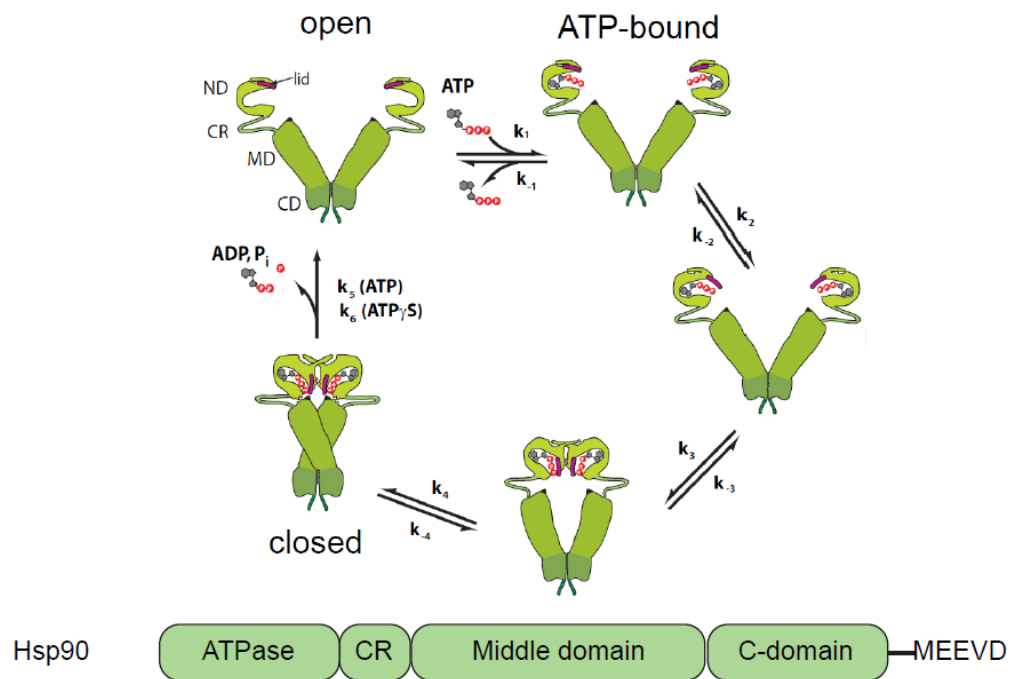


Figure 1.4 Conformational cycle and schematic domain organization of Hsp90

During different phases of the chaperone cycle Hsp90 binds more than 20 co-chaperones through both the N- and C-termini of the protein, some of which play the tuning roles by either activating or inhibiting the ATPase activity of Hsp90.⁸⁸⁻⁹⁰ Hsp90 contains several drugable sites at both its N- and C-terminal domains and for this reason, Hsp90 inhibitors are divided into several groups. Traditional Hsp90 inhibitors block the binding of the ATP at N-terminal domain, they include natural compounds, as geldanamycin (GDA) and radicicol (RDC),^{91,92} and synthetic molecules such as geldanamycin and

Introduction

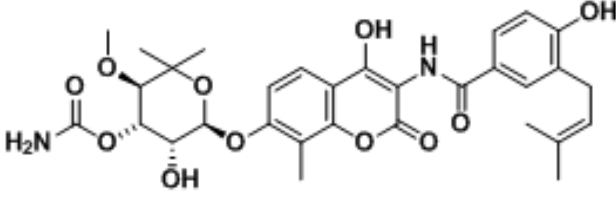
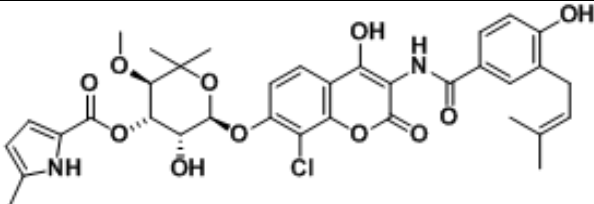
radicol derivatives,⁹³⁻⁹⁷, purines derivatives,⁹⁸⁻¹⁰⁰ pyrazoles derivatives,¹⁰¹ sulfonamide derivatives,¹⁰² C₉-type iridoid (verminoside)¹⁰³ and the three chimeric compounds of radicol and geldanamycin radamide, radester and radanamycin.¹⁰⁴⁻¹⁰⁶ Even today, there are over 50 clinical trials testing different N-terminal Hsp90 inhibitors (ClinicalTrials.gov database) undergoing clinical evaluation.^{107,108} However, clinical trials have shown many limitations, including poor solubility and toxicity of these drugs that limit their use.¹⁰⁹ The most well-known side effect is the induction of a cytoprotective mechanism termed as *heat shock response* (HSR),^{110,111} which induces drug-resistance and anti apoptotic mechanisms.^{112,113} A promising strategy to overcome these problems is to regulate Hsp90 function by targeting the C-terminal domain, as its inhibition does not induce the unsought HSR.^{114,115} Unfortunately, the few structural information on Hsp90 C-terminal domain currently obtainable have not provided the resolution necessary for structure-based drug design of new synthetic inhibitors. The development of more efficacious C-terminal inhibitors is desired to better understand the ramifications of C-terminal inhibition and to probe the mechanism by which Hsp90 interacts with client proteins.¹¹⁶ The first C-terminal inhibitor was discovered in 2000 by Neckers and co-workers, they showed the capabilities of the Hsp90 C-terminus to bind novobiocin.¹¹⁷ Novobiocin is not the only product which inhibits the Hsp90 activity through C-terminus modulation, but related family members such as chlorobiocin and coumermycin A1 were showed to bind this domain and induce a dose-dependent degradation of Hsp90 client proteins in a manner similar to Hsp90 N-terminal inhibitors.¹¹⁸ However, these inhibitors have micromolar and millimolar IC₅₀ values (Novobiocin \approx 700 μ M in SKBr3 cells) and it is not sufficient for clinical application,¹¹⁵ but it give a starting point for the development of new more efficacious C-terminal inhibitors. Furthermore, structural optimization of

Introduction

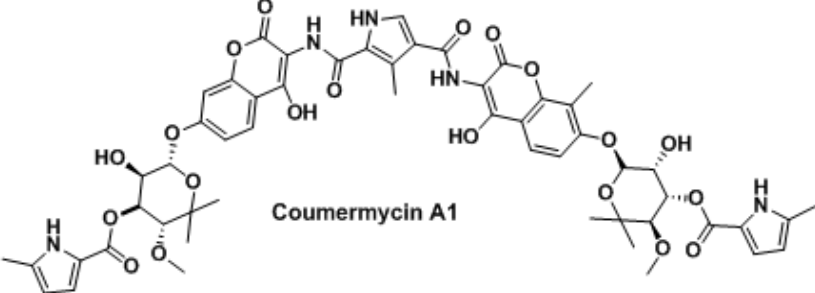
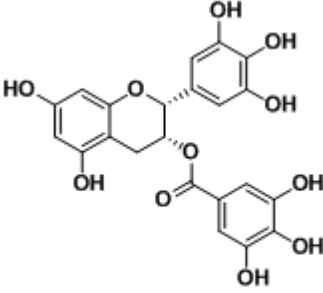
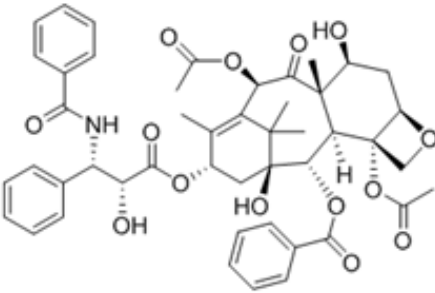
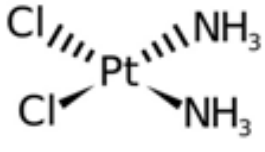
novobiocin has led to analogues with more potent antiproliferative profiles than the starting compound.¹¹⁹⁻¹²² Many other inhibitors that bind C-terminal domain exist, they include epigallocatechin-3-gallate,¹²³ taxol,¹²⁴ cisplatin¹²⁵ and sansalvamide A derivatives (Table 1).^{126,127}

The latter are the allosteric modulators that bind the N-middle domain and block the binding of Hsp90 to client proteins and co-chaperones that bind to the C terminus of the protein.¹²⁸ Until now, only natural and/or semi-synthetic compounds have been described. Recently, *Strocchia et al.* have identified the first synthetic compound able to inhibit C-terminal domain of the Hsp90 (Table 1).¹²⁹ The principal benefit of C-terminal inhibitors is that they do not seem to be associated with the heat shock response than N-terminal inhibitors.¹³⁰

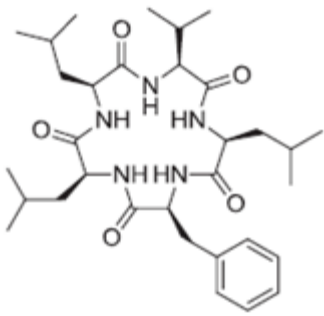
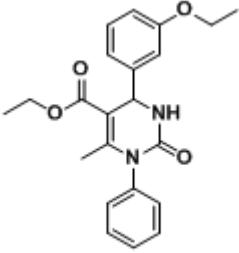
Table 1. Hsp90 C-terminal inhibitors and their IC₅₀ value.

Inhibitor	IC ₅₀
 Novobiocin	700 μM In SKBr3
 Chlorobiocin	80 μM In SKBr3

Introduction

 <p style="text-align: center;">Coumermycin A1</p>	<p>70 μM In SKBr3</p>
 <p style="text-align: center;">(+)-Epigallocatechin-3-gallate</p>	<p>100.16 μM In SKBr3</p>
 <p style="text-align: center;">Taxol</p>	<p>-</p>
 <p style="text-align: center;">Cisplatin</p>	<p>-</p>

Introduction

 <p>Sansalvamide A</p>	46.7 μ M against an NCI 60 panel cell line
 <p>DHPM Compound</p>	20.8 μ M in Jurkat cell line

As described before, Hsp90 is the central point of the protein folding machine, because there are many binding sites for co-chaperones. So, each protein-protein interaction presents the opportunity for disruption the protein folding process. Nowadays, only a few protein-protein interactions have been targeted such as interactions between Hsp90 and the co-chaperones Cdc37,¹³¹ p50,¹³² and the interactions between Hsp90 and the partner protein HOP.¹³³ However, the modulation of Hsp90 through the last two strategies (C-terminal inhibitors and disrupt protein-protein interaction), may allow to develop of new potential modulators of Hsp90 which could be used as anticancer agents and are expected to be free from side effects associated to the induction of heat shock response.

1.6 Microsomal prostaglandin E₂ synthase-1 (mPGES-1)

Prostaglandins (PGs) and thromboxane A₂ (TXA₂), collectively termed prostanoids, are a group of physiologically active lipid mediators derived enzymatically from fatty acids. This class of mediators are involved in homeostatic functions and mediate pathogenic mechanisms, including inflammatory response.

Inflammation is the body's natural response to infection and injury against an organ or tissue and has been implicated in the pathogenesis of arthritis, cancer and stroke, as well as in neurodegenerative and cardiovascular disease.¹³⁴ Furthermore, inflammatory diseases increase the risk of developing many types of cancer such as bladder, cervical, gastric, intestinal, oesophageal, ovarian, prostate and thyroid cancer.^{135,136} There are four principal bioactive prostaglandins generated: prostaglandin E₂ (PGE₂), prostacyclin (PGI₂), prostaglandin D₂ (PGD₂) and prostaglandin F_{2α} (PGF_{2α}).¹³⁷ Biosynthesis of prostanoids starts by release of arachidonic acid (AA) from cell membrane phospholipids catalyzed by phospholipase A₂ (PLA₂). Subsequently AA is converted to Prostaglandin H₂ (PGH₂) in two steps by cyclooxygenase 1/2 (COX-1, COX-2), bifunctional enzymes that contain cyclooxygenase and peroxidase activity, in the first step AA was oxidized to generate PGG₂, then this intermediate is reduced into PGH₂.¹³⁸ The COX pathway produces PGG₂ and PGH₂, which then are converted into PGI₂ by prostacyclin synthase, TXA₂ by thromboxane synthase, and PGE₂, PGD₂ and PGF_{2α} by their respective synthase enzymes (**Figure 1.5**).¹³⁹

Among the prostaglandins, PGE₂ is the most abundant in physiological conditions and plays a crucial role in several organs and tissues such as kidney and gastrointestinal tract.^{139,141} Further studies suggest that PGE₂ had immunosuppressive effects by regulating the expression of EP₂, EP₃ and

Introduction

EP₄,¹⁴² also, PGE₂ protected the gastrointestinal mucosa and regulated the renal flow, natriuresis and blood pressure by modulating the expression of EP₁ and EP₂.¹⁴³ Under physiological conditions, the level of PGE₂ is regulated by three enzyme, the prostaglandin E₂ synthases (PGEs), that including the cytosolic PGES (cPGES) and two membrane-bound proteins mPGES-1 and mPGES-2.¹⁴⁴

cPGES and mPGES-2 are constitutively expressed in various cells and tissues, and their levels were not significantly increased under inflammatory conditions, but high levels of mPGES-2 was observed in human colorectal cancer, human gliomas and activated microglia.¹⁴⁵ mPGES-1 is considered as an induced enzyme like COX-2, because, in normal conditions it is expressed at low level but under pathological conditions, this enzyme is significantly activated leading to over-production of PGE₂.¹⁴⁶

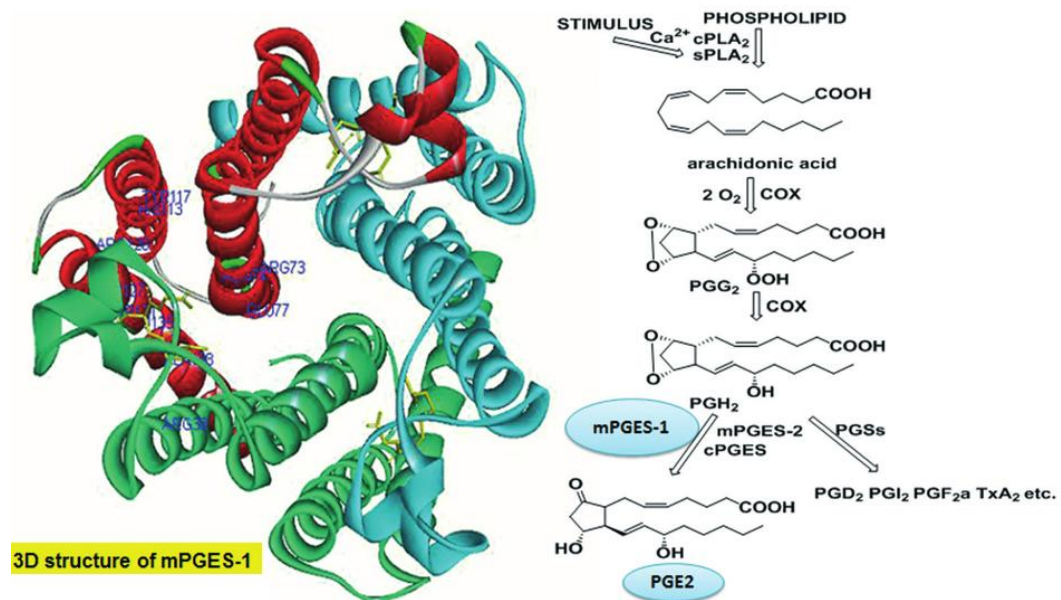


Figure 1.5 3D structure of mPGES-1 and arachidonic acid (AA) cascade

Introduction

A variety of signal transduction pathways are involved in the regulation of mPGES-1, its expression increase in response to various inflammatory stimuli and mediators, for example, cytokines (LPS, IL-1b and TNF- α).^{147,148}

It is clear how mPGES-1 could represent a drug target associated with inflammation, fever and pain,¹⁴⁹ so, the modulation of this enzyme could be a promising alternative in anti inflammatory therapy. mPGES-1 plays a key role, similar to COX-2, in the development of cancers. Several studies suggest that mPGES-1 was overexpressed in colon cancer,^{150,151} lung cancer,¹⁵² head and neck cancer, breast cancer, stomach cancer,^{153,154} and Alzheimer's disease tissues.¹⁵⁵ Furthermore, several publications reported that mPGES-1 could cause lung metastatic tumor formation and growth, induce EGFR expression, and mediate EGFR-dependent tumor growth in prostate cancer.¹⁵⁶ Moreover, mPGES-1 expression was hugely correlated with vascular invasion and worse prognosis in colorectal cancer.^{157,158}

Pharmacological inhibition of mPGES-1 reduced squamous carcinoma growth by suppression of PGE₂ mediated-EGFR signalling and impairing tumor-associated angiogenesis. These findings highlight also the potential of mPGES-1 inhibitors as agents capable of reducing tumor growth.¹⁵⁹

The discovery of mPGES-1 is attributed to Jackbsson in 1999¹⁶⁰ who recognized it as a member of the Membrane-Associated Proteins in Eicosanoid and Glutathione Metabolism (MAPEG) superfamily.¹⁶¹ In this family, there are many other members including leukotriene C₄ synthase (LTC₄S), 5-lipoxygenase-activating protein (FLAP) and microsomal glutathione transferases (MGST) 1-3.^{162,163} The most closely related MAPEG member is the microsomal glutathione transferase-1 (MGST1), which shares 39% sequence identity with mPGES-1.¹⁶⁴

Recently a study by *Sjögren et al.* showed that the accuracy of mPGES-1's structure reached a higher resolution of 1.2 Å x-ray in-plane *via* electron

Introduction

crystallography.¹⁶⁵ Human mPGES-1 is a membrane homotrimer with four transmembrane α -helices (TM₁-TM₄) enclosing an inner core, which looked like a funnel-shaped opening towards the cytoplasm between TM₁ and TM₂ in each monomer (**Figure 1.6A**). Glutathione (GSH) is an essential co-factor for active binding in the U-shapes conformation at the interface between subunits in the proteins¹⁶⁶⁻¹⁶⁹ and attacked the peroxide group of PGH₂ in the active site *via* its thiol group in the catalytic cycle process.¹⁶⁴

GSH forms hydrogen bond with several amino acid residues such as, Arg73, Asn74, Glu77, His113, Tyr117, Arg126 and Ser127 from helices II and IV, and Arg38 from helix I. In addition, GSH forms a π -stacking interaction with Tyr130 due to its glutamate and its cysteine (**Figure 1.6B**).

The active site of mPGES-1 consists of three gatekeepers and a residue of Arg, all of that are located within the transmembrane-helix IV.^{166,170-172} In order to work its catalytic activity the active site of the mPGES-1 must be open to be able ensure the PGH₂ access.¹⁶⁸ The N-terminal region of helices II and IV jointly with the C-terminal portion of helix I and the C-cytoplasmatic domain from neighboring molecule forms a deep cavity,¹⁷³ researchers suggest that this is the active site based on the form, the size and the favorable interactions that this pocket has with PGH₂.^{174,175}

The proposed mechanism for PGH₂ isomerization to PGE₂ by GSH suggests that Ser127 activates the thiol of GSH to form a thiolate anion that acts as nucleophilic and directly attack on the endoperoxide oxygen atom at the C-9 carbon of PGH₂ to produce an unstable intermediate. Deprotonation in 9-position and cleavage of S-O bond lead to a bidentate complex with Arg126. This results in the regeneration of the reactive thiolate anion (regeneration of GSH) and the formation of the product PGE₂ (**Figure 1.6C**).¹⁶⁵

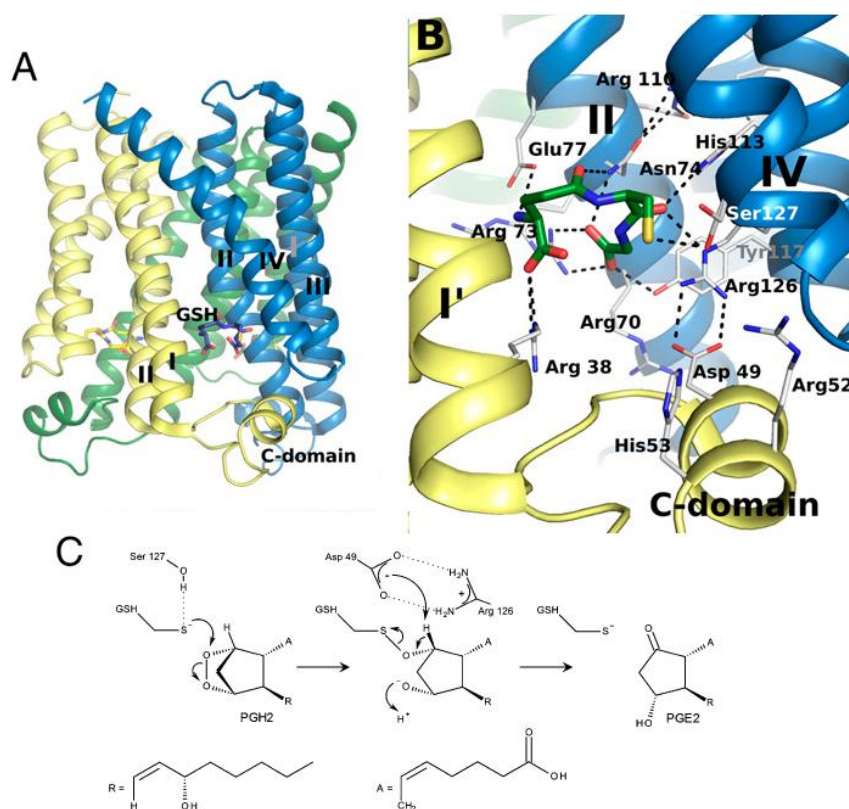


Figure 1.6 (A) Structure of the mPGES-1 trimer. (B) Interactions between mPGES-1 and GSH. (C) Suggested mechanism of PGH2 isomerization to PGE2 by mPGES-1.

Inhibition of mPGES-1 offers many therapeutic opportunities in several pathologies, in fact, the suppression of massive PGE₂ biosynthesis is a reasonable pharmacological strategy in many pathological conditions such as fever, inflammation, cardiovascular disease and cancer.¹⁷⁶⁻¹⁷⁸ Traditional anti-inflammatory agents are not selective towards this enzyme, drugs that target mPGES-1 are considered as valuable alternatives to NSAIDs/coxib and they may offer a better safety profile and, thus, lower risk of side effects that are usually associated with NSAIDs and coxib.¹⁷⁹⁻¹⁸² NSAIDs not only inhibit the production of PGs but also annihilates the release of bradykinin, change lymphocyte reactions and decrease the migration of phagocytosis of

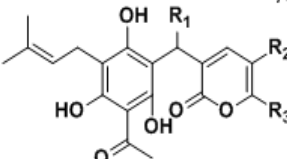
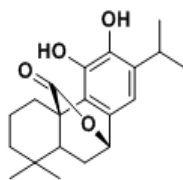
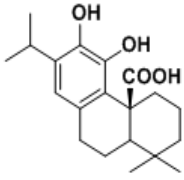
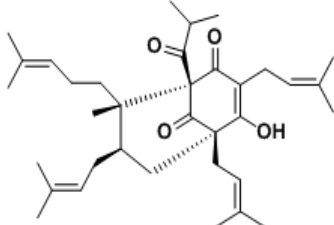
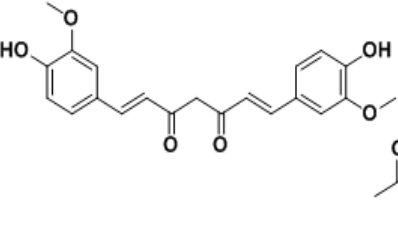
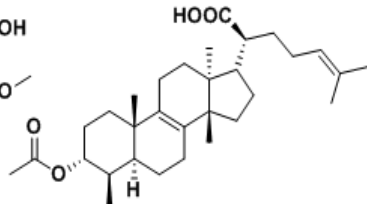
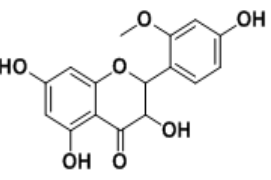
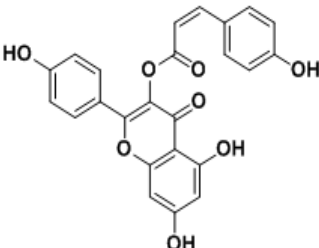
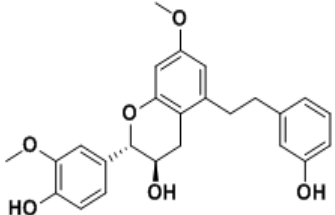
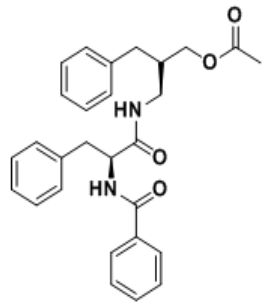
Introduction

granulocytes and monocyte in the inflammatory process. However, unselective NSAID are not able to differentiate between the two COXs, and this is the reason of their gastric side effects, because, PGE₂ is clearly known to have the protective effects on the gastrointestinal mucosa.¹⁸³ In order to overcome the side effects of NSAIDs selective inhibitors of the inducible COX-2 (COXibs) were discovered.¹⁸⁴ These products modulate the COX-2 as well as the downstream PGEs enzymes. However, after the marketing of this class of medicine, they have proved to be associated with the increased cardiovascular risk in patients after long-term therapies, probably due to imbalance of PGI₂ and TXA₂ in the vasculature.^{185,186} In this field, mPGES-1 inhibitors constitute an attractive pharmacological approach which could overcome the classic side effects associated with COX-inhibitors, in fact, blocking the mPGES-1 enzyme we expect to selectively inhibit increased PGE₂ production, without affecting other prostanoids of physiological importance. Despite that mPGES-1 was reported as a drug target already in 1999, progress in drug discovery of mPGES-1 has been very slow. Up to now, a number of compounds with different chemotypes have been identified, but none have entered clinical trials.^{187,188} Even today there are many problems to be studied and solved in developing real selective mPGES-1 modulators for humans, because, the phenotypic differences between human and murine enzyme have hampered research on the effects of mPGES-1 inhibition in cancer and in inflammatory diseases.¹⁸⁹ For example, the variation of certain amino acids in the active site of mPGES-1 may lead to partial or complete loss the activity of potent inhibitors. Three amino acids located in transmembrane helix IV of mPGES-1 are not conserved between human and rat/mouse enzyme, these residues are the gatekeepers of the active site and the variation of these amino acids intercept the access of modulators for steric reasons.¹⁹⁰ In the **Table 2** were reported the most known mPGES-1 inhibitors and their IC₅₀ valeus, grouped

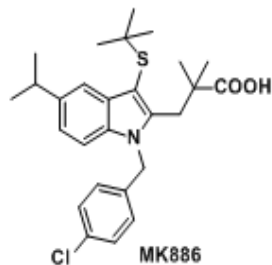
Introduction

in three main ways: natural products and derivatives, synthetic compounds and dual inhibitors of mPGES-1 and 5-lipoxygenase (5-LO).

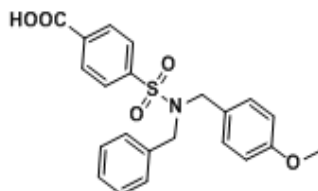
Table 2. Some mPGES-1 inhibitors

Natural products and derivatives		
 <p>Arzanol $R_1=H; R_2=CH_3; R_3=CH_2CH_3$ $IC_{50}=0,4\mu M^a$ $R_1=Ph; R_2=CH_3; R_3=CH_2CH_3$ $IC_{50}=0,8\mu M^a$ $R_1=Ph; R_2=H; R_3=CH_3$ $IC_{50}=1,0\mu M^a$</p>		
Arzanol and its synthetic derivatives ^{191,192}		
 <p>Carnosol¹⁹³ $IC_{50}=5,0\mu M^a$</p>	 <p>Carnosic acid¹⁹³ $IC_{50}=5,0\mu M^a$</p>	 <p>Hyperforin¹⁸⁴ $IC_{50}=1,0\mu M^a$</p>
 <p>Curcumin¹⁹⁵ $IC_{50}=0,2-0,3\mu M^a$</p>	 <p>Boswellic acid¹⁹⁶ $IC_{50}=0,4\mu M^a$</p>	 <p>Flavonoids¹⁹⁷ $IC_{50}=63,5^b; 94,3\%^c$</p>
 <p>Castilliferol¹⁹⁸ $IC_{50}=35,8^b$</p>	 <p>Shanciol B¹⁹⁸ $IC_{50}=63,5^b$</p>	 <p>Aurantiamide acetate¹⁹⁸ $IC_{50}=29,9^b$</p>

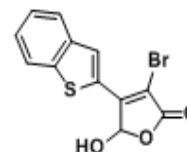
Synthetic Compounds



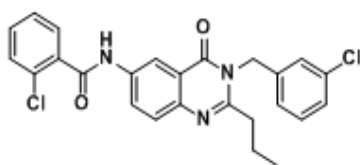
Indole¹⁹⁹ IC₅₀ = 1,6μM^a



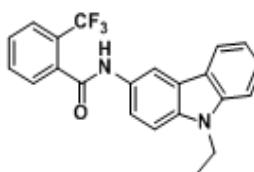
Benzenesulfonamides²⁰⁰ IC₅₀ = 13,8μM^a



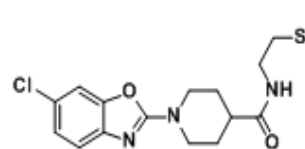
Benzenethiophene²⁰¹ IC₅₀ = 1,8μM^a



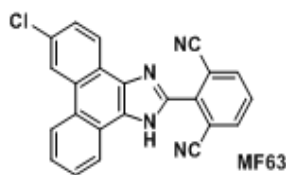
Quinazolinones²⁰² IC₅₀ = 0,67μM^d



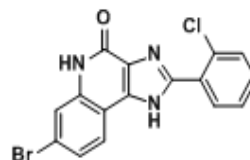
Carbazoles¹⁵⁹ IC₅₀ = 0,6μM^a



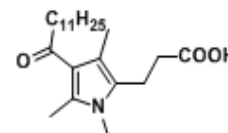
Benzoxazoles²⁰³ IC₅₀ = 1,2μM^a



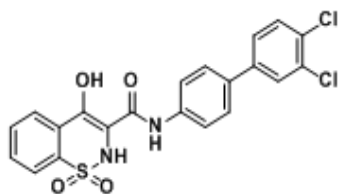
Phenanthreneimidazole²⁰⁴ IC₅₀ = 0,001μM^a



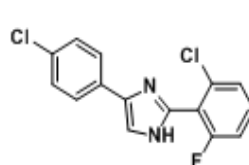
Imidazoquinolines²⁰⁵ IC₅₀ = 0,062μM^a



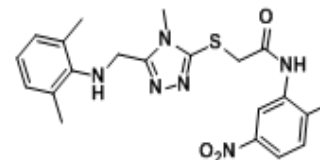
Pyrrole²⁰⁶ IC₅₀ = 0,67μM^a



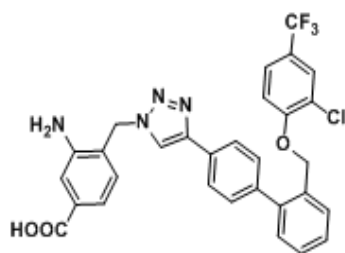
Oxicam²⁰⁰ IC₅₀ = 0,016μM^a



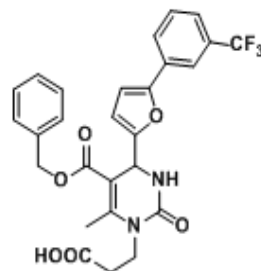
Biarylimidazoles²⁰⁷ IC₅₀ = 0,66μM^a



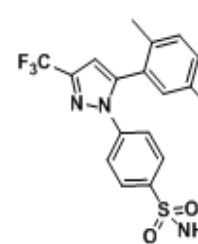
1,2,4 Triazoles²⁰⁸ IC₅₀ = 0,7μM^a



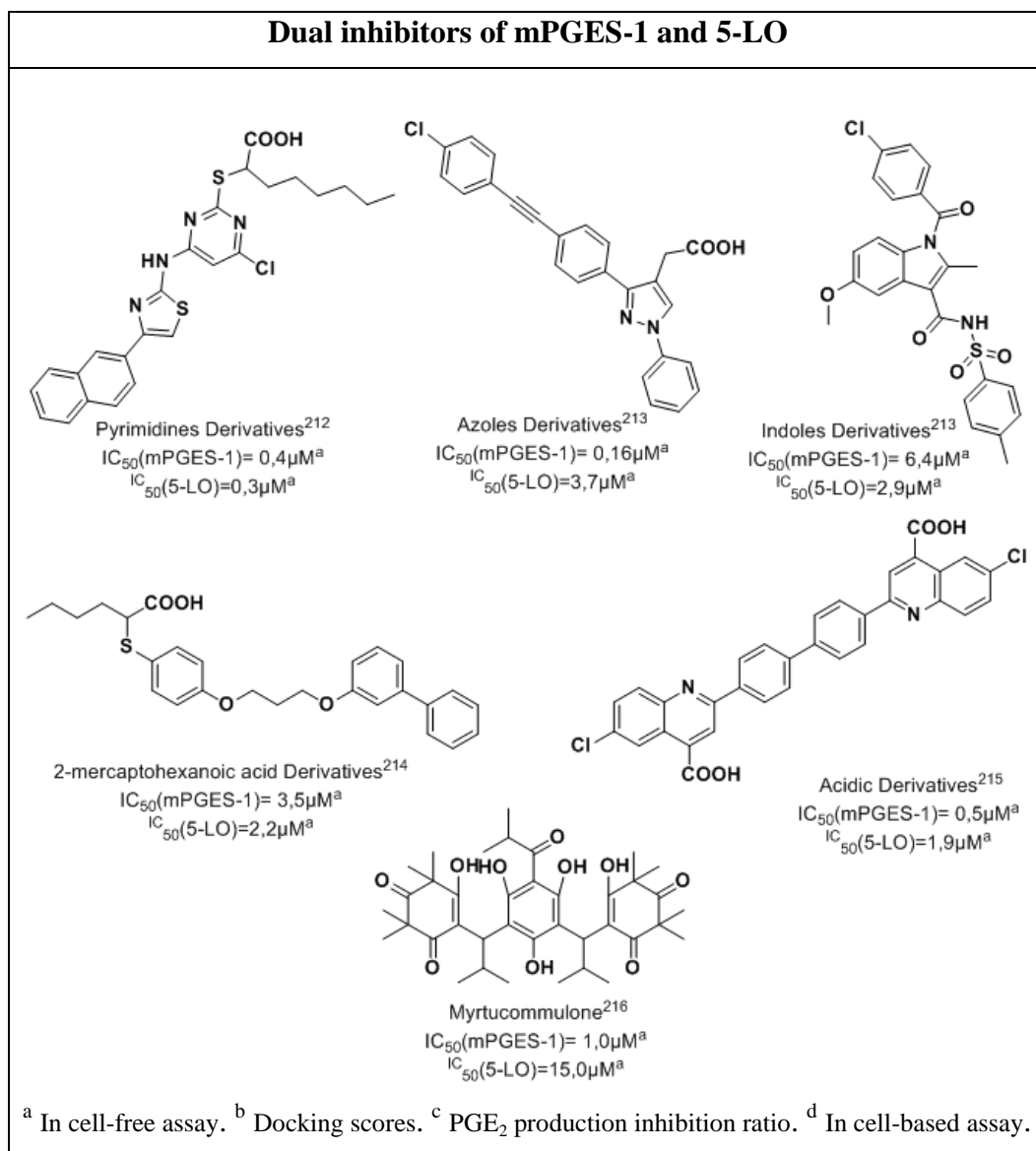
1,2,3 Triazoles²⁰⁹ IC₅₀ = 0,7μM^a



Dihydropyrimidines²¹⁰ IC₅₀ = 0,41μM^a



Sulfonamides²¹¹ IC₅₀ = 3,0μM^a



Despite good results have been obtained for some products with different chemical motifs, currently there is still no selective modulators acting on mPGES-1 in clinics.^{217,218} Many industrial and academic groups have worked to develop mPGES-1 modulators. Their results show any excellent IC₅₀ values in cell-free assay but they are not stable so they have a poor cell potency, another reason which blocks the drug development of mPGES-1 inhibitors, as

Introduction

previously mentioned, are the specific differences between the enzyme isoforms in various species.²¹⁹ The rational inhibitors design of mPGES-1 was started in 2013 with the three-dimensional crystal structure of mGES-1 determined by Sjögren et al.¹⁶⁵ The rational design through computational methods was complicated, because, the active site is shallow and located within the membrane-spanning region. In 2015, a crystal structures binding to four inhibitors of mPGES-1 including MF63 and MK886 (see Table 2: synthetic inhibitors) was reported by J.G. Luz et al., they clarified the binding mode between inhibitors and amino acid residues and explained the mechanism of isomerization from PGH₂ to PGE₂.²²⁰ However, the ultimate goal is to discover more effective, highly selective and highly safe drugs for the treatment of pain, inflammatory diseases and cancer, and in this context, the discovery of new mPGES-1 modulators is highly demanded, so, this crystal structure can expand our knowledge with regard to designing and pharmacologically validating inhibitors of mPGES-1.

1.7 How to proceed in the research project

My PhD program is aimed to the design, synthesis and biological evaluation of new chemical compounds able to modulate the activity of the two biological target described before. Therefore, the scientific activity carried out during the PhD was focused on the synthesis of small libraries of compounds in order to identify new products to guide the development of new modulators with inhibitory activity against the C-terminal domain of Hsp90 and mPGES-1.

The research was focused on the analysis of data currently available in the literature, also taking advantage the information about Structure Activity Relationship (SAR) of known inhibitors of the two targets proteins.

Introduction

The general methodology used in this study can be described through these main steps:

1. Analysis of data currently available in the literature in order to identify some chemical motifs able to interact with the two biological targets;
2. Design and synthesis of the compounds through suitable synthetic strategies;
3. Biological evaluation and individuation of new possible hits or lead compounds;
4. Rationalisation of ligand/protein interaction by computational analysis.

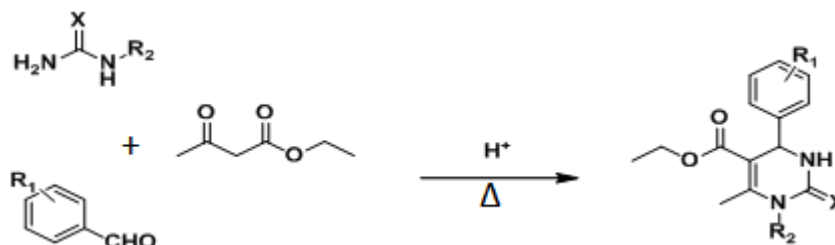
Concerning step 1, analysis data present in the literature was used for the identification of a few scaffolds poorly explored, able to interfere with the target of interest. In particular, the 3,4-dihydropyrimidin-2(1*H*)-one (DHPM) core for the Hsp90,¹²⁶ while carbazole, dyaryl and pyrazol-5-one scaffolds for mPGES-1.

These chemical moieties are seen as “privileged structures” in medicinal chemistry, because they possess significant biological activity, in fact, adequately decorated, they can selectively bind many enzymes, receptors or channels having different pharmacological effects.²²¹⁻²²⁴

In respect to step 2, appropriate synthetic procedures were used and optimized in order to obtain the desired products in good yield. For the synthesis of DHPM core were used the well-known Biginelli condensation, a multiple-component chemical reaction that creates 3,4-dihydropyrimidin-2(1*H*)-ones core under acidic conditions from three component, aryl aldehydes, urea or its derivatives and β -ketoesters. This one-pot reaction was first reported by Pietro Biginelli in 1893 (**Scheme 1.1**).²²⁵

Introduction

Scheme 1.1 Biginelli condensation between urea derivatives, aryl aldehydes and ethyl acetoacetate



Although the original reaction conditions suffered from poor yields, in the last decades, the discovery of dihydropyrimidine biological activity has led to a renewed exploration of the reaction conditions, revealing a variety of compatible solvents, acid catalysts, and an expanded substrate scope.²²⁶ Some of these procedures have replaced the traditional Brønsted acids²²⁶⁻²²⁸ with different Lewis acids such as TMSCl,²²⁹ FeCl₃,²³⁰ Yb(OTf)₃,²³¹ Cu(OTf)₂.²³² Moreover, different techniques have been described as the use of solvent-free conditions,²³³ solid-phase approaches,²³⁴ phase-transfer and polymer supported catalyst,^{235,236} ionic liquids,²³⁷ asymmetric methodology.²³⁸

Another optimization of the methodology concerned the usage of several high-speed microwave-assisted protocols in order to improve the yield of products and reduce the reaction time.²³⁹⁻²⁴¹ For the synthesis of our compounds, DHPMs derivatives have been obtained through a protocol of Biginelli reaction supported by microwave-irradiation and chlorotrimethylsilane (TMSCl).²⁴²

Regarding the carbazoles derivatives has been used a synthetic strategy in two steps, the first step was performed through a classic Suzuki-Miyaura cross-coupling reaction in order to obtain 2-nitrobiaryl derivatives, while the second step was carried out *via* Cadogan cyclization protocol. This approach allows the reductive cyclization of 2-nitrobiphenyl compounds in the presence of suitable organophosphorus reagents.^{243,244}

Introduction

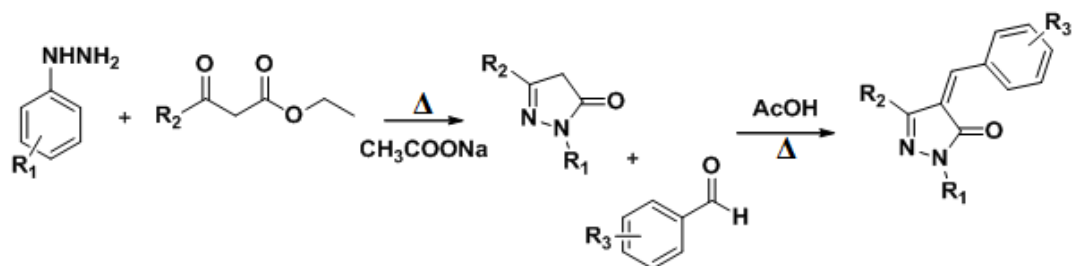
The reaction of these compounds were conducted using an excess of triethyl phosphite ($\text{P}(\text{OEt})_3$), under solvent-free conditions and supported by microwave-irradiation.

This synthetic methodology, compared to others, provides a greater tolerance of functional groups on the substrate and more precise regiocontrol of functional group placement within the product. Since the biaryl compounds have been obtained in the same manner of the first step of carbazole compounds. Suzuki-Miyaura reaction is an organic reaction between organic boron compounds and organic halides catalyzed by a palladium(0) complex and it is widely used to synthesize substituted biphenyls.²⁴⁵

Cross-coupling reactions is one of the most straightforward methodologies for various carbon-carbon bond formations and it has many advantages, in fact, the reactants are readily available, nontoxic, and air- and water-stable. They react under mild conditions and are amenable to a variety of reaction conditions, including the use of aqueous solvents and substrate supports. The inorganic boron byproduct can be easily removed after the reaction.²⁴⁶ In our case, biaryl compounds were obtained using a classical Suzuki-Miyaura protocol promoted by $\text{Pd}(\text{PPh}_3)_4$, Tetrakis(triphenylphosphine)palladium(0) and potassium carbonate, K_2CO_3 as base.

Concerning the pyrazol-5-one derivatives has been used a synthetic strategy in two steps, in the first step there is the preparation of the pyrazol-5-one core using a tandem condensation and thermal cyclization between β -ketoesters and hydrazines. In the second step was performed through an aldol condensation, taking advantage of C4 (methylene group) reactivity with aldehydes (**Scheme 1.2**).^{247, 248}

Scheme 1.2 *Synthesis of pyrazol-5-one derivatives*



Lastly concerning step 3, biological evaluation of the synthesized products were performed using appropriately assay for each of two investigated targets, e.g. Surface Plasmon Resonance (SPR), cytotoxicity, western blot assay and limited proteolysis assay in the case of Hsp90, a cell-free assay using the microsomal fraction of interleukin- 1β -stimulated human A549 cells to evaluate the effect of several compounds on mPGES-1 activity. Regarding step 4, the rationalization of ligand/protein interaction has been performed using docking studies.

RESULTS AND DISCUSSION

- CHAPTER 2 -

Exploration of the structural elements of a 3,4-dihydropyrimidin-2(1H)-ones (DHPM) core, driving toward more potent Hsp90 C-terminal inhibitors.

Based on : Terracciano S., **Foglia A.**, Chini M.G., Vaccaro M.C., Russo A., Dal Piaz F., Saturnino C., Riccio R., Bifulco G., Bruno I. *RSC Adv.* (2016), **6**, 82330-82340.
And Terracciano S., Chini M.G., Vaccaro M.C., Strocchia M., **Foglia A.**, Vassallo A., Saturnino C. Riccio R., Bifulco G., Bruno I. *Chem. Commun.* (2016), **52**, 12857-12860.

2.1 The need to develop Hsp90 C-terminal inhibitors

As outlined above, many Hsp90 N-terminal inhibitors have been shown excellent antitumor activity have some drawbacks in clinical application.²⁴⁹⁻²⁵²

In contrast to this strategy, an alternative approach to Hsp90 modulation for the treatment of cancer is represented by the C-terminal inhibitors, as they don't induce the heat shock response, a well-established compensatory mechanism that has likely limited the clinical impact of N-terminal Hsp90 inhibitors in cancers treatments.²⁵³⁻²⁵⁵

The heat shock response (HSR) is a cellular mechanism in response to stress, bacterial infections, heat, toxins and heavy metals.²⁵⁶

It is mediated by heat shock factor-1 (HSF-1), which activates transcription of heat shock genes.²⁵⁷ HSF-1 is ubiquitously expressed and has the principal role in the stress-induced expression of Hsp genes,²⁵⁸ this protein is a monomer in complex with Hsp90 and in this form it is unable to bind to DNA.²⁵⁹

In stress condition, HSF-1 is released from the chaperone complex then trimerized and it is transported into the nucleus where it undergoes hyperphosphorylation and binds to DNA containing heat shock elements sequence.^{260, 261} Herein it directs the transcription of Hsp genes which lead the increase of cellular resistance by elevating the expression of multiple heat shock proteins,²⁵⁴ including Hsp27, Hsp70 and Hsp90 (**Figure 2.1**).²⁶² The N-terminal inhibitors of Hsp90 induce the dissociation of HSF-1 from Hsp90 and, with the same mechanism, trigger the pro-survival heat shock response that enables cancer cells to escape the cytotoxic effect, in fact, this cascade of events facilitates oncogenic growth and stops tumor cells from undergoing apoptosis.²⁶³

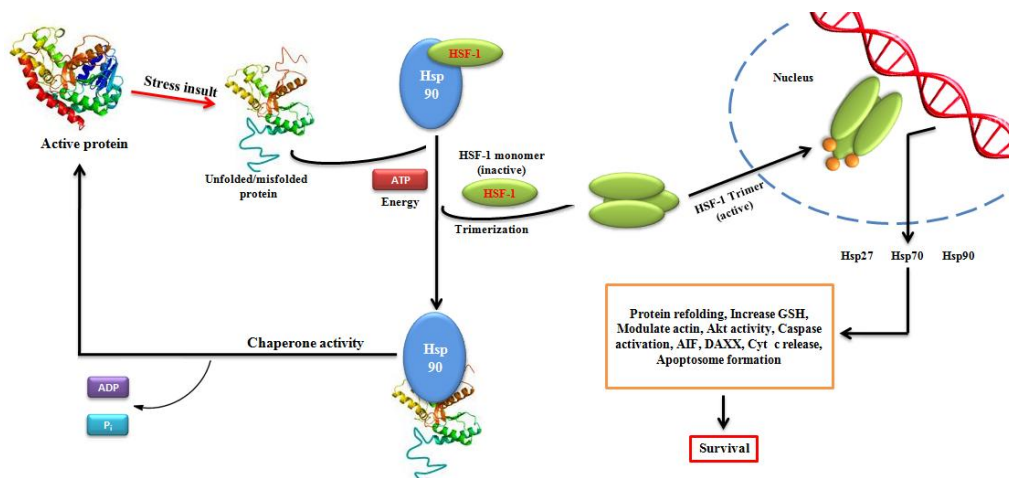


Figure 2.1 Heat Shock Response

In addition, this attractive cytoprotective mechanism has driven researchers to find alternative molecules that repress Hsp90 activity without inducing HSR. The C-terminal modulation has an opposite effect, because C-terminal inhibitors block HSF-1 in its inactive form promoting its degradation via ubiquitin-proteasome pathway.²⁶³⁻²⁶⁵

In this context, the research is enormously engaged in the development and discovery of new molecules that bind the C-terminal domain of Hsp90, but the vast conformational space of this region is still a strong limitation for the rational design of a selective inhibitors.

2.2 Where do we start?

With the aim of identify new promising and more potent C-terminal inhibitors of Hsp90 published data were used. For the first time in 2015 *Strocchia et al.*¹²⁹ reported a new 3,4-dihydropyrimidin-2(1H)-one derivative able to interact with C-terminal domain of Hsp90.

This compound was designed starting from one assumption, *Csermely et al.*^{78, 80} reported that the C-terminal region is able to interact with both purine and

pyrimidine nucleotides (GTP and UTP preferentially), so take in advantage the structural analogy between uridine triphosphate (UTP) and the DHPM core they synthesized seventeen DHPM derivatives through Biginelli multicomponent reaction.

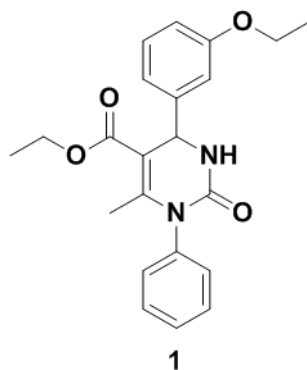


Figure 2.2 *First non-natural inspired modulator of C-terminal domain*

Moreover, compound **1** (**Figure 2.2**) represents the first non-natural inspired product able to modulate the C-terminal domain of Hsp90 with a good antiproliferative profile (IC_{50} values 50.8 ± 0.2 and 20.8 ± 0.3 mM in A375 and Jurkat cell lines, respectively) without any apparent cytotoxic activity in non-tumor cells. Western blot analysis confirmed that the antitumor activity of this compound was provided by degradation of some Hsp90 client oncoproteins, moreover, they showed that the compound does not cause an increase of the levels of Hsp90 and Hsp70 demonstrating that the undesired HSR was not induced.

Finally, limited proteolysis assay showed that the compound **1** binds the C-terminal region of Hsp90.

2.3 Influence of the chemical functionalization on the phenyl ring at C4 position of DHPM core based Hsp90 C-terminal inhibitors.

The great interest aroused by C-terminal Hsp90 inhibitors as potential therapeutic agent and the recent discovery of compound **1** as C-terminal Hsp90 inhibitor drove us to improve the exploration of this promising scaffold.

With the purpose to improve the information about the structure-activity relationship and to explore the influence of the chemical functionalization on the phenyl ring at C4 position of DHPM core a second collection of different decorated DHPM derivatives was synthesized (compounds **2-13**, **Figure 2.3**), by a microwave-assisted Biginelli multicomponent reaction²⁴² through the combination of the following synthons:

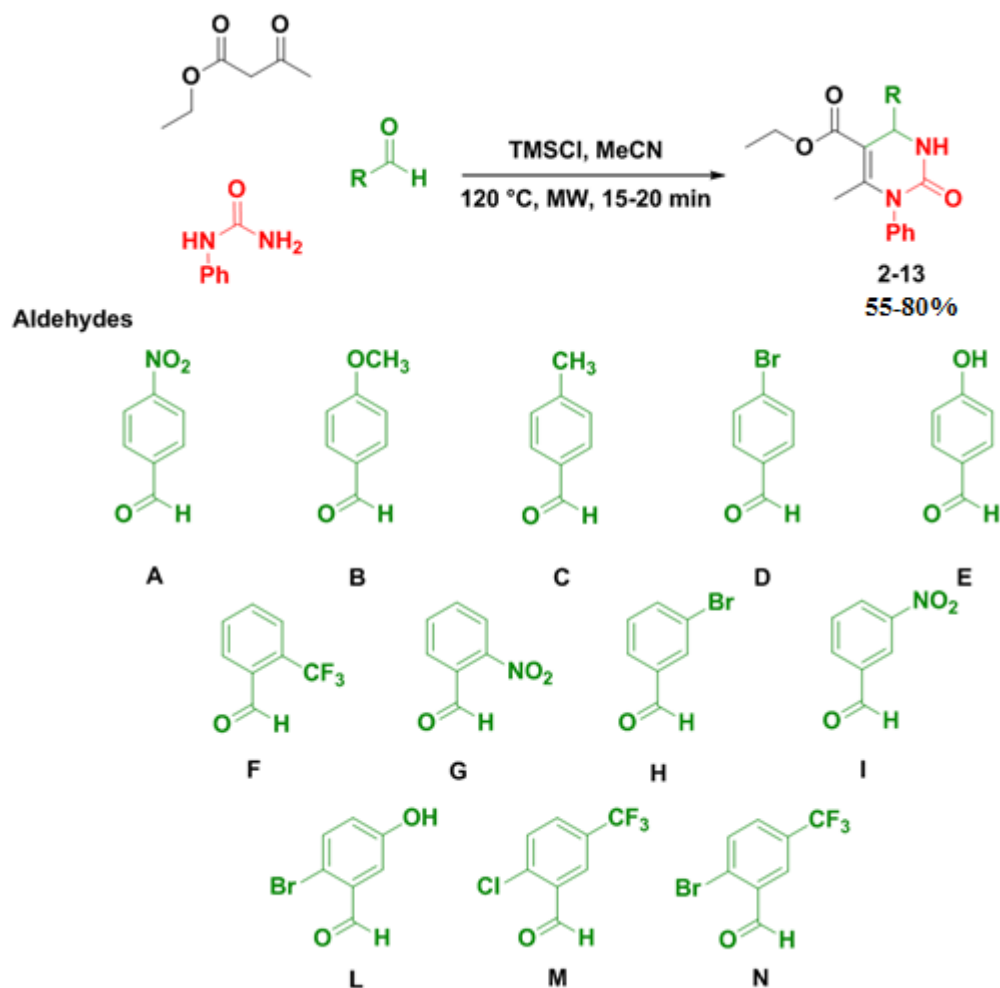
- twelve different aldehydes (**A-N**);
- N-phenylurea;
- Ethyl acetoacetate.

N-phenylurea and ethyl acetoacetate have been used to maintain the same functionalizations present on the other positions on DHPM core of compound **1**. These compounds were obtained by using chlorotrimethylsilylane (TMSCl) as the mediator of Biginelli reaction, especially for the synthesis of N1-substituted dihydropyrimidinones more difficult to obtain using a microwave-assisted Biginelli protocol (**Scheme 2.1**).^{222, 240}

In particular, with the aim of shedding more light on the influence of chemical diversity around the phenyl ring at C4 position of this scaffold, diverse aryl aldehydes available in laboratory were chosen. These aldehydes have different substituents in the *o*-, *m*-, *p*- and *o*-, *m*- positions with either electron-withdrawing or electron-donating groups.

Exploration of the structural element of 3,4-dihydropyrimidin-2(1H)-ones (DHPM) core, driving toward more potent Hsp90 C-terminal inhibitors

Scheme 2.1 General synthetic procedure for the synthesis of compounds **2-13** and structures of the aryl aldehydes used to generate the second collection of DHPMs derivatives.



Following the synthetic procedure described before compounds **2-13** were prepared in short reaction time (15-20 min) and with a good yields (55-80%).

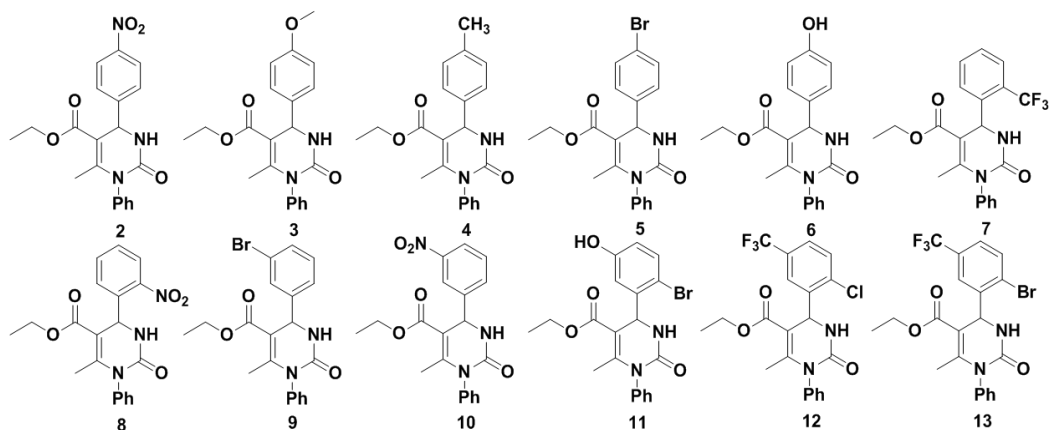


Figure 2.3 Structures of compounds 2-13

Biological evaluation has been conducted in collaboration with Professor Fabrizio Dal Piaz, Dr. Maria Carmela Vaccaro and Dr. Alessandra Russo of Salerno University.

2.3.1 Surface Plasmon Resonance assay

Once synthesized the compounds **2-13** were evaluated for their ability to interact with the recombinant Hsp90 α by a Surface Plasmon Resonance (SPR) based binding assay.^{266, 267} On the basis of this screening, 7 out of 12 tested compounds efficiently interact with the immobilized protein with low kinetic dissociation constant (K_D) values (**Table 2.1**). The lead compound **1** and the known Hsp90 inhibitor 17-*N*-allylamino-17-demethoxygeldanamycin (**17-AAG**)²⁶⁸ were used as positive controls. Checking the results obtained compounds **2-6**, **8** and **11** exhibit high affinity against the molecular chaperone with low K_D values in the nM range, ranging from 2.9 to 76.2 nM. Analyzing the data obtained, all the compounds synthesized using *p*-substituted aromatic aldehydes were able to interact with the molecular chaperone, showing an increased affinity compared **1** against Hsp90 except for **2**.

Exploration of the structural element of 3,4-dihydropyrimidin-2(1H)-ones (DHPM) core, driving toward more potent Hsp90 C-terminal inhibitors

Table 2.1 Thermodynamic constants measured by SPR for the interaction between tested compounds and immobilized Hsp90 α

Entry	K _D (nM)	Entry	K _D (nM)
1 ^a	75.6 ± 7	8	2.9 ± 0.8
2	76.2 ± 1.9	9	No Binding
3	17.6 ± 4.9	10	No Binding
4	13.0 ± 4.9	11	23.6 ± 0.7
5	12.0 ± 1.9	12	No Binding
6	3.7 ± 0.9	13	No Binding
7	No Binding	17-AAG ^{a,b}	388 ± 89

^a Data previously reported ^b 17-N-Allylamino-17-demethoxygeldanamycin

In addition, the presence of a nitro group at *ortho* position (compound **8**) increased the affinity toward the chaperone than in *para* position (compound **2**) (K_D 2.9 ± 0.8 nM and 76.2 ± 1.9 nM, respectively), while in the same position the trifluoromethyl group is not tolerated (compound **7**). Moreover, molecules synthesized with m-substituted aldehydes (compounds **9** and **10**) were inactive. Finally, the three products obtained by the *ortho-meta* disubstituted aromatic aldehydes showed a not homogenous results, indeed, compound **11** interacts with the immobilized Hsp90 α with a good affinity (K_D 23.6 ± 0.7 nM), whereas **12** and **13** were inactive.

In conclusion, this initial screening has highlighted the capacity of this second generation of DHPM derivatives to bind the immobilized protein.

2.3.2 Antiproliferative assay and Western Blot analysis

The new eight identified Hsp90 α binders (**2-6**, **8**, **11**) were investigated for their potential cytotoxic effect in A375 (human melanoma) and Jurkat (human leukemic) cell lines. The IC₅₀ values are reported in **Table 2.2**. The known C-

terminal inhibitor novobiocin and the *lead compound 1* were used as reference compounds in this assay.

Antiproliferative assay has proven the cytotoxic ability of this second generation of DHPM derivatives, identifying three new compounds **4**, **5** and **11**, endowed with moderate cytotoxic effects at micromolar concentration in both cancer cell lines.

Table 2.2 IC_{50} values of new binders, compound **1** and novobiocin on A375 and Jurkat cell lines

Entry	A375		Jurkat	
	IC_{50} (μ M) 24h	IC_{50} (μ M) 48h	IC_{50} (μ M) 24h	IC_{50} (μ M) 48h
2	-	-	-	-
3	-	-	-	86.1 \pm 0.9
4	-	-	51.2 \pm 0.8	40.3 \pm 0.6
5	85.1 \pm 0.8	74.2 \pm 1.1	55.0 \pm 0.6	43.5 \pm 1.0
6	-	-	-	-
8	-	-	-	-
11	81.0 \pm 1.2	70.5 \pm 1.4	21.3 \pm 0.9	15.2 \pm 1.1
Novobiocin	550.3 \pm 1.3	460.5 \pm 0.9	170.6 \pm 1.1	150.5 \pm 0.7
1^a	50.8 \pm 0.2		20.8 \pm 0.3	

^a Data previously reported

Interestingly how all compounds show a better antiproliferative profile than novobiocin and a comparable profile to that remarked for the lead compound **1**. Referring to human leukemic cell line the best result was obtained for **11**, whereas compounds **4** and **5** showed a comparable potency with an IC_{50} value around 50 μ M, compound **3** shows a moderate effect only after 48h of treatment. Finally, the DHPM derivatives **2**, **6** and **8** seem to have no effect on cell viability. Furthermore, these products haven't negative effect on PHA-stimulated proliferating PBMC, used as control non-tumor cell line, for which the percentage of non-viable cells after 24h of treatment was similar to that

observed control cells treated with DMSO. To establish that the cytotoxic effect pointed out by compounds **4**, **5** and **11** was associated with changes of the Hsp90 modulation, the expression levels of some Hsp90 client oncoproteins was verified in the same treated and untreated cell lines used in the antiproliferative assay, by western blot analysis (**Figure 2.4**).

Both cell lines were exposed for 24h to DMSO or **4**, **5** and **11** used at concentrations corresponding to the IC₅₀ values. Actin is not an Hsp90-dependent protein and that is why it has been used as control in the experimental.

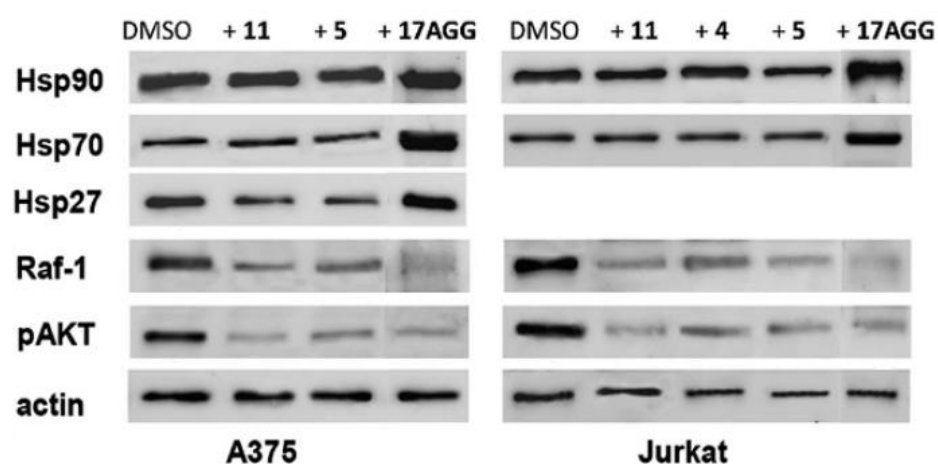


Figure 2.4 *Effect of compounds 4, 5 and 11 on Hsp90 client proteins levels in A375 and Jurkat cells. The shown blots are representative of three different experimental with similar results.*

Western blot analysis has shown that all tested compounds induced a strong down-regulation of Hsp90-dependent clients Raf-1 and p-Akt (about 60-80% less compared to untreated cells, by densitometric estimation). Notably, the exposure of compounds **5** and **11** in A375 and **4**, **5** and **11** in Jurkat cell lines did not cause any significant increase in the level of Hsp90, Hsp70 and Hsp27, evidencing that they did not trigger the undesired HSR, unlike the **17-AAG** which cause a marked up-regulation of Hsp90, Hsp70 and Hsp27 protein levels.

Furthermore, treatment with compounds **5** and **11** in A375 cell line for 24h has revealed a decrease in the Hsp27 protein levels, whereas, according with Sedlackova, *et al.*²⁶⁹ the Jurkat cell line was completely Hsp27 negative. These results confirm that the synthesized compounds **4**, **5** and **11**, as the reference lead compound, inhibit Hsp90 by modulation of the C-terminus

2.3.3 Molecular docking studies

Taken together the interesting biological results obtained by the dihydropyrimidin-2(1H)-scaffold and considering the poor number of synthetic products that modulate the Hsp90 activity at C-terminal domain, in collaboration with the research group of Professor Bifulco a computational study was performed in the attempt to explore the influence of these different substituents of the aromatic ring at position 4 on biological activity, leaving unchanged the other part of the molecule with respect to lead compound **1** (Figure 2.5).

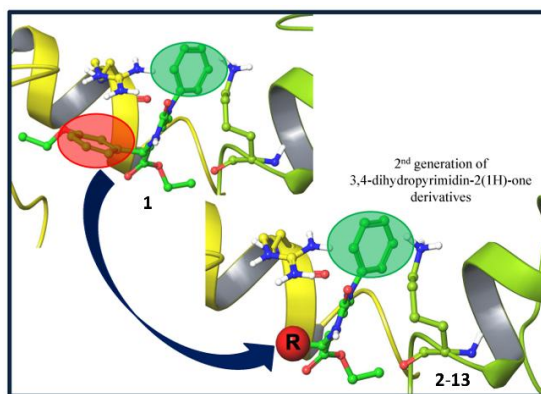


Figure 2.5 3D representation of binding mode of *compound 1* and new DHPM-based *compounds 2-13*.

This small set of molecules is closely linked to **1**, so referring to the same site and binding mode of lead compound **1** toward Hsp90,¹²⁹ an Induced Fit Docking protocol of Schrodinger Suite²⁷⁰ was used, considering the region at interface between the C-terminal chains of Hsp90 α homologue as the area of pharmacologic interest. The chosen model receptor for computational analyses

Exploration of the structural element of 3,4-dihydropyrimidin-2(1H)-ones (DHPM) core, driving toward more potent Hsp90 C-terminal inhibitors

was the ATP-bound active state of Hsp82, yeast homolog of Hsp90 α (PDB code: 2CG9),²⁷¹ and its sequence alignment with the human protein reported by Lee *et al.*²⁷² The key interactions with Arg591 and Lys594 were considered as fundamental to account the inhibitory activity for this kind of molecules. In more details, computational analysis highlight two different binding modes for products with mono or disubstituted aromatic ring at C4 position: (a) the first subset includes compounds having the two substitutions (*o*, *m*- position), **11-13**; (b) the second one regards compounds containing the *para* substitution **2-6**. Analyzing the computational results of compound **11**, the presence of disubstituted ring at C4 position directs efficiently the binding mode in the C terminal domain (**Figure 2.6A**).

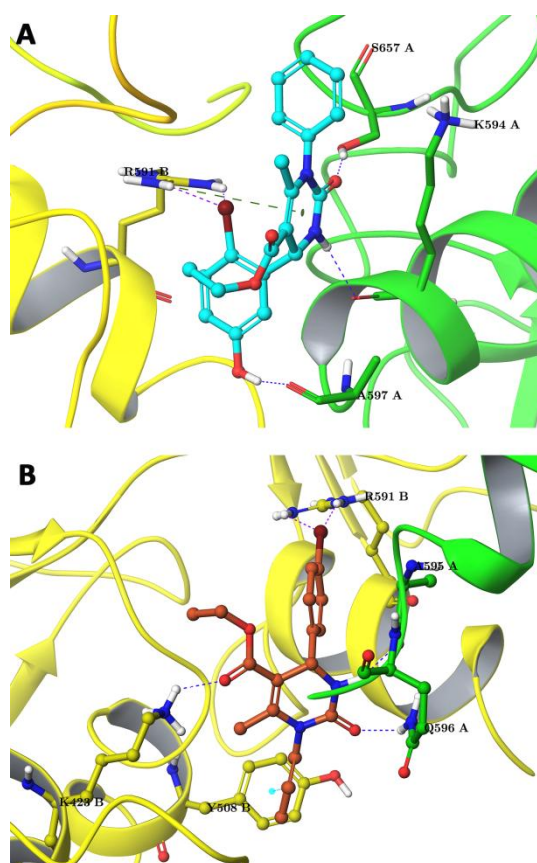


Figure 2.6 Three dimensional model of **11** (cyan sticks) and **5** (light brown sticks) in the Hsp90 C-terminal domain.

The bromide atom forms a crucial halogen bonds with the side chain of Arg591_{Chain B} and the hydroxyl group establishes a hydrogen bonds with backbone of Ala597_{Chain A}. Moreover, the dihydropyrimidin-2(1H)-one ring creates a π - π interaction with Arg591_{Chain B} and two hydrogen bonds with Ser657_{Chain A} and Lys594_{Chain A}. The key role of bromide atom on the aromatic ring at C4 is also confirmed by the biological profile exhibited for **5**, in which, it forms a halogen bonds with Arg591_{Chain B} (**Figure 2.6B**).

On the other hand, even if the bromide atom of compound **13** form a halogen bond with Ala597_{Chain A}, the CF₃ group decrease the affinity of molecule-target complex creating an ugly interaction with the key amino acid Arg591_{Chain B}.

The same trend is also observed for **12**, where the CF₃ group negatively affects its activity forming a bad interaction with the Lys423_{Chain B}. The high influence of the substitution of the aromatic ring at C4 position is also confirmed by the complete biological inactivity of **7**, in which the CF₃ group at *orto* position forms a bad interaction with key Arg591_{Chain B} drafting this group as not favorable in the design new Hsp90 C-terminal inhibitors. Considering the molecules **2-4** and **6** with *para* substitution (**Figure 2.7**), they show a good calculated interactions between the key aminoacids Arg591, Lys594 and the ring at C4.

These results showed the fundamental role of the decoration on the phenyl ring at C4 position, that strongly affect the modulation of Hsp90 activity, as showed from a not homogeneous (**4**, **5** vs **2**, **3** and **6**) profile in antiproliferative assay. In conclusion, structural studies have disclosed the halogen bonding between bromide atom and the side chain of Arg591_{Chain B} as a new key interaction suitable for the design of novel DHPM derivatives.

Exploration of the structural element of 3,4-dihydropyrimidin-2(1H)-ones (DHPM) core, driving toward more potent Hsp90 C-terminal inhibitors

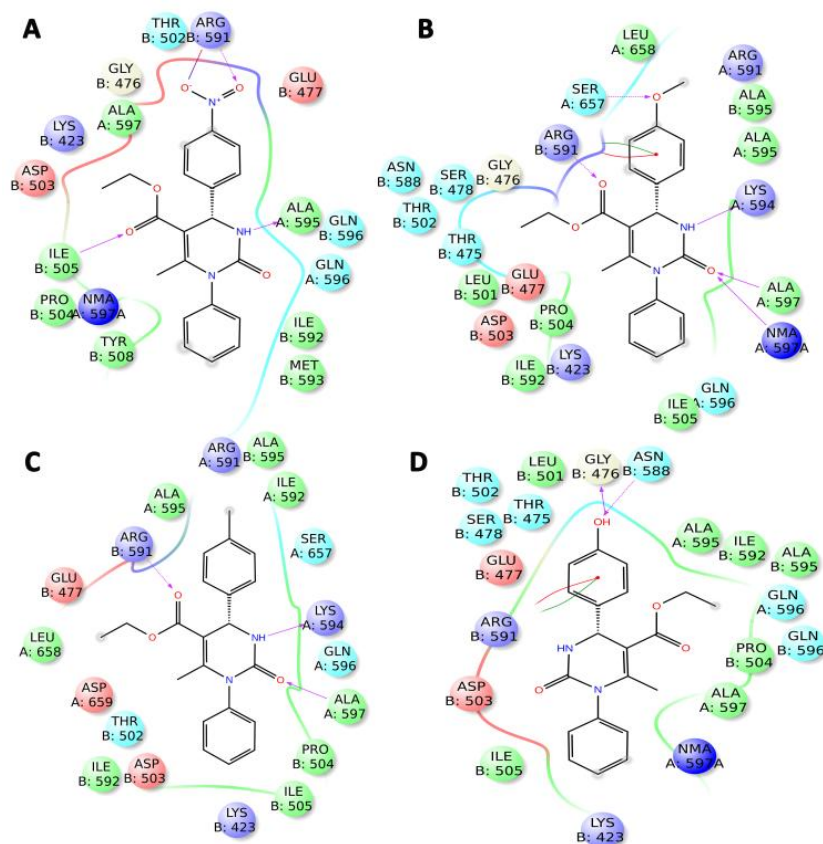


Figure 2.7 2D panels represent the interactions between 2 (A), 3 (B), 4 (C), 6 (D) and the residues of C-terminal Hsp90 binding site. Positive charged residues are colored in violet, negative charged residues are colored in red, polar residues are colored in light blue, hydrophobic residues are colored in green. The π - π stacking interactions are indicated as green lines, and H-bond (side chain) are reported as dotted pink arrows.

Moreover, these findings outline that only punctual changes at specific position on the aromatic ring at C4 position of Biginelli's scaffold are tolerated, reflecting a high sensitive steric environment within the C-terminal domain, and prompted us to further optimize the biginelli core in order to identify more powerful Hsp90 inhibitors.

2.4 Enhanced inhibitory activity of C-terminal Hsp90 domain through substitution of DHPM core at C2 position.

The data so far collected have underlined an highly sensitive steric environment within this protein domain. In light of the findings obtained, with the aim of expanding the investigation on the DHPM scaffold in order to identify more effective Hsp90 C-terminal inhibitors, a third collection was synthesized by expanding the functionalization at C2 position of the DHPM core, which was previously unexplored (**Figure 2.8**).

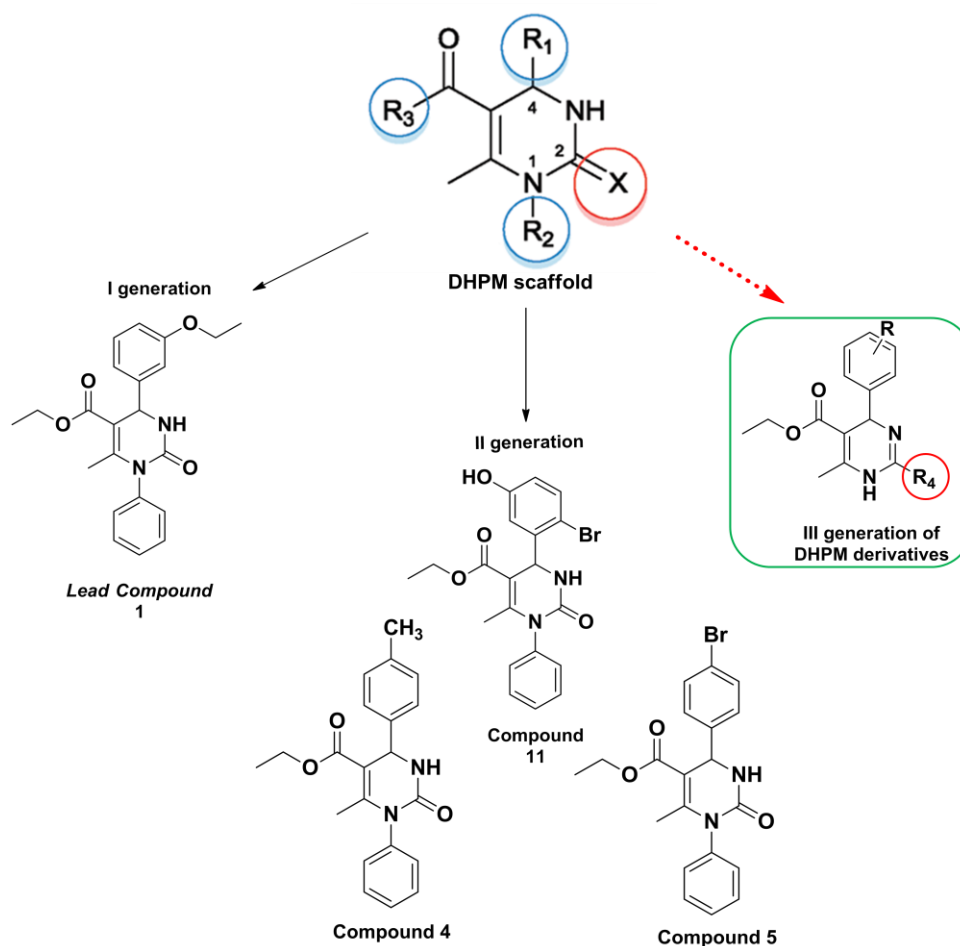


Figure 2.8 Evolution of DHPM derivatives as Hsp90 C-terminal inhibitors

The synthesis of this generation (compounds **15-22**, **Scheme 2.2**) has been achieved in high yields using a two step procedure, under microwave-heated conditions.

Briefly, in the first step were generated the dihydropyrimidine-2-thiones precursors **14a** and **14b** (**Scheme 2.2**) from the Biginelli reactions by means of the previously reported protocol, and subsequently, final desired compounds were obtained through a Liebeskind-Srogl cross-coupling.²⁷³⁻²⁷⁵

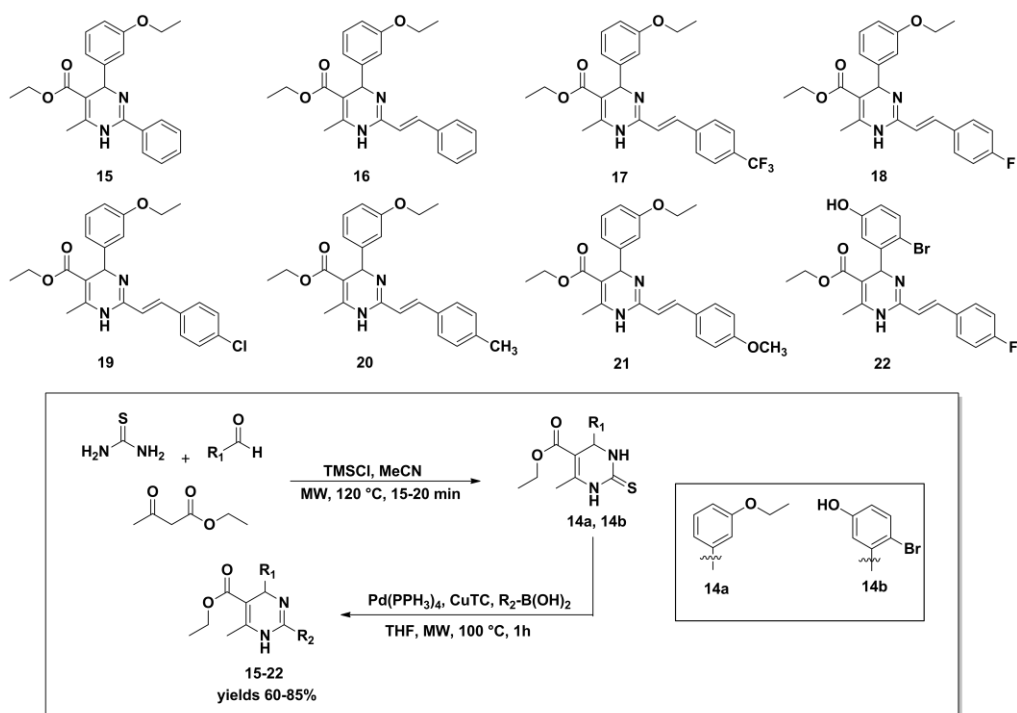
Liebeskind-Srogl reaction is a cross-coupling where a new carbon-carbon bond has been formed through the use of the palladium(0)-catalyzed, copper(I)-mediated reaction of a variety of different thioorganic products with boronic acids under neutral conditions.²⁷⁶⁻²⁷⁸

The disulfitative carbon-carbon coupling requires stoichiometric amounts of a copper(I) carboxylate, such as Cu(I)-thiophene-2-carboxylate (CuTC) as metal cofactor.²⁷⁹ This cross-coupling reaction is useful for scaffold decoration of heterocycles and it can be used to cyclic thioureas such as the dihydropyrimidine-2-thiones.²⁸⁰

Hence, this synthetic procedure was exploited to synthesize compounds **15-22**, using Tetrakis(triphenylphosphine)palladium(0) (Pd(PPh₃)₄) as palladium source, CuTC as copper(I) source and THF as solvent system, under microwave irradiation at 100 °C (**Scheme 2.2**).

Exploration of the structural element of 3,4-dihydropyrimidin-2(1H)-ones (DHPM) core, driving toward more potent Hsp90 C-terminal inhibitors

Scheme 2.2 Structures of 15-22 and synthetic procedure



Biological evaluation has been accomplished in collaboration with Dr. Maria Carmela Vaccaro, Dr. Alessandra Russo of Salerno University and Dr. Antonio Vassallo of Basilicata University.

2.4.1 Surface Plasmon Resonance assay

Compounds **15-22** were evaluated for the binding to the recombinant Hsp90 α by a Surface Plasmon Resonance (SPR)-based assay that give us a detailed view about their affinity toward the molecular chaperone. In **Table 2.3** have been shown the results obtained of this preliminary screening.

Table 2.3 Thermodynamic constants measured by SPR for the interaction between tested compounds and immobilized Hsp90 α

Entry	KD (nM)
15	No Binding
16	12.7 \pm 3.2
17	2.1 \pm 0.9
18	7.8 \pm 1.1
19	397 \pm 3
20	18.1 \pm 4.4
21	6.5 \pm 2.7
22	47.5 \pm 9.1
17-AAG^a	388 \pm 89
1^a	75.6 \pm 7

^a Data previously reported

In the second generation one can see the importance of the phenyl ring at N1 for the binding to the protein counterpart, and for this reason a directly analogue **15** has been synthesized. Interestingly to note the effect of the shifting of phenyl ring from N1 to the C2 position on the DHPM ring, in fact, SPR results indicated that analogue **15** did not binds to Hsp90 α . Afterwards, in order to evaluate if a spacing out between the scaffold and the aromatic ring could enhance the activity, compounds **16–22** have been designed and synthesized. Finally, SPR data showed that all tested compounds **16–22** bind to Hsp90 with low K_D values (**Table 2.3**), indicative of an optimal interaction with the chaperone protein.

2.4.2 Antiproliferative assay, Western Blot analysis and effect on cell cycle progression

The seven new identified Hsp90 α binders (**16-22**) were tested for their antiproliferative effect in A375 (human melanoma) and Panc-1 (human pancreatic carcinoma cell line), cells type of aggressive human cancers that usually acquire drug resistance in monotherapy. The amazing results obtained are shown in **Table 2.4**.

Table 2.4 IC_{50} values of 16-22 in A375 and Panc-1 cell lines after 24h of treatment

Compound	IC_{50} (μM) in A375	IC_{50} (μM) in Panc-1
16	2.5 \pm 0.2	5.3 \pm 0.1
17	2.2 \pm 0.1	5.0 \pm 0.2
18	2.1 \pm 0.3	5.1 \pm 0.2
19	3.5 \pm 0.3	6.0 \pm 0.3
20	8.7 \pm 0.2	14.5 \pm 0.2
21	7.1 \pm 0.1	10.0 \pm 0.1
22	4.2 \pm 0.2	11.5 \pm 0.2
17-AAG	2.1 \pm 0.3	>10

All tested compounds exhibited a strong increased antiproliferative potency compared with lead **1** (IC_{50} 50.8 \pm 0.2 μ M in A375). In particular, compounds **16-18** showed the highest potency with an IC_{50} values about 25 fold greater compared to lead compound **1** against both cancer cell lines. 17-AAG (17-(allylamino)-17-demethoxygeldanamycin), a well-known Hsp90 inhibitor, was used as a control in both cancer cell lines under the same experimental conditions. Moreover, no negative effect was observed for the above mentioned compounds in PHA-stimulated proliferating PBMCs, used as the control non-tumor cell line. In fact, the non-viable cells after 24 h of treatment with compounds **16-18**, used with concentrations close to IC_{50} values (about 9 \pm 1.2%, 8 \pm 1.5%, 9.5 \pm 1.8%, respectively), showed similar responses to that

observed in DMSO treated control cells (about $7 \pm 0.9\%$). As it was done with the second generation, to ascertain that the cytotoxic effect of these compounds were associated with changes in Hsp90 modulation, the level of expression of some Hsp90 client protein was verified in treated and untreated cancer cell lines, by western blot analysis using compound **18** as a representative compound of this new class of Hsp90-ligands (**Figure 2.9**).

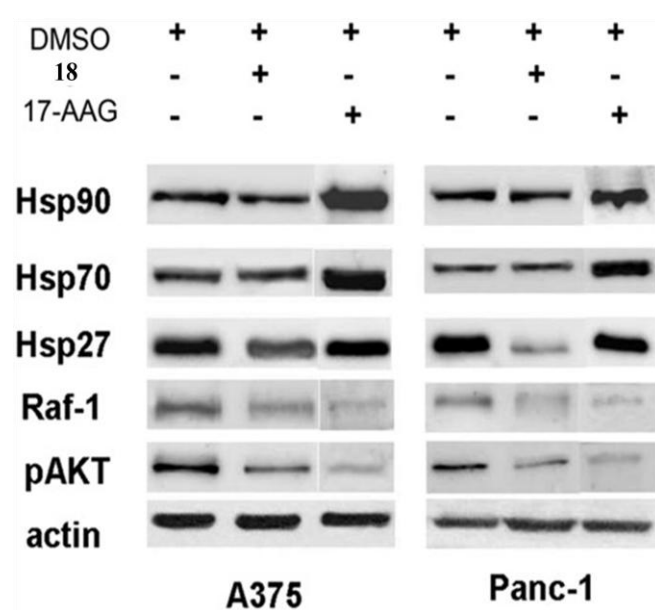


Figure 2.9 Western blot analysis of total cellular proteins, extracted 24 h after treatment with **18** (2 or 5 mM), using specific antibodies. Actin was used as a loading control. The blots shown are representative of three different experiments with similar results

Following 24h exposure to compound **18** (or **17-AAG** used as a positive control) causes a significant down-regulation of the expression levels of client protein Raf-1 and p-Akt in A375 and Panc-1 cell lines. Moreover, it is worth to note that exposure to compound **18** did not cause any alteration in the level of Hsp90, Hsp70 an Hsp27 in both cancer cell lines, this means that also this set of molecules did not induce the undesired HSR, unlike the N-terminal

ligand **17-AAG**. However, it is interesting to note the levels of Hsp27 was downregulated, Hsp27 prevents apoptosis and induces drug-resistance, so the depletion of this protein make these compounds as attractive candidates for drug development.

To further investigate the cytotoxic effects induced by the most potent compounds **16-18**, the cell cycle progression of treated cancer cells versus normal cell PHA-stimulated PBMC was analyzed, using flow cytometric analysis.²⁸¹ The A375, Panc-1 and PBMC cells were incubated for 24h or 48h with concentrations close to IC₅₀ values of **16-18**. The effects of these products were compared to the effect of **17-AAG** used at a concentration of 2 μ M in A375 and 2.5 μ M in Panc-1 cells, on the basis of a preliminary cell cycle distribution analysis with increasing concentrations of **17-AAG** (0.5–2.5 μ M) (data not shown).

Previous data reported that Panc-1 cells are poorly responsive to **17-AAG** after 24 h and the exposure to 0.5 μ M **17-AAG** did not cause any change in the cell cycle distribution.²⁸² Cell cycle distribution analysis indicated that **18** induced different responses from **17-AAG** depending on the cell type. Indeed, after exposure of **18** the A375 cells were mainly arrested in the G2/M phase of the cycle after 24 h and 48 h, with a moderate increase of the subG0/G1 DNA content after 48 h, indicative of apoptotic/necrotic cell death (**Figure 2.10A**). Conversely, the **18**-treated Panc-1 cells were accumulated in the S and G2/M cell cycle phases, with a 13% fraction of subG0/G1 cells after 48 h (**Figure 2.10B**).

Moreover, **16** and **17** showed a similar effect on the cell cycle status but gave a smaller fraction of subG0/G1 cells after 48 h (**Figure 2.10C, D**). These products did not exhibit any pro-death or cytostatic activity in PHA-stimulated proliferating PBMC (data not shown).

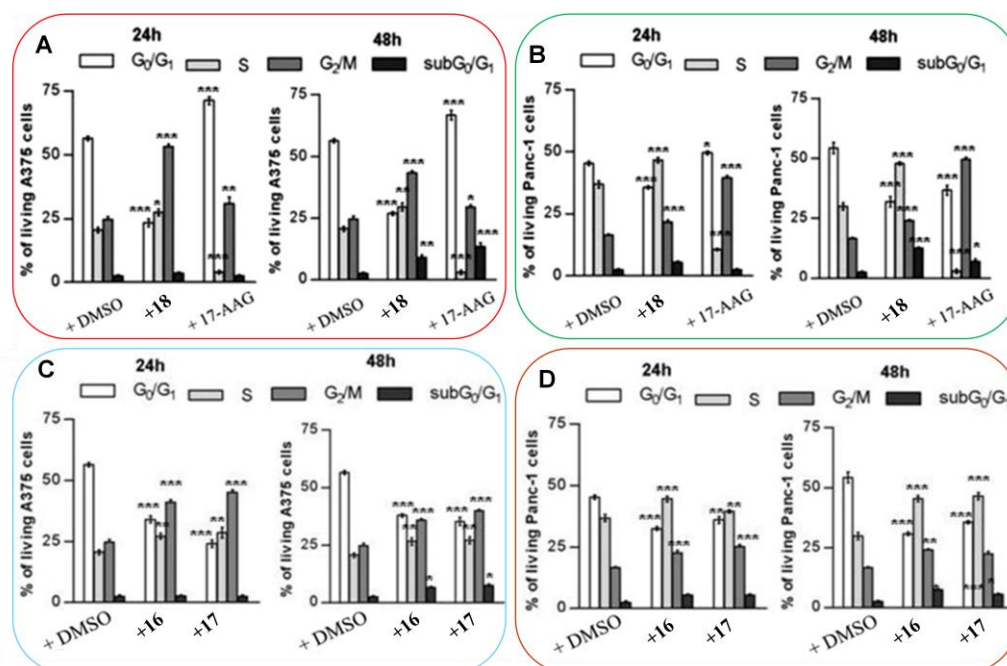


Figure 2.10 Effect of compound **18**, **16** or **17** on cell cycle distribution in A375 and Panc-1 cells. Quantification of cell cycle distribution of viable A375 (A, C) or Panc-1 (B, D) cells treated with DMSO, compound **18**, **16** or **17** (2 or 5 μ M, respectively) or 17-AAG (2 or 2.5 μ M, respectively) for 24 h, S13 evaluated by PI staining. Results are expressed as means \pm SD of three independent experiments, performed in duplicate (***P < 0.001, **P < 0.01, *P < 0.05 versus control).

2.4.3 Study of Hsp90 α /18 interaction

With the aim of identifying the Hsp90 α region involved in the binding of **18**, a limited proteolysis-mass spectrometry-based technique in analyzing the Hsp90 α /**18** complex was employed. The efficiency of this technique, in the investigation of Hsp90 α /inhibitor interaction, relies on the evidence that exposed, weakly structured and flexible regions of a target protein can be recognized by a proteolytic enzyme and, therefore, the observed differences in the proteolytic patterns, in the presence or in the absence of a putative protein ligand, can be useful to identify the protein regions involved in the molecular interactions.^{127, 283, 284} The proteolytic patterns obtained both on Hsp90 α and

on the Hsp90 α /**18** complex, using trypsin or chymotrypsin as proteolytic agents, are summarized in **Figure 2.11**. Comparing the differential peptides derived from the digestion of native Hsp90 α or of the Hsp90 α /**18** complex, by mass spectrometry analysis, confirmed a direct interaction between **18** and the chaperone and it was compared to Hsp90 α /novobiocin complex.

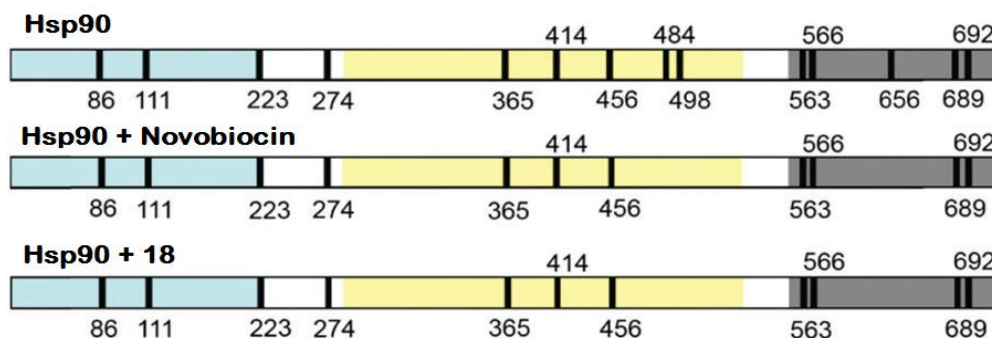


Figure 2.11 Schematic representation of limited proteolysis experiments. The preferential cleavage sites detected on recombinant Hsp90 α , Hsp90 α /novobiocin and Hsp90 α /**18** complexes are indicated in black. The Hsp90 α N-terminal domain is highlighted in light blue, the middle domain is highlighted in yellow and the C-terminal domain is highlighted in grey.

Indeed, it was observed that the peptide bonds following Lys484, Lys498 and Lys656, preferential cleavage sites of the native chaperone in absence of **18**, were protected in the complex, thus indicating that the middle and C-terminal domain of Hsp90 α are likely involved in the ligand binding. In addition, the conformational changes of Hsp90 induced by compound **18** are similar to the cleavage sites detected on Hsp90 α /novobiocin, a well known Hsp90 C-terminal inhibitor used as an internal reference.²⁸⁵⁻²⁸⁷

2.4.4 Molecular docking studies

In order to rationalize the biological effects of this new set of DHPM derivatives, molecular docking studies between **16–22** and Hsp90 α proteins was performed.

As mentioned before, a yeast Hsp90 α homologue (PDB code: 2CG9)²⁷¹ was used as a model receptor and its sequence alignment with the human protein, reported by *Lee et al.*,²⁷² was used as the reference during the comparative experimental–computational analysis. Considering the high plasticity of the Hsp90 during its mechanism of action, we have used the Induced Fit Docking protocol of the Schrödinger Suite²⁷⁰ was employed to account for both ligand and receptor flexibility.²⁸⁸ Starting from biological evaluation reported above, the region at interface between the C-terminal chains of Hsp90 α homologue was considered as the area of pharmacologic interest.^{127, 289} As already mentioned, small structural modifications on the heterocyclic core have caused a shift of the site of interaction; in more detail, besides Lys640, other positively charged amino acids such as Arg628 and Arg670 also play a fundamental role in the binding of these new Hsp90 C-terminal inhibitors. In fact, the aromatic ring at C2 of **18** (**Figure 2.12**), **16** (**Figure 2.13**), **20** and **21** (**Figure 2.15**) positively interacts with Arg628_{Chain A}, while the phenyl ring of **22** interacts with Arg670_{Chain A} (**Figure 2.15**). Moreover, except for **15**, the inactive one, the other molecular portions of **16–22** also form hydrogen bonds with Asp641_{Chain A} and Thr638_{Chain A} (**Figure 2.12, 2.13, 2.14** and **2.15**), contributing to the stability of the ligand–target complexes. In summary, the exact distances of the aromatic portion at C2 from the central core, in association with the best substituents on the phenyl ring at C4 position of DHPM core, identified from the results of the first generation (compound **1**) and second generation (compound **11**), allowed to discovery the most active Hsp90 C-terminal inhibitors among these three series. This new generation, in

Exploration of the structural element of 3,4-dihydropyrimidin-2(1H)-ones (DHPM) core, driving toward more potent Hsp90 C-terminal inhibitors

fact, showed a remarkably increased of potency against A375 and overall against Panc-1 cancer cell lines, the more aggressive type of human tumors, highlighting the efficacy of Biginelli's scaffold as a privileged structure to obtain new leads in the drug discovery process.

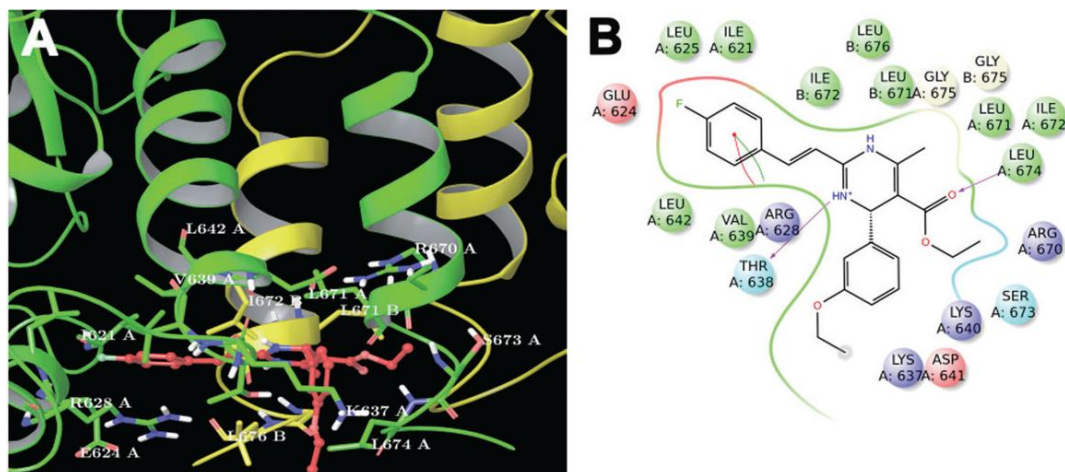


Figure 2.12 Three dimensional (panel A) and bi-dimensional (2D) (panel B) diagrams of interactions of **18** with the C-terminal domain of the HSP82 yeast analogue of Hsp90a (PDB: 2CG9). Positively charged residues are colored in violet, negatively charged residues are colored in red, polar residues are colored in light blue, and hydrophobic residues are colored in green. The p-p and cation-p stacking interactions are indicated as green and red lines, and H-bonds (side chains) are indicated as dotted pink arrows. Illustrations of the 2D and 3D models were generated using Maestro software.²⁹⁰

Exploration of the structural element of 3,4-dihydropyrimidin-2(1H)-ones (DHPM) core, driving toward more potent Hsp90 C-terminal inhibitors

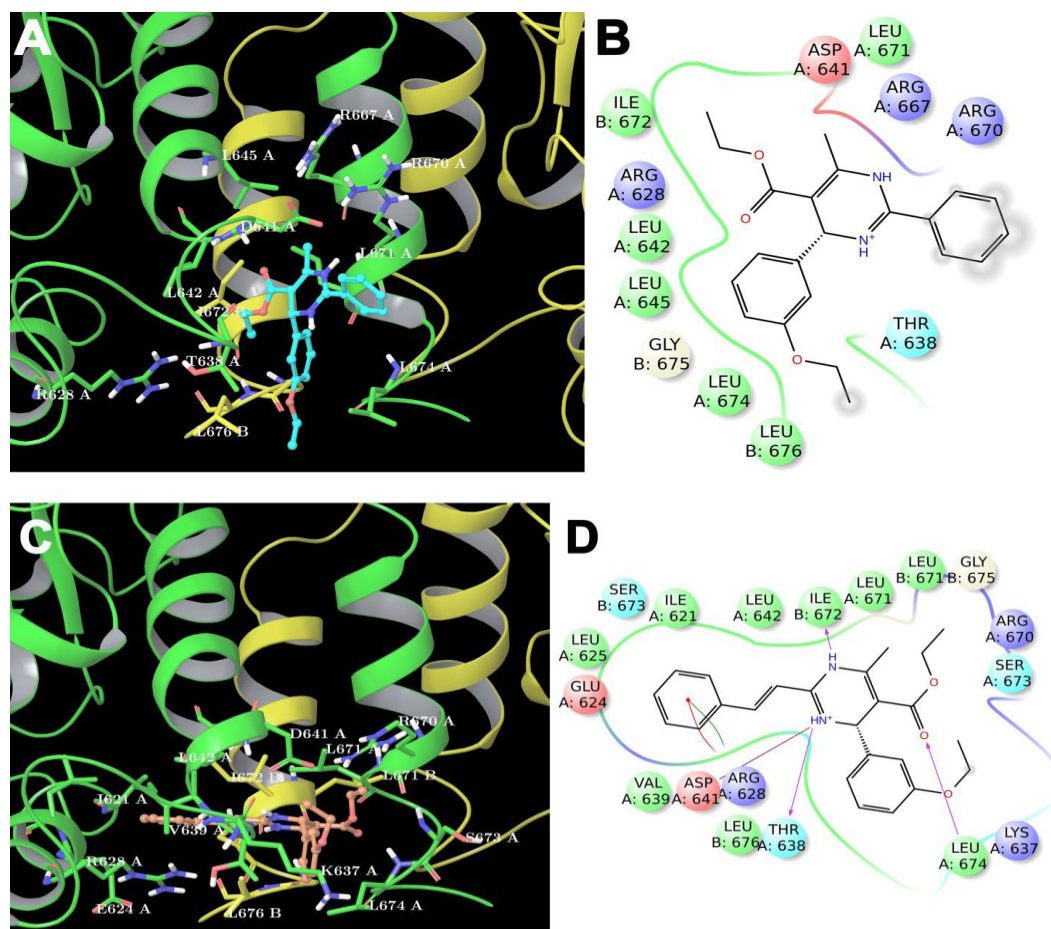


Figure 2.13 Three dimensional models (panel A and C) and 2D diagram interactions (panel B and D) of **15** (cyan) and **16** (orange) with C-terminal domain of HSP82 yeast analogue of Hsp90 α (PDB: 2CG9). In the panels A and C, the protein is reported as colored ribbons: chain A is depicted in green and chain B is depicted in yellow. The aminoacids interacting with each ligand are reported in green (chain A) and yellow (chain B) sticks. In the panels B and D, positive charged residues are colored in violet, negative charged residues are colored in red, polar residues are colored in light blue, hydrophobic residues are colored in green. The π - π stacking interactions are indicated as green lines, and H-bond (side chain) are reported as dotted pink arrows.

Exploration of the structural element of 3,4-dihydropyrimidin-2(1H)-ones (DHPM) core, driving toward more potent Hsp90 C-terminal inhibitors

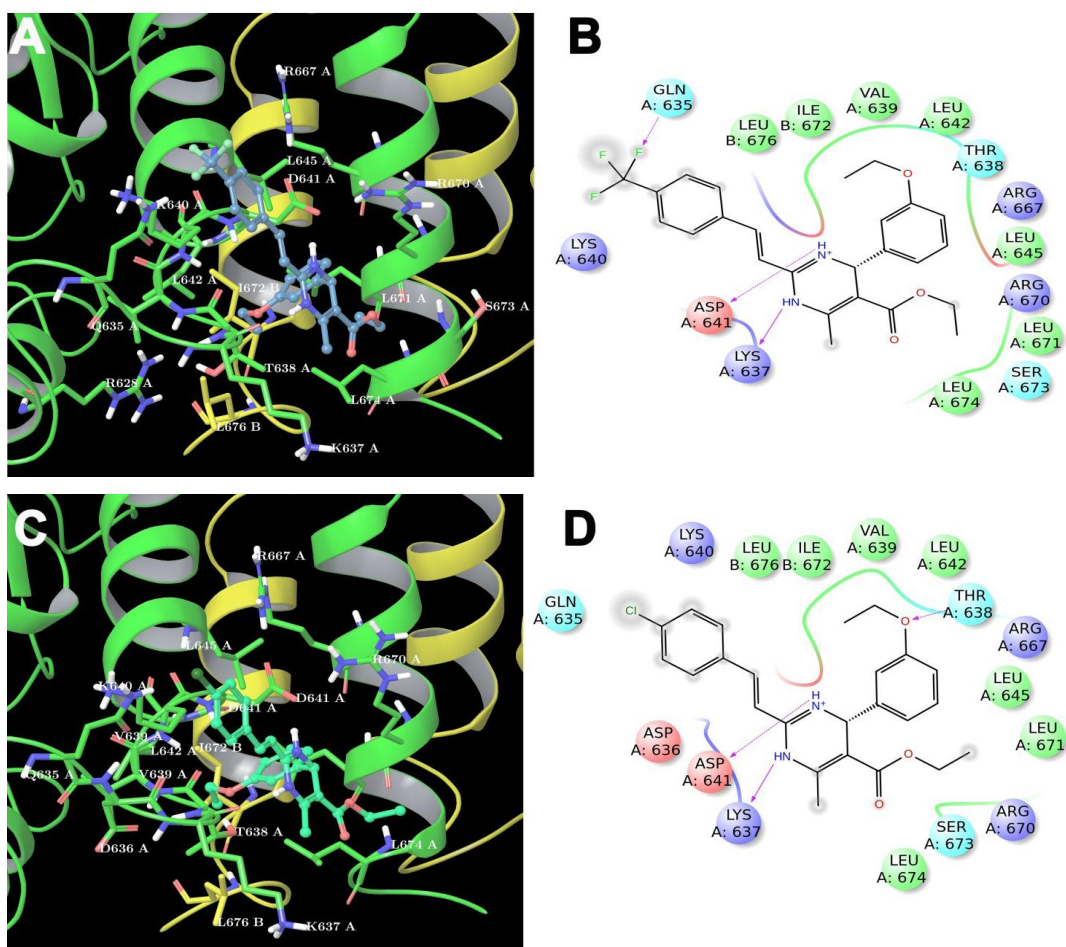


Figure 2.14 Three dimensional models (panel A and C) and 2D diagram interactions (panel B and D) of **17** (blue) and **19** (light green) with C-terminal domain of HSP82 yeast analogue of Hsp90 α (PDB: 2CG9). In the panels A and C, the protein is reported as colored ribbons: chain A is depicted in green and chain B is depicted in yellow. The aminoacids interacting with each ligand are reported in green (chain A) and yellow (chain B) sticks. In the panels B and D, positive charged residues are colored in violet, negative charged residues are colored in red, polar residues are colored in light blue, hydrophobic residues are colored in green. The π - π stacking interactions are indicated as green lines, and H-bond (side chain) are reported as dotted pink arrows.

Exploration of the structural element of 3,4-dihydropyrimidin-2(1H)-ones (DHPM) core, driving toward more potent Hsp90 C-terminal inhibitors

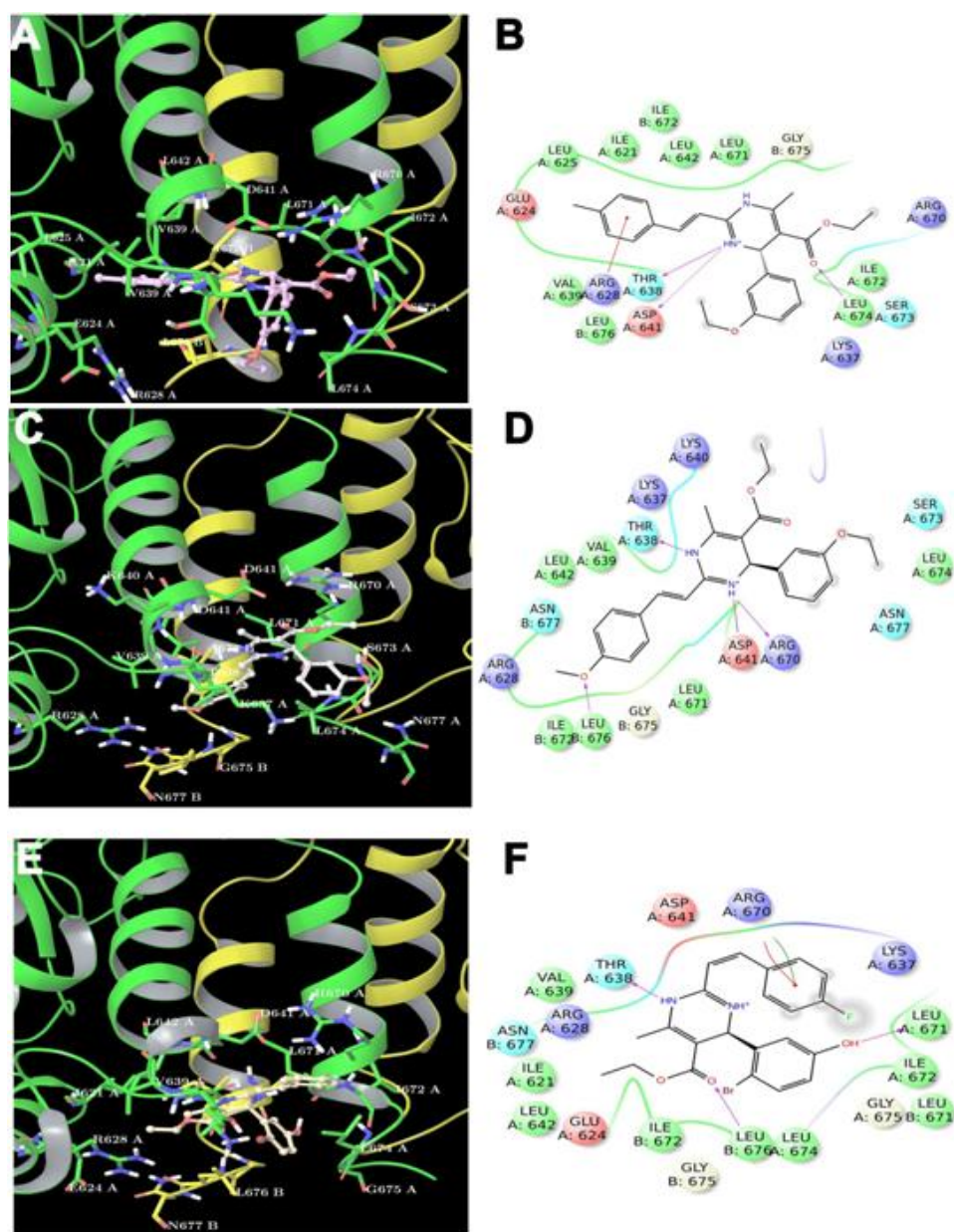


Figure 2.15 Three dimensional models (panel A, C and E) and 2D diagram interactions (panel B, D and F) of **20** (pink), **21** (white), and **22** (beige) with C-terminal domain of HSP82 yeast analogue of Hsp90 α (PDB: 2CG9). In the panels A, C and E, the protein is reported as colored ribbons: chain A is depicted in green and chain B is depicted in yellow. The aminoacids interacting with each ligand are reported in green (chain A) and yellow (chain B) sticks. In the panels B, D and F, positive charged residues are colored in violet, negative charged residues are colored in red, polar residues are colored in light blue, hydrophobic residues are colored in green. The π - π stacking interactions are indicated as green lines, and H-bond (side chain) are reported as dotted pink arrows.

- CHAPTER 3 -

*Targeting mPGES-1: design and synthesis of promising inhibitors
as new anti-inflammatory agents*

3.1 Why mPGES-1?

With the term anti-inflammatory defined each substance or treatment that reduces inflammation or swelling. Nowadays, the most widely used class in anti-inflammatory therapy are the Nonsteroidal anti-inflammatory drugs (NSAIDs), that act suppressing the biosynthesis of prostaglandins (PGs) through the activity inhibition of cyclooxygenases (COX-1/2).²⁹¹ Prostaglandins are bioactive mediators involved in key physiological functions but also in several other pathologic conditions, such as tumorigenesis.²⁹² As described before, is noteworthy the correlation between inflammatory events and the development of pre-cancerous lesions at various anatomic sites. Proliferation, invasion and migration processes are promoted by inflammatory events and, indeed, the identification of new anti-inflammatory drugs could be synergic in the context of anticancer pharmacological strategies.²⁹³ However, the side effects caused by anti-inflammatory drugs currently available such as cardiovascular, gastrointestinal and renal side,²⁹⁴ make the development of safer alternatives especially for long-term therapies more required.^{295, 296} In this scenario, drugs that targeting mPGES-1 represent valuable approach for the development of new anti-inflammatory/anticancer agents with reduced side effects. Indeed, mPGES-1 is responsible for the biosynthesis of inducible PGE₂ as a response to inflammatory stimuli²⁹⁷ and it doesn't affect on the constitutive levels of PGE₂ involved in crucial physiological functions. Today there are two main strategies employed in the modulation of mPGES-1 activity. The first consists in the negative modulation of its expression, while the second one concerns the direct and selective inhibition of the enzyme. Scientific community focused the attention on this promising target with the aim of developing products able to act either directly on the enzyme or to affect its expression. therefore, some structurally different molecules able to potently inhibit mPGES-1 activity have been developed.

3.2 Looking for new molecular platforms

In literature there are various templates able to inhibit mPGES-1 activity, our attentions has been targeted on two molecular platforms: the 5-Pyrazolone and the carbazole motifs, afterwards by carbazoles compounds was obtained a third collection of molecules with a biaryl motif. The chosen chemical motifs was made through a careful search based on various inhibitors of the receptor counterpart,^{136, 179, 188, 298} in addition, these scaffolds represent “privileged structures” because they were interact with different biological targets.^{299, 300}

3.2.1 Design and synthesis of 5-Pyrazolone compounds

For the construction of the virtual 5-pyrazolone compounds library was used CombiGlide software, a powerful software which allows to build in silico combinatorial libraries of compounds in automated manner and in a short time, starting from a scaffold (5-pyrazolone) of departure that will be replaced by user in specific positions.

For the realization of the library have been downloaded from the Sigma-Aldrich database, 3012 aryl aldehydes, 23 arylhydrazines and 19 β -ketoesters. After that, with *reagent preparation*, a CombliGlide application that splits the various substituents on the basis of their functional group and also it allows to choose the part of the molecule that will bind the scaffold, the chosen building blocks were used as substituents of the 5-pyrazolone scaffold. Position 1 of the initial scaffold was substituted with the collection of the 23 arylhydrazines, position 3 with the collection of 19 β -keto esters and finally, position 4 with the collection of 3012 arylaldehydes, thus generating all possible combinations.

After the construction of the virtual library, the compounds have been filtered using ADME/tox (absorption, distribution, metabolism, excretion and toxicity) filtering in

Targeting mPGES-1: design and synthesis of promising inhibitors as new anti-inflammatory agents.

an attempt to work with databases of molecules with acceptable physical properties and chemical functionalities. In these perspectives has been used a Qikprop software, called Lipinski filter in order to eliminate the products "non-drug-like". The drug-like compounds were then subjected to the structure-based virtual screening towards mPGES-1, through the "Virtual screening workflow" form of the Schrödinger LLC.²⁷⁰ Finally, the final products were chosen taking into account the docking score, selecting only those promising compounds with excellent predicted affinity towards the biological target (binding energy values of -8.0 kcal / mol) (**Figure 3.1**).

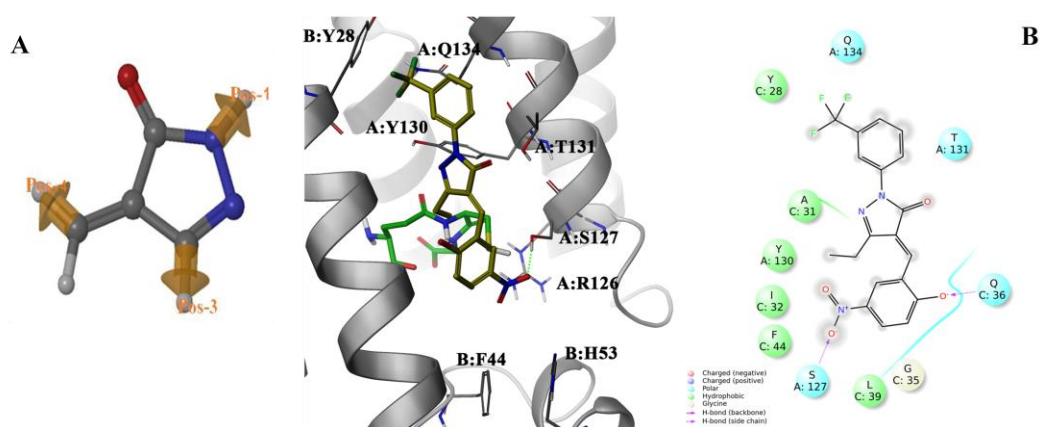
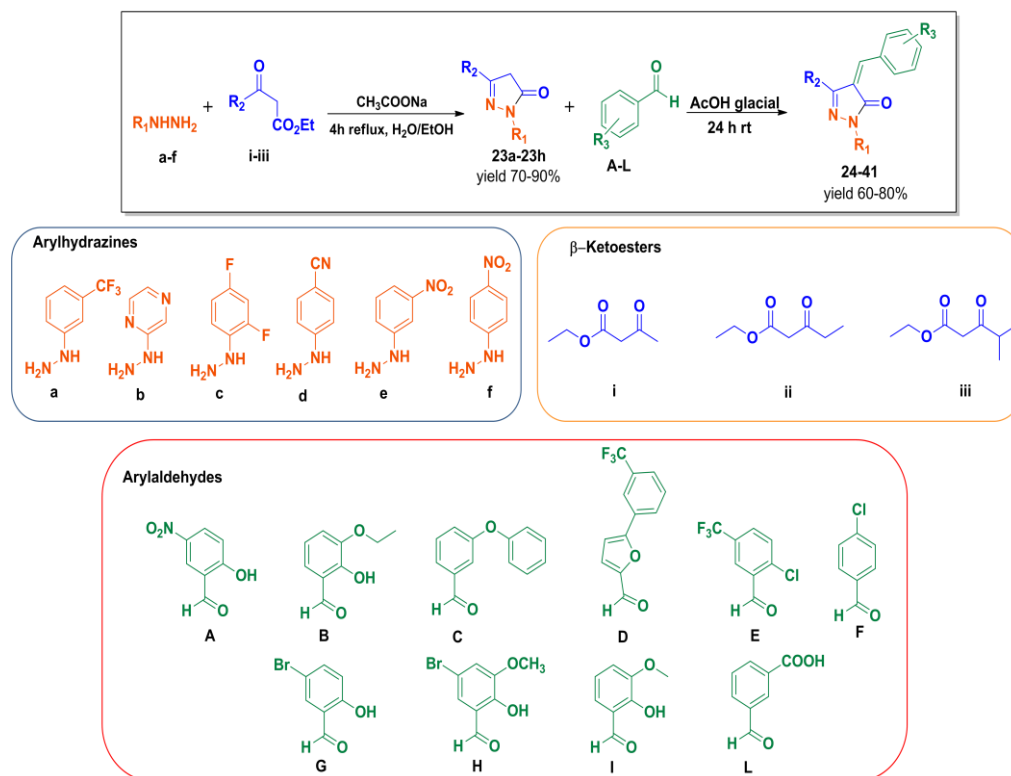


Figure 3.1 (A) Graphical interface of the software CombiGlide (B) representative binding mode of 4-arylidene-1,3-disubstituted-5-pyrazolone.

The pyrazol-5-one compounds was synthesized in two-step procedure: firstly, the 1,3-disubstituted-5-pyrazolones precursor **23a-23h** were produced by refluxing in a mixture of water and ethanol using a tandem condensation and thermal cyclization between arylhydrazines (**a-f**) and appropriate β -ketoesters (**i-iii**) with a small amount of sodium acetate, subsequently, final desired 4-arylidene-1,3-disubstituted-5-pyrazolone compounds **24-41** were obtained taking in advantage a reactive methylene group that react at C4 position with arylaldehydes (**A-L**) (**Scheme3.1**).

Targeting mPGES-1: design and synthesis of promising inhibitors as new anti-inflammatory agents.

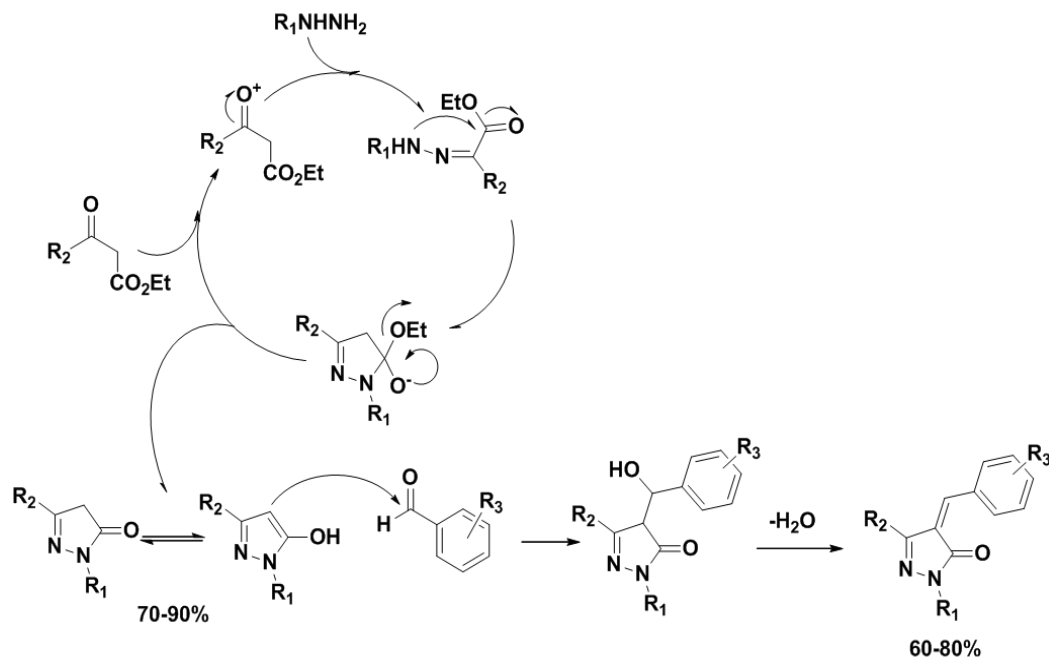
Scheme 3.1 General synthetic procedure for the synthesis of compound **24-41** and structures of the building blocks used to generate the 4-arylidene-1,3-disubstituted-5-pyrazolones.



Several workers reported that the condensation of 1,3-disubstituted-5-pyrazolones with aromatic aldehydes were performed in the presence of a catalyst (ethylenediammonium diacetate (EDDA),³⁰¹ magnesium oxide (MgO),³⁰² lithium bromide,³⁰³ potassium fluoride,³⁰⁴ or triethylamine³⁰⁵), for these compound glacial acetic acid was used.³⁰⁶

Targeting mPGES-1: design and synthesis of promising inhibitors as new anti-inflammatory agents.

Scheme 3.2 Reactions mechanism of 4-arylidene-1,3-disubstituted-5-pyrazolone compounds.



In collaboration with professor Oliver werz of Friedrich Schiller University (Germany), the interference of the synthesized 4-arylidene-1,3-disubstituted-5-pyrazolones on mPGES-1 activity was investigated in a cell-free assay using the microsomal fraction of interleukin-1 β -stimulated human A549 cells. The tested compounds (**Figure 3.2A**) in most cases showed a moderate inhibitory activity against mPGES-1. In particular, mPGES-1 remaining activity, after treatment with 10 μ M of **24-41**, was no effected in all the case, except for products **24** and **33** which manifested to inhibit the enzyme of about 45% and 50% (**Figure 3.2B**).

Targeting mPGES-1: design and synthesis of promising inhibitors as new anti-inflammatory agents.

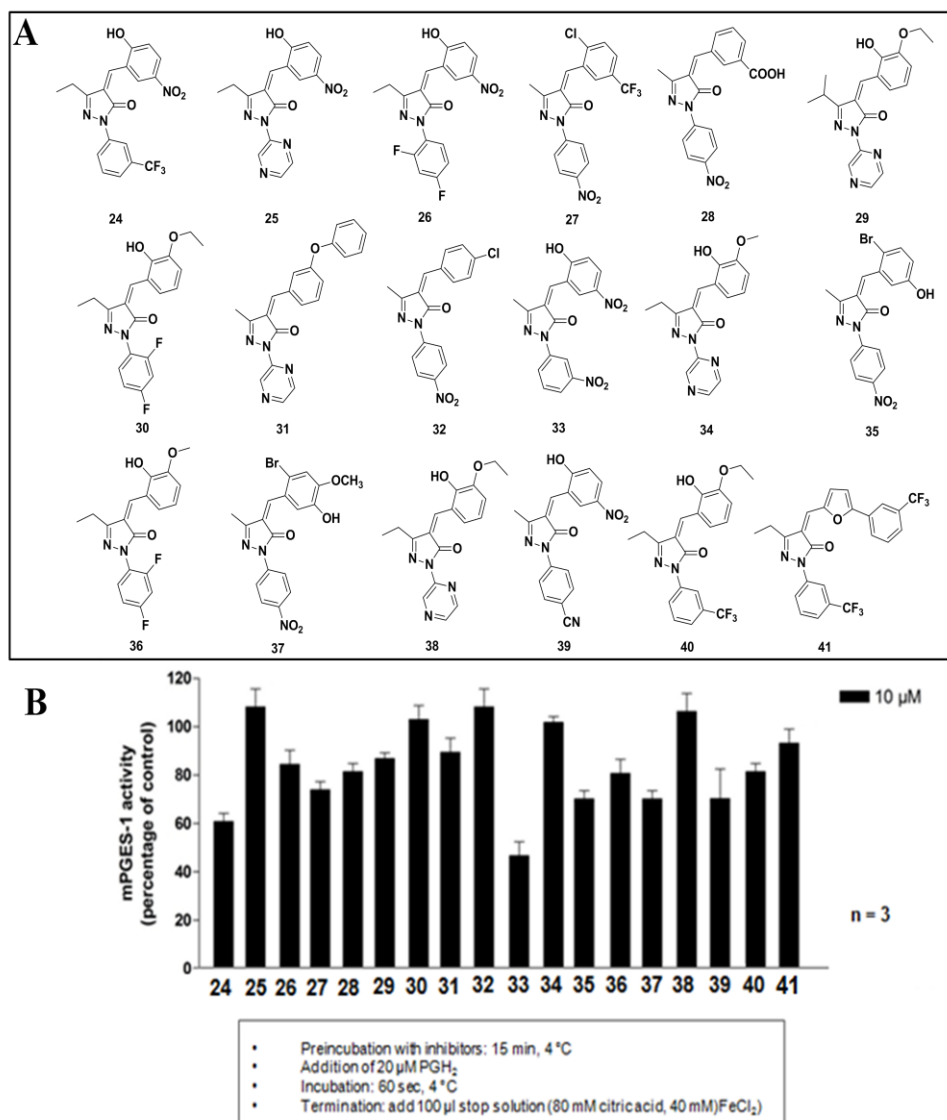


Figure 3.2 (A) Structures of compounds 24-41 (B) Effect of compounds 24-41 on the mPGES-1 activity. Experiments were performed in triplicate.

Nevertheless, since the maximal inhibition value was lower than 50%, the IC₅₀ values could not be obtained.

3.2.2 Design and synthesis of Carbazole compounds

Starting from the well-known inhibitor of mPGES-1 with carbazole core,¹⁵⁹ a small group of 2-trifluoromethyl-7(or 5)-substituted-carbazole compounds were designed. The synthesis of carbazole compounds recently have gained considerable interest, due to their widespread applications as light-emitting devices,³⁰⁷ conjugate polymers,³⁰⁸ dendrimers,³⁰⁹ etc. In addition, there has been much interest on the biological activities of the carbazole analogues in recent years and a great number of carbazole alkaloids has been isolated and synthesized.³¹⁰ Furthermore, the synthesis of aromatic fused systems like benzo- and indolocarbazoles, have found a rapidly increasing interest of the pharmaceutical industry due to their versatile and potent, but still scarcely explored, biological activities. Chemically the carbazole skeleton (**Figure 3.3**) is a modest nucleophile that can be readily functionalized with a wide variety of electrophiles (tertiary alkyl, acyl, nitro, halogen, etc.).³¹¹⁻³¹⁴

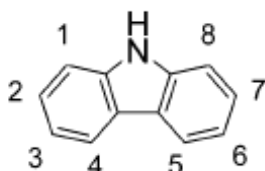


Figure 3.3 Structure of carbazole ring system

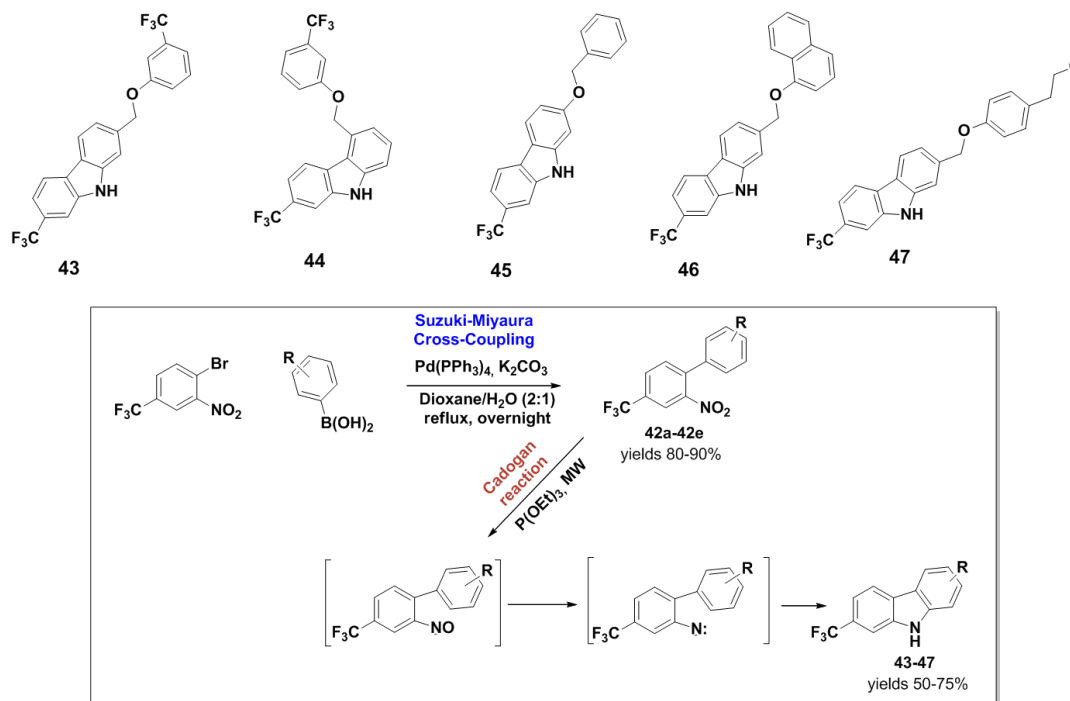
Electrophilic substitution reacts preferentially on the 3 and 6 position (more reactive) and to a lesser extent, the 1 and 8 positions, which often require more drastic reaction conditions. When we want to functionalize the 2, 4, 5, or 7 ring positions, or when mono and/or asymmetrical substitution patterns are desired, and/or when functional groups not easily introduced by electrophilic substitution are needed, other synthetic procedures are indispensable.³¹⁵ Fortunately several methods exist for the synthesis of carbazoles, however, the

majority of the work concerning the synthesis of carbazoles derivatives is based on the phosphite-mediated Cadogan reductive cyclization of the corresponding 2-nitrobiaryls.³¹⁶⁻³¹⁸

This synthetic method has a number of advantages which include increased substrate scope and functional group tolerance, and more precise regiocontrol of functional group placement within the product. However, this nitrene-mediated reductive cyclization procedure often demands drastic conditions and long reaction times, making it a less-favored synthetic method. Today, microwave irradiation has emerged as a valuable tool in organic chemistry,³¹⁸⁻³²⁰ in fact, when the reactions are carried out under microwave irradiation, improvements in yields and reduction in reaction times are often observed. In particular, the synthesis of these molecules were performed in two-step tandem procedures: a Suzuki–Miyaura cross-coupling reaction between 1-bromo-2-nitro-4-(trifluoromethyl) benzene and appropriate phenylboronic acids in order to produce the 2-nitrobiaryl precursors **42a-42e**, subsequently, final desired carbazoles **43-47** were obtained through a microwave-assisted Cadogan reductive cyclization. The reaction is commonly conducted using an excess of P(OEt)₃ (triethyl phosphite), as both the reductant and reaction solvent, under microwave irradiation at a maximum irradiation power of 300 W for 15 min at a pre-selected temperature of 210 °C (**Scheme 3.3**).

Targeting mPGES-1: design and synthesis of promising inhibitors as new anti-inflammatory agents.

Scheme 3.3 Structures of carbazole compounds 43-47 and synthetic strategies



As mentioned above, interference of the carbazole products with mPGES-1 activity was investigated in a cell-free assay, using the microsomal fraction of interleukin-1 β -stimulated human A549 cells. Unfortunately also for this collection of compounds have not shown inhibit the mPGES-1 activity after treatment with 10 and 1 μ M of **43-47**, so an IC₅₀ value could not be obtained (Figure 3.4).

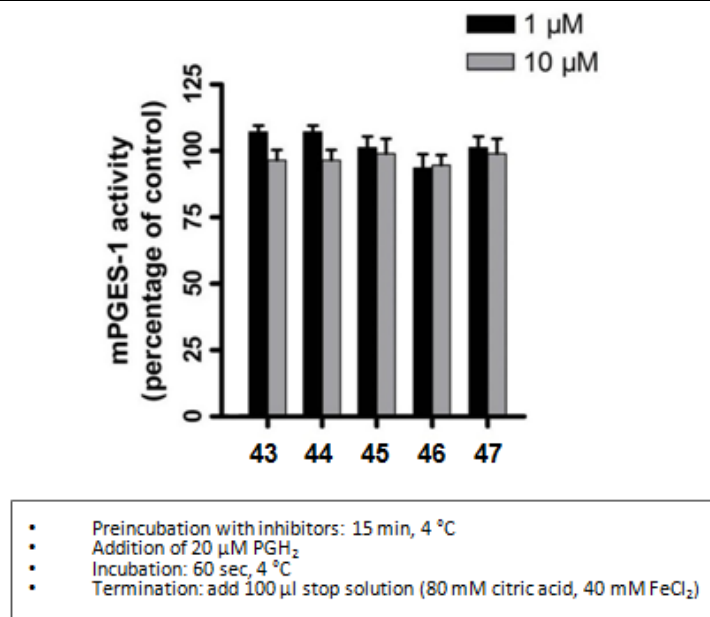


Figure 3.4 Effect of compounds **43-47** on the activity of mPGES-1. Experiments were performed in triplicate.

Looking the results obtained by the two classes of molecules synthesized is right to draw some conclusions. In the case of 4-arylidene-1,3-disubstituted-5-pyrazolones the data were not in accordance with modeling predictions, thus suggesting that the rational design made was not enough.

While in the case of carbazole compounds the substitution with variously decorated benzyloxy groups in position 7 (or 5) is arguably not useful. In order to understand the binding mode of these products and rationalize the results obtained a molecular docking study was needed. Actually, this study showed how the products are not able to interact with receptor counterpart, in fact as shown in Figure 3.5, the representative carbazoles **43** and **46**, fail to create good interactions with active site of mPGES-1, probably this happens for the planar carbazole ring system that does not allow good accommodation of the functional groups within the active site of mPGES-1.

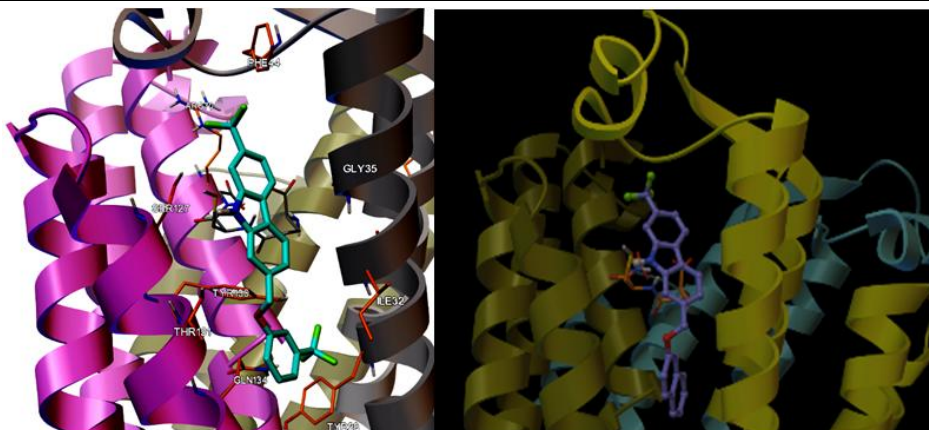
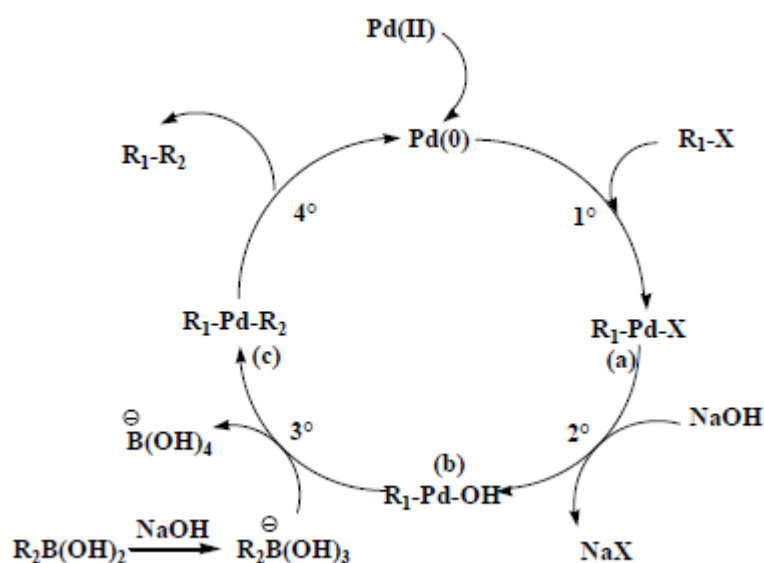


Figure 3.5 Binding mode of **43** and **46** in the active site of mPGES-1.

3.2.3 Design, synthesis and biological evaluation of Biaryl compounds

Therefore, starting from the assumption described before and with the purpose of optimize the few results obtained until now a collection of biaryl compounds has been designed. In order to synthesize the biaryl compounds a Suzuki-Miyaura cross-coupling reaction has been used. The Suzuki-Miyaura reaction is widely used for the construction of a C-C bond, because the building block used in this reaction are easy to handle and the experimental procedure is very simple. This reaction involving the coupling of an organoboron reagent and an organic halide in the presence of a catalyst (usually palladium or nickel) and a base.³²² Basically Suzuki coupling takes place among an aryl- or vinyl-boronic acid acting as nucleophile with an aryl-, vinyl- or an alkyl-halide and is catalyzed by Ni(0) and Pd(0). As reported in Scheme 3.1, the mechanism of the catalytic cycle of Suzuki coupling reaction involves three basic steps: 1) oxidative addition, 2) transmetallation and 3) reductive elimination.³²³

Scheme 3.1 Catalytic cycle of Pd(0) in Suzuki cross-coupling reaction



The reaction begins with the oxidative addition of aryl halide to a Pd(0) species affording a stable trans- δ -palladium(0) complex (a). After that it proceeds with complete retention of configuration for alkenyl halides and with inversion for allylic and benzylic halides. Oxidative addition is the decisive step for the speed in the catalytic cycle; hence it is crucial that the supports are sufficiently reactive for the oxidative addition. Subsequently, the halogen atom bonded on the organo-palladium (II) is readily displaced by the base anion to provide the reactive R₁-Pd-OH complex (b).³²⁴ Because of the low nucleophilicity of organic group on boron atom, the cross coupling reaction requires the presence of a suitable base that coordinates the organic group on boron atom and enhances its nucleophilicity.

Indeed, the transmetalation of activated organic group to the Pd (II) complex with the consequent formation of trans R₁-Pd-R₂ (trans-c) is facilitated by the quaternization of the boron with negatively charged.³²⁶ Cross-coupling reaction has many advantages that include the mild reaction conditions, ready availability of organoboron reagents, which are inert to water and related solvents, as well as oxygen, and generally thermally stable, tolerant toward

Targeting mPGES-1: design and synthesis of promising inhibitors as new anti-inflammatory agents.

various functional groups and low toxicity of starting materials and by-products.^{327,328} Hence, this synthetic approach was employed to synthesize the biaryl compounds **48-64** (Figure 3.6), using Pd(PPh₃)₄, as a catalyst, K₂CO₃ as a base and a mixture of dioxane and water (2:1) as solvent system (Scheme 3.4).

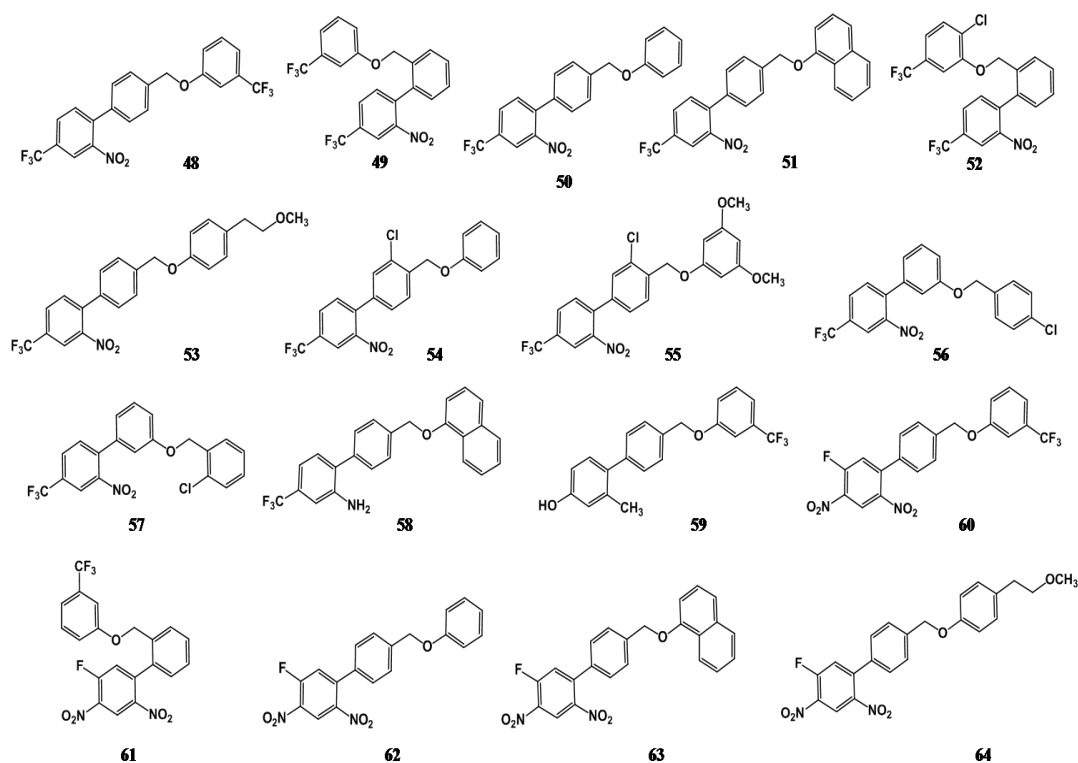


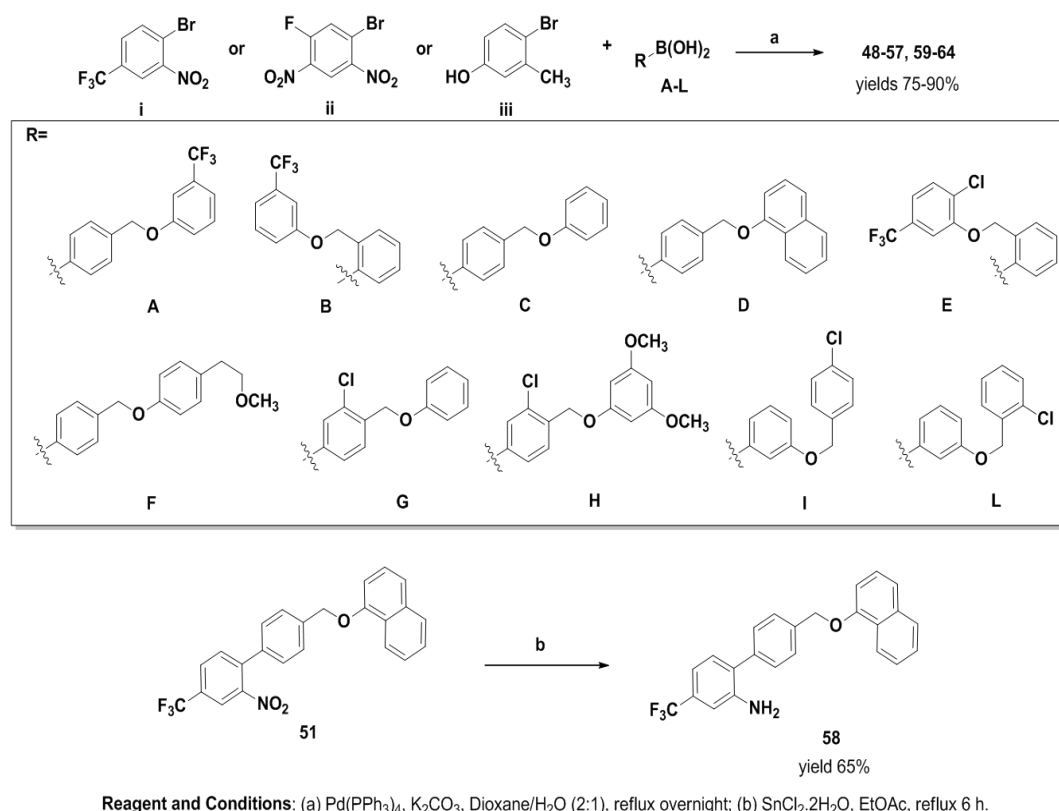
Figure 3.6 Structures of synthesized biaryl derivatives **48-64**

The first group of compounds **48-57** was synthesized using the same aryl halide employed in the synthesis of precursors of the carbazole compounds in combination with various arylboronic acids; however, in order to increase the chemical variability of the substituents on the biaryl skeleton another two aryl halide have been used (compounds **59, 60-64**). Finally, compound **58** (*o*-amine derivatives) was synthesized *via* nitro group reduction procedure starting from

Targeting mPGES-1: design and synthesis of promising inhibitors as new anti-inflammatory agents.

the compound **51**. The reduction of aromatic nitrocompound **51** to the corresponding amino derivative **58** was made by commercial $\text{SnCl}_2 \cdot 2\text{H}_2\text{O}$ (Tin (II) chloride dehydrate) and ethylacetate as solvent, the reaction was conducted in reflux condition under an inert atmosphere (**Scheme 3.4**).

Scheme 3.4 General procedures for the synthesis of biaryl compounds



Therefore through a cell-free assay using the microsomal fraction of interleukin- 1β -stimulated human A549 cells the interference of biaryl compounds with mPGES-1 activity was investigated in the same manner used for the first two classes of compounds (4-arylidene-1,3-disubstituted-5-pyrazolones and carbazoles) described before. The results obtained shown that compounds **48-59** have no inhibitory activity toward mPGES-1, after

Targeting mPGES-1: design and synthesis of promising inhibitors as new anti-inflammatory agents.

treatment with 10 μM of tested compounds, whereas compounds **60-64** showed an amazing inhibitory activity against mPGES-1 (**Figure 3.7**).

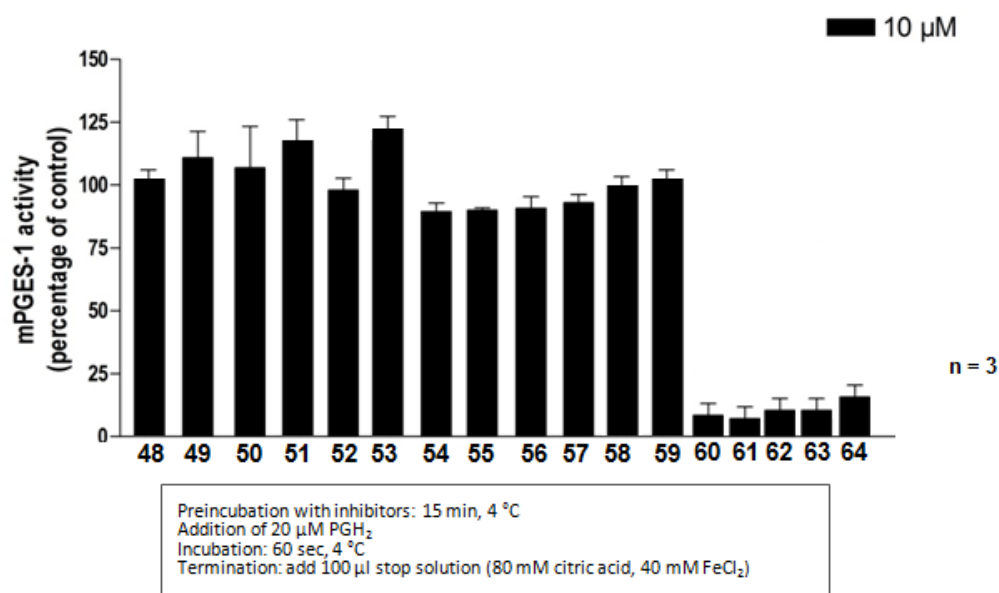


Figure 3.7 Effect of compounds 48-64 on the activity of mPGES-1.

Experiments were performed in triplicate.

Among the tested compounds, interesting IC_{50} values were detected for compounds **60-64** (**Table 3.1**). In particular, the best result was obtained by compound **63** that shows an IC_{50} value of $0.18 \pm 0.03 \mu\text{M}$.

Table 3.1 mPGES-1 inhibition by tested compounds 60-64. Experiments were performed in triplicate

Entry	$\text{IC}_{50} \pm \text{SD} (\mu\text{M})$
60	$0.26 \pm 0.09 \mu\text{M}$
61	$0.54 \pm 0.07 \mu\text{M}$
62	$0.60 \pm 0.05 \mu\text{M}$
63	$0.18 \pm 0.03 \mu\text{M}$
64	$1.64 \pm 0.08 \mu\text{M}$

Targeting mPGES-1: design and synthesis of promising inhibitors as new anti-inflammatory agents.

Analyzing the data obtained, all the tested compounds synthesized using 1-bromo-5-fluoro-2,4-dinitrobenzene as aryl halide in the Suzuki-Miyaura reaction, exhibit high inhibitory activity against the mPGES-1 with low IC₅₀ values in the μM range, ranging from 0.18 to 1.64 μM. On the other hand, compound **48-57** and **59** were synthesized using the other two aryl halides (1-bromo-2-nitro-4-(trifluoromethyl)benzene and 4-bromo-3-methylphenol) manifested no effect on the mPGES-1 activity, this allows to understand how the functionalization present on the first aromatic ring are essential for the inhibitory activity toward this enzyme. In conclusion, previous studies showed that carbazole compounds **43-47** did not interact with the active site of mPGES-1, so with the aim to optimize the results obtained a novel class of compounds has been synthesized. Promising biaryl compounds **60-64** has been identified as new potent mPGES-1 inhibitors. In addition, modifications of the nitro groups on the first aromatic ring of the biaryl skeleton were resulted in a loss of activity towards mPGES-1. Finally, compound **63** showed the best inhibitory activity on mPGES-1 (IC₅₀ = 0.18 ± 0.03 μM) that could be a really promising anti-inflammatory drug realized with a simple synthetic strategy.

-CONCLUSION-

Conclusion

In conclusion, in the course of my PhD program an efficient approach toward the development of new agents able to modulate the C-terminal domain of Hsp90 and mPGES-1 enzyme have been discovered. In particular, with the aim to discover new chemical agents able to modulate C-terminal domain of Hsp90, we started from compound **1** which emerged as the first non-natural inspired inhibitor of Hsp90 C-terminus, two generation of different DHPMs derivatives have been synthesized. The second generation was designed in order to explore the chemical influence of the functionalization on the aromatic ring at C4 position of DHPM core, while the third generation was synthesized with the aim of improving the inhibitory profile of this class of compound through the functionalization of C2 position of Biginelli's scaffold. The exploration and optimization processes of DHPM core were able to discover the third generation possessing a better antiproliferative profile compared to the lead compound **1**. These results support the importance of the DHPM core as a potent scaffold able to inhibit the C-terminal domain of Hsp90, moreover, these products could be useful to extend the still few structural knowledge related to this region. Concerning the development of new products able to interfere with mPGES-1 enzyme, three collections of compounds were successfully realized. Taking into account the molecular modelling studies and basing either on the highly efficient a first collection of 4-arylidene-1,3-disubstituted-5-pyrazolone was synthesized. Whereas, taking in consideration the well-known carbazole inhibitor of mPGES-1, a small set of carbazole compounds was designed. Biological evaluation, performed in collaboration with the research group of professor Oliver Werz, showed that no compound is able to inhibit the enzyme of interest. Based on the negative results reported by the carbazole products a third series of biaryl compounds was synthesized.

Fortunately, biological studies of this class of molecules allowed us to identify five interesting products (compounds **60-64**) able to inhibit the action of mPGES-1 which showed IC₅₀ values in the low micromolar range.

EXPERIMENTAL SECTION

-CHAPTER 4-

Synthesis of second and third generation of DHPM derivatives as
Hsp90 C-terminus inhibitors: experimental procedures.

4.1 General information

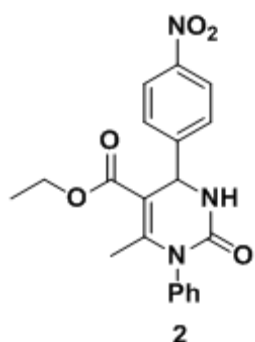
All commercially available starting materials were purchased from Sigma-Aldrich and were used as received. All solvents used for the synthesis were of HPLC grade; they were purchased from Sigma-Aldrich and Carlo Erba Reagenti. NMR spectra (^1H , HMBC, HSQC) were recorded on a Bruker 400 MHz instrument. All compounds were dissolved in 0.5 mL of 99.95% CDCl_3 (Carlo Erba, 99.95 Atom % D). Coupling constants (J) are reported in Herz, and chemical shifts are expressed in parts per million (ppm) on the delta (δ) scale relative to CHCl_3 (7.26 ppm for ^1H and 77.2 ppm for ^{13}C) as internal reference. Electrospray mass spectrometry (ESI MS) was performed on a LCQ DECA TermoQuest (San Josè, California, USA) mass spectrometer. Reactions were monitored on silica gel 60 F254 plates (Merck) and the spots were visualized under UV light. Analytical and semi-preparative reversed-phase HPLC was performed on Agilent Technologies 1200 Series high performance liquid chromatography using a Jupiter Proteo C18 reversed-phase column (250 x 4.60mm, 4 μ , 90 Å, flow rate = 1 mL/min; 250 x 10.00mm, 10 μ , 90 Å, flow rate = 4 mL/min respectively, Phenomenex[®]). The binary solvent system (A/B) was as follows: 0.1% TFA in water (A) and 0.1% TFA in CH_3CN (B). The absorbance was detected at 280 nm. The purity of all tested compound (>97%) was determined by HPLC analysis. All microwave irradiation experiments were carried out in a dedicated CEM-Discover[®] Focused Microwave Synthesis apparatus, operating with continuous irradiation power from 0 to 300 W utilizing the standard absorbance level of 300 W maximum power. Microwave reactions were performed on a CEM Discover[®] single mode platform using 10 mL pressurized vials. The DiscoverTM system also offers controllable ramp time, hold time (reaction time) and uniform stirring. The temperature was monitored using the CEM-Discover built-in-vertically-

focused IR temperature sensor. After the irradiation period, the reaction vessel was cooled rapidly (60-120 s) to ambient temperature by air jet cooling.

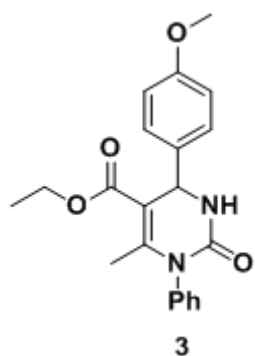
4.2 Methods and materials

4.2.1 General procedure for synthesis of the second generation of DHPMs derivatives by microwave-assisted Biginelli reaction.

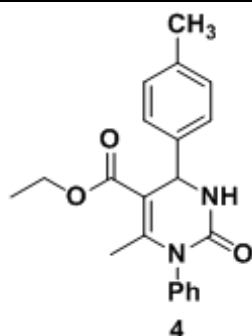
A mixture of appropriate aldehyde (1.0 mmol), *N*-phenylurea (1.5 mmol), ethyl acetoacetate (1.0 mmol) in acetonitrile (1.5 mL) was placed in a 10 mL microwave glass vial equipped with a small magnetic stirring bar. TMSCl (1.0 mmol) was added and the mixture was then stirred under microwave irradiation at 120°C for 15-20 min. After irradiation, the reaction mixture was cooled to ambient temperature by air jet cooling, cold water was added and the vial was poured into crushed ice and then at 4°C overnight. The resulting precipitate was filtered and washed with a cold mixture of ethanol/water (1:1) (3x3 mL), to give the desired product in good yields (55-80%). HPLC purification was performed by semi-preparative reversed-phase HPLC (on a Jupiter Proteo C₁₈ column: 250 x 10.00mm, 10μ, 90 Å, flow rate = 4 mL/min) using the gradient conditions reported below for each compound. The final products were obtained with high purity (>95%) as detected by HPLC analysis and were fully characterized by ESMS and NMR spectra.



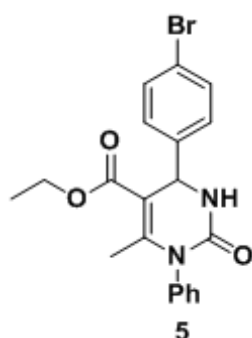
Compound **2** was obtained by following the general procedure as a yellow solid (200.0 mg, 66% yield). RP-HPLC tR = 33.5 min, gradient condition: from 5% B to 100% B in 50 min, flow rate of 4 mL/min, $\lambda = 280$ nm. ^1H NMR (400 MHz, CDCl_3): $\delta = 1.21$ (t, $J = 7.1$ Hz, 3H), 2.13 (s, 3H), 4.16 (q, $J = 7.0$ Hz, 2H), 5.61 (s, 1H), 7.14 (brs, 2H), 7.41-7.50 (m, 3H), 7.55-7.60 (d, $J = 8.5$ Hz, 2H), 8.22 (d, $J = 8.4$ Hz, 2H); ^{13}C NMR (100 MHz, CDCl_3): $\delta = 15.2, 19.6, 54.5, 61.0, 105.6, 122.6, 125.0, 128.3, 128.9, 130.6, 133.5, 138.3, 143.4, 148.1, 166.5$. ESMS, calcd for $\text{C}_{20}\text{H}_{19}\text{N}_3\text{O}_5$ 381,1; found $m/z = 382.5$ $[\text{M} + \text{H}]^+$.



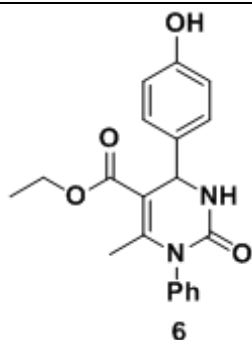
Compound **3** was obtained by following the general procedure as a yellow gelatinous solid (210.0 mg, 60% yield). RP-HPLC tR = 33.2 min, gradient condition: from 5% B to 100% B in 50 min, flow rate of 4 mL/min, $\lambda = 280$ nm. ^1H NMR (400 MHz, CDCl_3): $\delta = 1.21$ (t, $J = 7.1$ Hz, 3H), 2.13 (s, 3H), 3.80 (s, 3H), 4.16 (q, $J = 7.0$ Hz, 2H), 5.60 (s, 1H), 6.82-6.97 (m, 2H), 7.12-7.24 (m, 4H), 7.28-7.36 (m, 3H), 8.20-8.25 (d, 2H); ^{13}C NMR (100 MHz, CDCl_3): $\delta = 14.6, 18.9, 55.0, 55.8, 60.1, 105.6, 113.8, 127.5, 128.4, 128.9, 132.8, 138.6, 150.3, 158.7, 167.5$. ESMS, calcd for $\text{C}_{21}\text{H}_{22}\text{N}_2\text{O}_4$ 366,4; found $m/z = 367.3$ $[\text{M} + \text{H}]^+$.



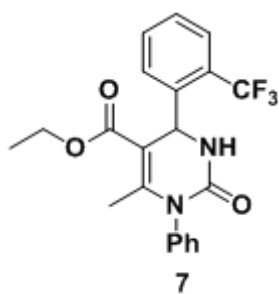
Compound **4** was obtained by following the general procedure as a yellow solid (200.0 mg, 75% yield). RP-HPLC t_R = 33.9 min, gradient condition: from 5% B to 100% B in 50 min, flow rate of 4 mL/min, λ = 280 nm. ^1H NMR (400 MHz, CDCl_3): δ = 1.24 (t, J = 7.1 Hz, 3H), 2.13 (s, 3H), 2.40 (s, 3H), 4.16 (q, J = 7.1 Hz, 2H), 5.50 (s, 1H), 7.18-7.22 (d, J = 7.8 Hz, 2H), 7.24 (s, 1H), 7.29-7.33 (m, 3H), 7.42-7.50 (m, 3H); ^{13}C NMR (100 MHz, CDCl_3): δ = 15.1, 19.6, 20.7, 55.5, 61.1, 104.9, 125.6, 127.9, 128.4, 128.9, 129.4, 136.5, 140.2, 147.8, 152.9, 166.7. ESMS, calcd for $\text{C}_{21}\text{H}_{22}\text{N}_2\text{O}_3$ 350.4; found m/z = 351.4 [$\text{M} + \text{H}$] $^+$.



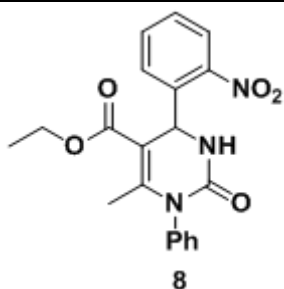
Compound **5** was obtained by following the general procedure as a yellow solid (190.0 mg, 65% yield). RP-HPLC t_R = 34.8 min, gradient condition: from 5% B to 100% B in 50 min, flow rate of 4 mL/min, λ = 280 nm. ^1H NMR (400 MHz, CDCl_3): δ = 1.24 (t, J = 7.1 Hz, 3H), 2.14 (s, 3H), 4.16 (q, J = 7.0 Hz, 2H), 5.50 (s, 1H), 7.20 (s, 2H), 7.28-7.31 (d, J = 8.5 Hz, 2H), 7.42-7.53 (m, 5H); ^{13}C NMR (100 MHz, CDCl_3): δ = 14.3, 19.5, 55.0, 61.3, 105.6, 122.8, 123.4, 128.9, 129.1, 132.8, 133.5, 138.6, 143.4, 149.7, 167.3. ESMS, calcd for $\text{C}_{20}\text{H}_{19}\text{BrN}_2\text{O}_3$ 415.3; found m/z = 415.5-417.5 [$\text{M} + \text{H}$] $^+$.



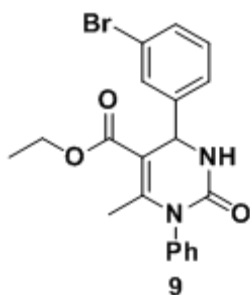
Compound **6** was obtained by following the general procedure as a yellow solid (200.0 mg, 75% yield). RP-HPLC $t_R = 29.4$ min, gradient condition: from 5% B to 100% B in 50 min, flow rate of 4 mL/min, $\lambda = 280$ nm. ^1H NMR (400 MHz, CDCl_3): $\delta = 1.27$ (t, $J = 7.1$ Hz, 3H), 2.40 (s, 3H), 4.16 (q, $J = 7.0$ Hz, 2H), 5.50 (s, 1H), 6.76 (d, $J = 8.4$ Hz, 2H), 7.07 (d, $J = 8.3$ Hz, 2H), 7.18 (t, $J = 9.4$ Hz, 3H), 7.28 (dd, $J = 8.5$ Hz, 2H); ^{13}C NMR (100 MHz, CDCl_3): $\delta = 15.3$, 16.8, 59.1, 61.0, 114.5, 124.6, 126.3, 128.1, 129.6, 130.1, 140.2, 148.7, 115.4, 167.2. ESMS, calcd for $\text{C}_{20}\text{H}_{20}\text{BrN}_2\text{O}_4$ 352.4; found $m/z = 353.4$ $[\text{M} + \text{H}]^+$.



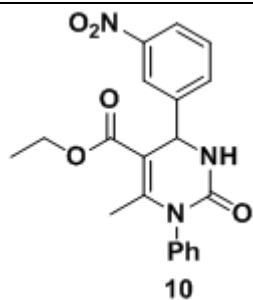
Compound **7** was obtained by following the general procedure as a white solid (190.0 mg, 55% yield). RP-HPLC $t_R = 36.6$ min, gradient condition: from 5% B to 100% B in 50 min, flow rate of 4 mL/min, $\lambda = 280$ nm. ^1H NMR (400 MHz, CDCl_3): $\delta = 1.04$ (t, $J = 7.1$ Hz, 3H), 2.28 (s, 3H), 4.02 (q, $J = 7.0$ Hz, 2H), 5.62 (s, 1H), 7.29 (s, 1H), 7.45-7.52 (m, 5H), 7.66-7.69 (d, $J = 6.6$ Hz, 2H), 7.73-7.76 (d, $J = 7.7$ Hz, 1H); ^{13}C NMR (100 MHz, CDCl_3): $\delta = 14.8$, 19.7, 51.2, 61.5, 103.5, 115.1, 123.2, 127.2, 128.9, 129.3, 129.6, 130.1, 133.6, 161.9. ESMS, calcd for $\text{C}_{21}\text{H}_{19}\text{F}_3\text{N}_2\text{O}_3$ 404.4; found $m/z = 405.5$ $[\text{M} + \text{H}]^+$.



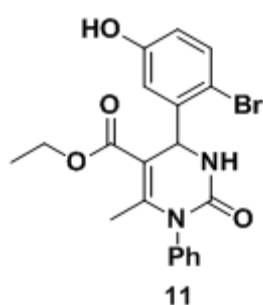
Compound **8** was obtained by following the general procedure as a white solid (200.0 mg, 70% yield). RP-HPLC $t_R = 34.7$ min, gradient condition: from 5% B to 100% B in 50 min, flow rate of 4 mL/min, $\lambda = 280$ nm. ^1H NMR (400 MHz, CDCl_3): $\delta = 0.98$ (t, $J = 7.1$ Hz, 3H), 2.27 (s, 3H), 3.98 (q, $J = 7.1$ Hz, 2H), 5.92 (s, 1H), 7.21-7.25 (s, 2H), 7.42-7.54 (m, 4H), 7.65-7.74 (m, 2H), 7.98 (dd, $J = 8.1, 1.3$ Hz, 1H); ^{13}C NMR (100 MHz, CDCl_3): $\delta = 14.8, 19.4, 51.3, 61.1, 101.6, 123.9, 128.2, 128.5, 133.0, 135.8, 136.2, 147.3, 148.1, 150.9, 152.6, 164.2$. ESMS, calcd for $\text{C}_{20}\text{H}_{19}\text{N}_3\text{O}_5$ 381.4; found $m/z = 382.3$ [$\text{M} + \text{H}$] $^+$.



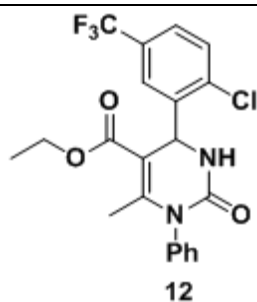
Compound **9** was obtained by following the general procedure as a colorless gelatinous solid (170.0 mg, 70% yield). RP-HPLC $t_R = 35.4$ min, gradient condition: from 5% B to 100% B in 50 min, flow rate of 4 mL/min, $\lambda = 280$ nm. ^1H NMR (400 MHz, CDCl_3): $\delta = 1.23$ (t, $J = 7.1$ Hz, 3H), 2.14 (s, 3H), 4.16 (q, $J = 7.0$ Hz, 2H), 5.47 (s, 1H), 7.25 (s, 2H), 7.36 (t, $J = 7.2$ Hz, 1H), 7.44-7.53 (m, 5H), 7.61 (s, 1H); ^{13}C NMR (100 MHz, CDCl_3): $\delta = 15.3, 19.5, 55.1, 61.5, 105.4, 124.2, 125.7, 128.0, 128.9, 130.5, 132.4, 147.2, 151.2, 154.9, 166.4$. ESMS, calcd for $\text{C}_{20}\text{H}_{19}\text{BrN}_2\text{O}_3$ 415.3; found $m/z = 415.5-417.5$ [$\text{M} + \text{H}$] $^+$.



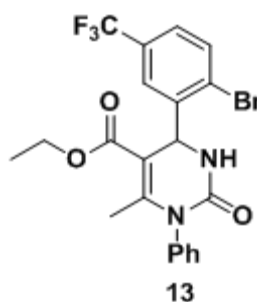
Compound **10** was obtained by following the general procedure as a white solid (200.0 mg, 70% yield). RP-HPLC $t_R = 34.2$ min, gradient condition: from 5% B to 100% B in 50 min, flow rate of 4 mL/min, $\lambda = 280$ nm. ^1H NMR (400 MHz, CDCl_3): $\delta = 1.26$ (t, $J = 7.1$ Hz, 3H), 2.20 (s, 3H), 4.17 (q, $J = 7.0$ Hz, 2H), 5.67 (s, 1H), 6.91 (s, 1H), 7.30 (s, 1H), 7.47-7.53 (m, 3H), 7.63 (t, $J = 8.1$ Hz, 1H), 7.78 (d, $J = 7.9$ Hz, 1H), 8.24 (d, $J = 8.4$ Hz, 1H), 8.36 (s, 1H); ^{13}C NMR (100 MHz, CDCl_3): $\delta = 13.9, 18.4, 53.7, 60.4, 104.0, 121.5, 122.8, 128.5, 129.5, 130.0, 132.2, 137.0, 145.2, 148.2, 149.6, 153.1, 165.1$. ESMS, calcd for $\text{C}_{20}\text{H}_{19}\text{BrN}_3\text{O}_5$ 381.4; found $m/z = 382.4$ $[\text{M} + \text{H}]^+$.



Compound **11** was obtained by following the general procedure as a pale yellow gelatinous solid (170.0 mg, 74% yield). RP-HPLC $t_R = 38.7$ min, gradient condition: from 5% B to 100% B in 50 min, flow rate of 4 mL/min, $\lambda = 280$ nm. ^1H NMR (400 MHz, CDCl_3): $\delta = 1.10$ (t, $J = 7.1$ Hz, 3H), 2.21 (s, 3H), 4.16 (q, $J = 7.1$ Hz, 2H), 5.83 (s, 1H), 6.64 (dd, $J = 8.6, 2.9$ Hz, 1H), 6.89 (br s, 1H), 7.17-7.24 (m, 2H), 7.39-7.45 (m, 4H); ^{13}C NMR (125 MHz, CDCl_3): $\delta = 13.9, 19.4, 53.4, 60.2, 114.4, 115.0, 116.9, 128.9, 129.2, 129.5, 133.5, 134.4, 138.6, 143.4, 149.7, 166.3$. ESMS, calcd for $\text{C}_{20}\text{H}_{19}\text{BrN}_2\text{O}_4$ 430.1; found $m/z = 431.0$ $[\text{M} + \text{H}]^+$.

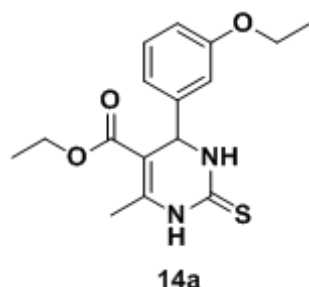


Compound **12** was obtained by following the general procedure as a white solid (150.0 mg, 70% yield). RP-HPLC $t_R = 38.2$ min, gradient condition: from 5% B to 100% B in 50 min, flow rate of 4 mL/min, $\lambda = 280$ nm. ^1H NMR (400 MHz, CDCl_3): $\delta = 1.13$ (t, $J = 7.1$ Hz, 3H), 2.27 (s, 3H), 4.13 (q, $J = 7.0$ Hz, 2H), 5.98 (s, 1H), 7.15-7.24 (m, 2H), 7.43-7.50 (m, 3H), 7.57 (s, 2H), 7.66 (s, 1H); ^{13}C NMR (100 MHz, CDCl_3): $\delta = 15.0, 19.6, 53.9, 61.3, 105.6, 121.9, 125.6, 127.1, 128.9, 129.8, 130.2, 129.2, 141.9, 149.7, 167.3$. ESMS, calcd for $\text{C}_{21}\text{H}_{18}\text{BrF}_3\text{N}_2\text{O}_3$ 483.3; found $m/z = 483.2$ -485.2 $[\text{M} + \text{H}]^+$.

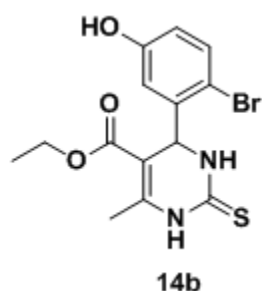


Compound **13** was obtained by following the general procedure as a colorless gelatinous solid (100.0 mg, 80% yield). RP-HPLC $t_R = 39.2$ min, gradient condition: from 5% B to 100% B in 50 min, flow rate of 4 mL/min, $\lambda = 280$ nm. ^1H NMR (400 MHz, CDCl_3): $\delta = 1.14$ (t, $J = 7.1$ Hz, 3H), 2.27 (s, 3H), 4.13 (q, $J = 7.0$ Hz, 2H), 5.97 (s, 1H), 7.18-7.24 (m, 2H), 7.43-7.50 (m, 4H), 7.66 (s, 1H), 7.78 (d, $J = 8.1$ Hz, 1H); ^{13}C NMR (100 MHz, CDCl_3): $\delta = 14.9, 19.2, 54.9, 61.9, 105.6, 121.9, 125.6, 127.1, 128.9, 129.8, 130.1, 129.2, 141.9, 149.7, 167.3$. ESMS, calcd for $\text{C}_{21}\text{H}_{18}\text{ClF}_3\text{N}_2\text{O}_3$ 438.8; found $m/z = 439.0$ $[\text{M} + \text{H}]^+$.

4.2.2 General procedure for synthesis of 14a and 14b by microwave-assisted Biginelli reaction.



A mixture of 3-ethoxybenzaldehyde (150 mg, 1.0 mmol), thiourea (115 mg, 1.5 mmol), ethyl acetoacetate (130 mg, 1.0 mmol) in acetonitrile (1.5 mL) was placed in a 10 mL microwave glass vial equipped with a small magnetic stirring bar. TMSCl (110 mg, 1.0 mmol) was added and the mixture was then stirred under microwave irradiation at 120°C for 20 min. After irradiation, the reaction mixture was cooled to ambient temperature by air jet cooling, cold water was added and the vial was poured into crushed ice and then left at 4°C overnight. The resulting precipitate was filtered and washed with a cold mixture of ethanol/water (1:1) (3x3 mL), to give the desired product as a yellow solid in 89% yields. RP-HPLC $t_R = 30.5$ min, gradient condition: from 5% B to 100 % B in 50 min, flow rate of 4 mL/min, $\lambda = 280$ nm. $^1\text{H NMR}$ (300 MHz, CDCl_3): $\delta = 1.18$ (t, $J = 7.1$ Hz, 3H), 1.45 (t, $J = 6.9$ Hz, 3H), 2.39 (s, 3H), 4.02-4.18 (m, 4H), 5.63 (s, 1H), 6.81-6.95 (m, 3H); 7.26 (t, $J = 8.0$ Hz, 1H). ESI-MS, calcd for $\text{C}_{16}\text{H}_{20}\text{N}_2\text{O}_3\text{S}$ 320.1; found $m/z = 321.0$ $[\text{M} + \text{H}]^+$.

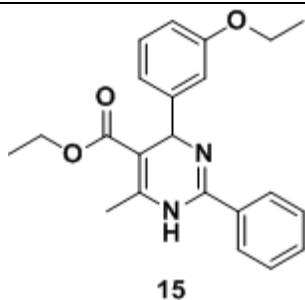


A mixture of 2-bromo-5-hydroxybenzaldehyde (200 mg, 1.0 mmol), thiourea (115 mg, 1.5 mmol), ethyl acetoacetate (130 mg, 1.0 mmol) in acetonitrile (1.5 mL) was placed in a 10 mL microwave glass vial equipped with a small magnetic stirring bar. TMSCl (110 mg, 1.0 mmol) was added and the mixture was then stirred under microwave irradiation at 120°C for 20 min. After irradiation, the reaction mixture was cooled to ambient temperature by air jet

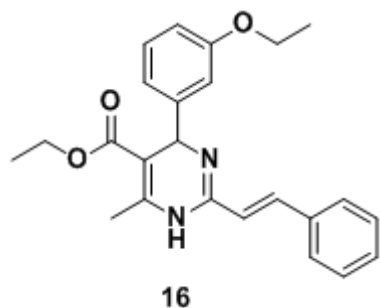
cooling, cold water was added and the vial was poured into crushed ice and then left at 4°C overnight. The resulting precipitate was filtered and washed with a cold mixture of ethanol/water (1:1) (3x3 mL), to give the desired product as a yellow solid in 89% yields. RP-HPLC t_R = 26.5 min, gradient condition: from 5% B to 100 % B in 50 min, flow rate of 4 mL/min, λ = 280 nm. ^1H NMR (300 MHz, CDCl_3): δ = 1.14 (t, J = 7.1 Hz, 3H); 2.47 (s, 3H); 4.12 (m, 2H); 5.65 (s, 1H); 6.95 (br s, 1H); 7.25 (br s, 2H). ESI-MS, calcd for $\text{C}_{14}\text{H}_{15}\text{BrN}_2\text{O}_3\text{S}$ 372.2; found m/z = 373.2 $[\text{M} + \text{H}]^+$.

4.2.3 General procedure for microwave-assisted Liebeskind-Srogl cross coupling reaction

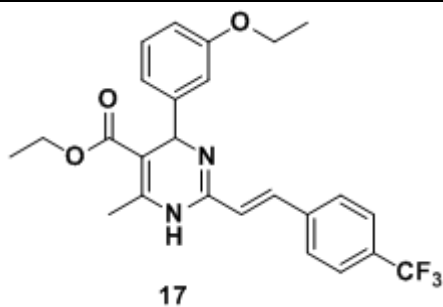
A dry microwave process vial was charged with dihydropyrimidinethione precursor **14a** or **14b** (1.0 mmol), the appropriate boronic acid (1.5 mmol), CuTC (3.0 mmol), and $\text{Pd}(\text{PPh}_3)_4$ (10 mol%). The reaction vessel was degassed and backfilled with nitrogen three times, and through the septum degassed dry THF (2.0 mL) was added. The mixture was subsequently heated in a microwave reactor at 100 °C for 60 min. After cooling, the mixture was transferred to a round-bottom flask and dried under reduced pressure. A solution of aqueous ammonia (25%) was added and the mixture was extracted three times with CHCl_3 . The combined organic layers were dried with anhydrous Na_2SO_4 and concentrated under vacuum. The crude residue was purified by HPLC to give the pure products in good yields (60-85%) and high purity (>95%).



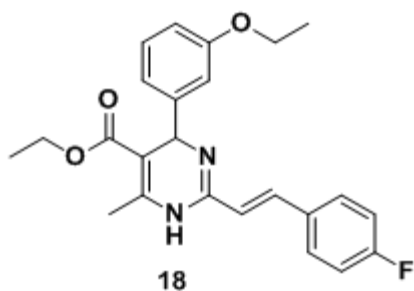
Compound **15** was obtained from **14a** following the general procedure. A portion of the crude product was then purified as follows: RP-HPLC $t_R = 21.6$ min, gradient condition: from 5% B to 100 % B in 50 min, flow rate of 4 mL/min, $\lambda = 280$ nm. 30.6 mg (85% yield, after HPLC purification step) as a pale yellow gelatinous solid. ^1H NMR (400 MHz, CDCl_3): $\delta = 1.17$ (t, $J = 7.1$ Hz, 3H); 1.35 (t, $J = 7.1$ Hz, 3H); 2.50 (s, 3H); 3.93-4.01 (m, 2H); 4.07-4.16 (m, 2H); 5.66 (s, 1H); 6.80-6.90 (m, 3H); 7.19-7.30 (m, 3H); 7.47 (br s, 1H); 7.72 (br s, 2H). ^{13}C NMR (100 MHz, CDCl_3): $\delta = 15.2, 15.9, 18.0, 54.5, 61.7, 64.6, 105.4, 112.5, 117.4, 123.8, 127.1, 128.1, 129.8, 133.3, 141.4, 155.5, 163.2$. ESI-MS, calcd for $\text{C}_{22}\text{H}_{24}\text{N}_2\text{O}_3$ 364.2; found $m/z = 365.1$ $[\text{M} + \text{H}]^+$.



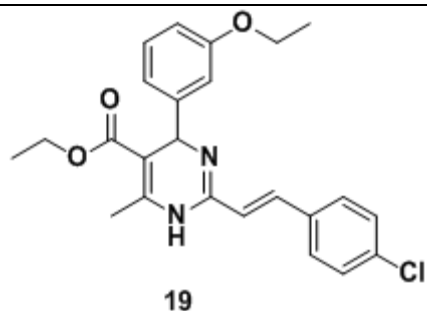
Compound **16** was obtained from **14a** by following the general procedure. A portion of the crude product was then purified as follows: RP-HPLC $t_R = 46.6$ min, gradient condition: from 5% B to 100 % B in 80 min, flow rate of 4 mL/min, $\lambda = 280$ nm. 16 mg (80% yield, after HPLC purification step) as a pale yellow gelatinous solid. ^1H NMR (400 MHz, CDCl_3): $\delta = 1.13$ (t, $J = 7.1$ Hz, 3H); 1.40 (t, $J = 6.9$ Hz, 3H); 2.34 (s, 3H); 4.01 (m, 4H); 5.33 (s, 1H); 6.80 (d, $J = 6.8$ Hz, 2H); 6.97 (d, $J = 16.1$ Hz, 1H); 7.21 (d, $J = 7.9$ Hz, 1H); 7.48 (s, 3H). 7.62 (m, 3H), 7.87 (d, $J = 16.3$ Hz, 1H). ^{13}C NMR (100 MHz, CDCl_3): $\delta = 14.8, 15.7, 18.3, 52.7, 59.2, 62.2, 103.7, 112.0, 117.6, 118.6, 127.5, 131.3, 132.0, 141.0, 145.9, 153.1, 158.6, 162.8$. ESI-MS, calcd for $\text{C}_{24}\text{H}_{26}\text{N}_2\text{O}_3$ 390.4; found $m/z = 391.4$ $[\text{M} + \text{H}]^+$.



Compound **17** was obtained from **14a** by following the general procedure. A portion of the crude product was then purified as follows: RP-HPLC $t_R = 38.9$ min, gradient condition: from 5% B to 100% B in 70 min, flow rate of 4 mL/min, $\lambda = 280$ nm. 13 mg (85% yield, after HPLC purification step) as a pale yellow gelatinous solid. ^1H NMR (400 MHz, CDCl_3): $\delta = 1.12$ (t, $J = 7.1$ Hz, 3H); 1.42 (t, $J = 7.1$ Hz, 3H); 2.42 (s, 3H); 4.05 (m, 4H); 5.46 (s, 1H); 6.87-6.81 (m, 3H); 6.99 (d, $J = 16.3$ Hz, 1H); 7.26 (s, 1H); 7.50 (m, 5H); 7.84 (d, $J = 16.2$ Hz, 1H). ^{13}C NMR (100 MHz, CDCl_3): $\delta = 14.8, 15.7, 18.3, 52.7, 59.2, 62.2, 103.7, 112.0, 117.6, 118.6, 127.5, 131.3, 132.0, 141.0, 145.9, 153.1, 158.6, 162.8$. ESI-MS, calcd for $\text{C}_{25}\text{H}_{25}\text{F}_3\text{N}_2\text{O}_3$ 458.4; found $m/z = 459.4$ $[\text{M} + \text{H}]^+$

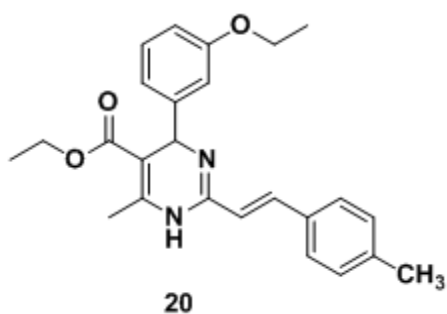


Compound **18** was obtained from **14a** by following the general procedure. A portion of the crude product was then purified as follows: RP-HPLC $t_R = 38.7$ min, gradient condition: from 5% B to 100% B in 50 min, flow rate of 4 mL/min, $\lambda = 280$ nm. 14.8 mg (75% yield, after HPLC purification step) as a pale yellow gelatinous solid. ^1H NMR (300 MHz, CDCl_3): $\delta = 1.10$ (t, $J = 7.1$ Hz, 3H); 1.36 (t, $J = 7.1$ Hz, 3H); 2.35 (s, 3H); 3.91-4.09 (m, 4H); 5.30 (s, 1H); 6.74-6.84 (m, 3H); 6.96 (br s, 2H); 7.20 (t, $J = 8.0$ Hz, 1H); 7.39-7.49 (m, 3H); 7.60 (br s, 1H). ESI-MS, calcd for $\text{C}_{24}\text{H}_{25}\text{FN}_2\text{O}_3$ 408.2; found $m/z = 409.1$ $[\text{M} + \text{H}]^+$.



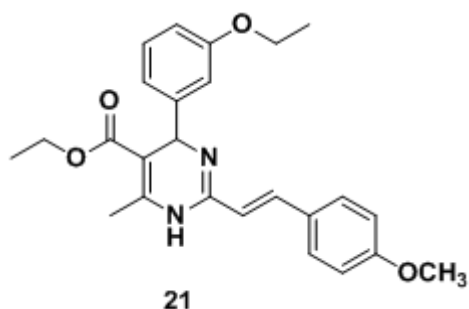
Compound **19** was obtained from **14a** by following the general procedure. A portion of the crude product was then purified as follows: RP-HPLC $t_R = 37.4$ min, gradient condition: from 5% B to 100 % B in 70 min, flow rate of 4 mL/min, $\lambda = 280$ nm.

10 mg (75% yield, after HPLC purification step) as a pale yellow gelatinous solid. ^1H NMR (400 MHz, CDCl_3): $\delta = 1.15$ (t, $J = 6.9$ Hz, 3H); 1.41 (t, $J = 6.6$ Hz, 3H); 2.41 (s, 3H); 4.05 (m, 4H); 5.39 (s, 1H); 6.82 (s, 1H); 7.52 (m, 4H); 7.64 (m, 5H). ^{13}C NMR (100 MHz, CDCl_3): $\delta = 14.8, 15.7, 18.3, 52.7, 59.2, 62.2, 103.7, 112.0, 117.6, 118.6, 127.5, 131.3, 132.0, 141.0, 145.9, 153.1, 158.6, 162.8$. ESI-MS, calcd for $\text{C}_{24}\text{H}_{25}\text{ClN}_2\text{O}_3$ 424.9; found $m/z = 425.5$ $[\text{M} + \text{H}]^+$



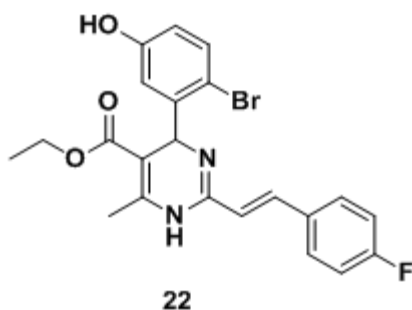
Compound **20** was obtained from **14a** by following the general procedure. A portion of the crude product was then purified as follows: RP-HPLC $t_R = 29.8$ min, gradient condition: from 5% B to 100 % B in 50 min, flow rate of 4 mL/min, $\lambda = 280$ nm.

10 mg (70% yield, after HPLC purification step) as a pale yellow gelatinous solid. ^1H NMR (400 MHz, CDCl_3): $\delta = 1.09$ (t, $J = 7.1$ Hz, 3H); 1.19 (t, $J = 6.9$ Hz, 3H); 2.32 (s, 3H); 2.38 (s, 3H); 4.02 (m, 4H); 5.33 (s, 1H); 6.81 (brs, 2H); 7.10 (d, $J = 7.4$ Hz, 2H); 7.25 (m, 3H); 7.42 (d, $J = 7.7$ Hz, 3H). 7.83 (d, $J = 16.0$ Hz, 1H). ^{13}C NMR (100 MHz, CDCl_3): $\delta = 14.8, 15.7, 18.6, 22.4, 54.9, 61.4, 64.1, 104.0, 111.0, 112.2, 113.2, 120.5, 128.1, 130.8, 132.1, 141.6, 145.9, 148.3, 153.8, 158.9, 162.4$. ESI-MS, calcd for $\text{C}_{25}\text{H}_{28}\text{N}_2\text{O}_3$ 404.5; found $m/z = 405.4$ $[\text{M} + \text{H}]^+$.



Compound **21** was obtained from **14a** by following the general procedure. A portion of the crude product was then purified as follows: RP-HPLC $t_R = 48.8$ min, gradient condition: from 5% B to 30% B in 5 min, increased to 100 % B in 60 min, flow rate of 4 mL/min, $\lambda = 280$ nm. 8 mg (60% yield,

after HPLC purification step) as a pale yellow gelatinous solid. ^1H NMR (400 MHz, CDCl_3): $\delta = 1.09$ (t, $J = 7.1$ Hz, 3H); 1.19 (t, $J = 6.9$ Hz, 3H); 2.32 (s, 3H); 3.50 (s, 3H); 4.02 (m, 4H); 5.33 (s, 1H); 6.81 (s, 2H); 7.10 (d, $J = 7.4$ Hz, 2H); 7.25 (m, 3H); 7.42 (d, $J = 7.7$ Hz, 3H). 7.83 (d, $J = 16.0$ Hz, 1H). ^{13}C NMR (100 MHz, CDCl_3): $\delta = 14.8, 15.6, 18.2, 55.5, 61.2, 64.4, 104.1, 114.2, 117.6, 118.6, 127.5, 131.3, 132.0, 141.0, 145.9, 153.1, 158.6, 162.8$. ESI-MS, calcd for $\text{C}_{25}\text{H}_{28}\text{N}_2\text{O}_4$ 420.5; found $m/z = 421.5$ $[\text{M} + \text{H}]^+$.



Compound **22** was obtained from **14b** by following the general procedure. A portion of the crude product was then purified as follows: RP-HPLC $t_R = 26.6$ min, gradient condition: from 5% B to 100 % B in 50 min, flow rate of 4 mL/min, $\lambda = 280$ nm. 10

mg (65% yield, after HPLC purification step) as a pale yellow gelatinous solid. ^1H NMR (300 MHz, CDCl_3): $\delta = 1.19$ (t, $J = 7.1$ Hz, 3H); 2.69 (s, 3H); 4.12 (m, 2H); 5.94 (s, 1H); 6.72 (m, 2H); 6.92 (s, 1H); 7.07 (t, $J = 8.1$ Hz, 1H); 7.36 (d, $J = 8.5$ Hz, 1H); 7.53 (d, $J = 7.2$ Hz, 2H); 7.85 (d, $J = 16.4$ Hz, 1H). ESI-MS, calcd for $\text{C}_{22}\text{H}_{20}\text{BrFN}_2\text{O}_3$ 459.3; found $m/z = 365.1$ $[\text{M} + \text{H}]^+$

-CHAPTER 5-

Development of new mPGES-1 inhibitors: experimental
procedures

5.1 General synthetic methods

All commercially available starting materials were purchased from Sigma-Aldrich and were used as received. All solvents used for the synthesis were of HPLC grade; they were purchased from Sigma-Aldrich and Carlo Erba Reagenti. All NMR spectra were recorded on a BrukerAvance 300 or 500 MHz instrument. All compounds were dissolved in 0.5 mL of 99.8% CDCl₃ (Sigma-Aldrich, 99.8 Atom % D). Coupling constants (*J*) are reported in Herz, and chemical shifts are expressed in parts per million (ppm) on the delta (δ) scale relative to CHCl₃ (7.26 ppm for ¹H and) as internal reference. Multiplicities are reported as follows: s, singlet; d, doublet; t, triplet; m, multiplet; dd, doublet of doublets. Reactions were monitored on silica gel 60 F254 plates (Merck) and the spots were visualized under UV light. Analytical and semi-preparative reversedphase HPLC was performed on Agilent Technologies 1200 Series high performance liquid chromatography using a Synergi Fusion C18 reversed-phase column (250 x 4.60mm, 4 μ , 80 Å, flow rate = 1 mL/min; 250 x 10.00mm, 10 μ , 80 Å, flow rate = 4 mL/min respectively, Phenomenex®). The binary solvent system (A/B) was as follows: 0.1% TFA in water (A) and 0.1% TFA in CH₃CN (B). The absorbance was detected at 280 nm. The purity of all tested compound (>95%) was determined by HPLC analysis.

5.2 General procedures for the preparation of 4-arylidene-1,3-disubstituted-5-pyrazolone compounds

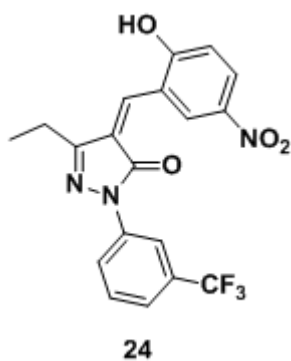
5.2.1 General procedure for the preparation of 5-pyrazolones 23a-23h

A mixture of appropriate β -ketoester (**i-iii**) (1 mmol.), arylhydrazine (**a-f**) (1.0 mmol.) and sodium acetate (0.6 mmol.) in 50% ethanol (2 mL) was refluxed for 4 hours. After the reaction, on cooling to room temperature a brown precipitate appeared. The precipitate was filtered off and dried to give the

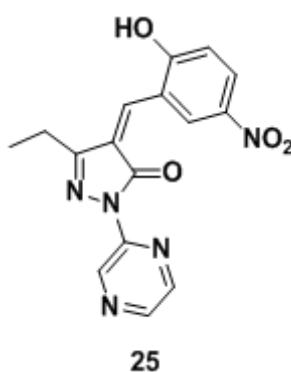
desired products **23a-23h**. The products were used in the next stage without further purification.

5.2.2 General procedure for the preparation of 24-41

A mixture of arylaldehyde (**A-L**) (1.3 eq.) and the appropriate 5-pyrazolone (**23a-23h**) (1.0 eq.) in acetic acid glacial (5 mL) was heated to reflux in oil bath for 24 h. After the reaction, the solvent was completely evaporated and residue was washed with cold water and filtered. The solid product was dried and the crude residue was purified by HPLC to give the desired products.

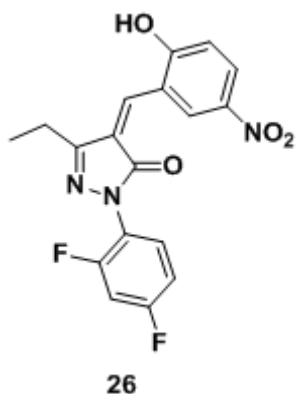


Compound **24** was obtained following the general procedures as an orange solid (190.0 mg, 65% yield). RP-HPLC $t_R = 26.6$ min, gradient condition: from 5% B to 100% B in 50 min, flow rate of 4 mL/min, $\lambda = 240$ nm. $^1\text{H NMR}$ (300 MHz, CDCl_3) δ 8.41 – 8.37 (m, 1H), 8.19 (d, $J = 6.6$ Hz, 2H), 7.85 (dt, $J = 7.1, 2.2$ Hz, 1H), 7.54 – 7.45 (m, 2H), 7.34 (d, $J = 1.0$ Hz, 1H), 7.05 (d, $J = 7.4$ Hz, 1H), 6.76 (s, 1H), 2.17 (q, $J = 8.0$ Hz, 2H), 1.05 (t, $J = 8.0$ Hz, 3H). ESI-MS, calcd for $\text{C}_{19}\text{H}_{14}\text{F}_3\text{N}_3\text{O}_4$ 405.3; found $m/z = 406.3$ [$\text{M} + \text{H}$] $^+$.



Compound **25** was obtained following the general procedures as an orange solid (150.0 mg, 60% yield). RP-HPLC $t_R = 24.5$ min, gradient condition: from 5% B to 100% B in 50 min, flow rate of 4 mL/min, $\lambda = 240$ nm. $^1\text{H NMR}$ (300 MHz, CDCl_3) δ 8.45 (d, $J = 7.5$ Hz, 1H), 8.38 (s, 1H), 8.28 – 8.20 (m, 3H), 7.63 (s, 1H), 7.32 (d, $J = 1.0$ Hz, 1H), 7.23 (d, $J = 7.4$ Hz,

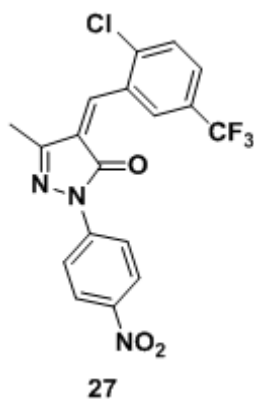
1H), 2.17 (q, $J = 8.0$ Hz, 2H), 1.04 (t, $J = 8.0$ Hz, 3H). ESI-MS, calcd for $C_{16}H_{13}N_5O_4$ 339.3; found $m/z = 340.3$ $[M + H]^+$.



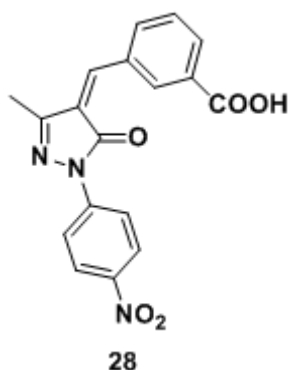
Compound **26** was obtained following the general procedures as an orange solid (100.0 mg, 62% yield).

RP-HPLC $t_R = 27.2$ min, gradient condition: from 5% B to 100% B in 50 min, flow rate of 4 mL/min, $\lambda = 240$ nm. 1H NMR (300 MHz, $CDCl_3$) δ 8.27 – 8.19 (m, 2H), 8.10 (dt, $J = 7.5, 5.7$ Hz, 1H), 7.33 (d, $J = 1.0$ Hz, 1H), 7.23 – 7.14 (m, 2H), 7.03 (td, $J = 8.9, 2.0$ Hz, 1H), 6.92 (ddd, $J = 9.2, 7.5, 2.0$ Hz, 1H),

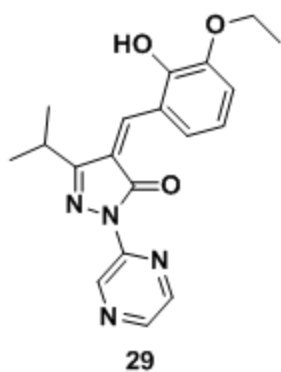
2.17 (q, $J = 8.0$ Hz, 2H), 1.06 (t, $J = 8.0$ Hz, 3H). ESI-MS, calcd for $C_{18}H_{13}F_2N_3O_4$ 373.1; found $m/z = 374.3$ $[M + H]^+$.



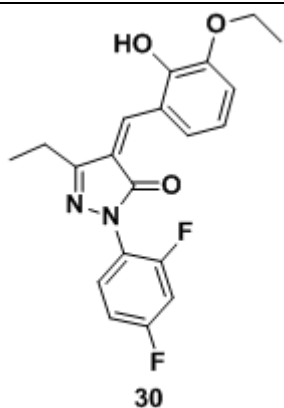
Compound **27** was obtained following the general procedures as an orange solid (90.0 mg, 60% yield). RP-HPLC $t_R = 24.9$ min, gradient condition: from 5% B to 100% B in 50 min, flow rate of 4 mL/min, $\lambda = 240$ nm. 1H NMR (300 MHz, $CDCl_3$) δ 8.31 – 8.25 (m, 2H), 7.94 – 7.88 (m, 2H), 7.58 – 7.47 (m, 3H), 7.43 – 7.38 (m, 1H), 2.30 (s, 3H). ESI-MS, calcd for $C_{18}H_{11}ClF_3N_3O_3$ 409.7; found $m/z = 410.9$ $[M + H]^+$.



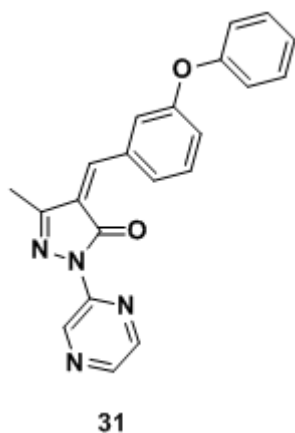
Compound **28** was obtained following the general procedures as an orange solid (120.0 mg, 60% yield). RP-HPLC $t_R = 21.2$ min, gradient condition: from 5% B to 100% B in 50 min, flow rate of 4 mL/min, $\lambda = 240$ nm. ^1H NMR (300 MHz, CDCl_3) δ 8.31 – 8.25 (m, 2H), 8.18 – 8.11 (m, 1H), 8.08 (q, $J = 1.6$ Hz, 1H), 7.94 – 7.88 (m, 2H), 7.62 – 7.53 (m, 2H), 7.28 (d, $J = 1.1$ Hz, 1H), 2.30 (s, 3H). ESI-MS, calcd for $\text{C}_{18}\text{H}_{13}\text{N}_3\text{O}_5$ 351.3; found $m/z = 352.4$ $[\text{M} + \text{H}]^+$.



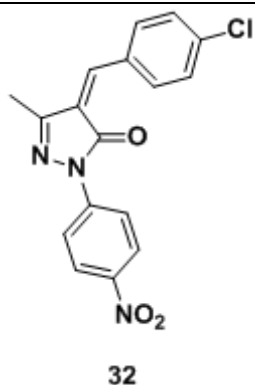
Compound **29** was obtained following the general procedures as an orange solid (130.0 mg, 70% yield). RP-HPLC $t_R = 26.2$ min, gradient condition: from 5% B to 100% B in 50 min, flow rate of 4 mL/min, $\lambda = 240$ nm. ^1H NMR (300 MHz, CDCl_3) δ 8.45 (d, $J = 7.5$ Hz, 1H), 8.38 (s, 1H), 8.25 (d, $J = 7.5$ Hz, 1H), 7.39 (d, $J = 0.9$ Hz, 1H), 6.97 (t, $J = 7.4$ Hz, 1H), 6.88 (ddd, $J = 7.6, 2.1, 1.0$ Hz, 1H), 6.83 (dd, $J = 7.3, 2.0$ Hz, 1H), 5.93 (s, 1H), 4.08 (q, $J = 8.0$ Hz, 2H), 2.72 (m, $J = 6.8$ Hz, 1H), 1.46 (t, $J = 8.0$ Hz, 3H), 1.11 (d, $J = 6.8$ Hz, 6H). ESI-MS, calcd for $\text{C}_{19}\text{H}_{20}\text{N}_4\text{O}_3$ 352.4; found $m/z = 353.4$ $[\text{M} + \text{H}]^+$.



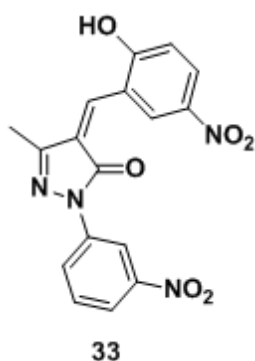
Compound **30** was obtained following the general procedures as an orange solid (150.0 mg, 75% yield). RP-HPLC $t_R = 24.5$ min, gradient condition: from 5% B to 100% B in 50 min, flow rate of 4 mL/min, $\lambda = 240$ nm. ^1H NMR (300 MHz, CDCl_3) δ 7.50 (dt, $J = 7.4, 5.7$ Hz, 1H), 7.40 (d, $J = 0.9$ Hz, 1H), 7.04 (td, $J = 9.0, 2.0$ Hz, 1H), 6.97 (t, $J = 7.5$ Hz, 1H), 6.94 – 6.86 (m, 2H), 6.83 (dd, $J = 7.4, 2.1$ Hz, 1H), 5.93 (s, 1H), 4.08 (q, $J = 8.0$ Hz, 2H), 2.17 (q, $J = 8.0$ Hz, 2H), 1.46 (t, $J = 8.0$ Hz, 3H), 1.05 (t, $J = 8.0$ Hz, 3H). ESI-MS, calcd for $\text{C}_{20}\text{H}_{18}\text{F}_2\text{N}_2\text{O}_3$ 372.4; found $m/z = 373.4$ $[\text{M} + \text{H}]^+$.



Compound **31** was obtained following the general procedures as an orange solid (130.0 mg, 74% yield). RP-HPLC $t_R = 23.4$ min, gradient condition: from 5% B to 100% B in 50 min, flow rate of 4 mL/min, $\lambda = 240$ nm. ^1H NMR (300 MHz, CDCl_3) δ 8.46 (d, $J = 7.5$ Hz, 1H), 8.37 (s, 1H), 8.27 (d, $J = 7.5$ Hz, 1H), 7.41 (t, $J = 7.5$ Hz, 1H), 7.38 – 7.30 (m, 2H), 7.23 (s, 1H), 7.19 – 7.13 (m, 1H), 7.13 – 7.07 (m, 2H), 7.02 – 6.96 (m, 2H), 6.91 (q, $J = 1.8$ Hz, 1H), 2.30 (s, 3H). ESI-MS, calcd for $\text{C}_{21}\text{H}_{16}\text{N}_4\text{O}_2$ 356.4; found $m/z = 357.4$ $[\text{M} + \text{H}]^+$.

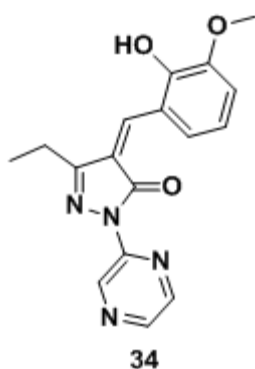


Compound **32** was obtained following the general procedures as an orange solid (130.0 mg, 74% yield). RP-HPLC $t_R = 23.4$ min, gradient condition: from 5% B to 100% B in 50 min, flow rate of 4 mL/min, $\lambda = 240$ nm. $^1\text{H NMR}$ (300 MHz, CDCl_3) δ 8.31 – 8.25 (m, 1H), 7.94 – 7.88 (m, 1H), 7.57 – 7.51 (m, 1H), 7.24 (hept, $J = 2.1$ Hz, 1H), 2.30 (s, 1H). ESI-MS, calcd for $\text{C}_{17}\text{H}_{12}\text{ClN}_3\text{O}_3$ 341.8; found $m/z = 342.7$ $[\text{M} + \text{H}]^+$.

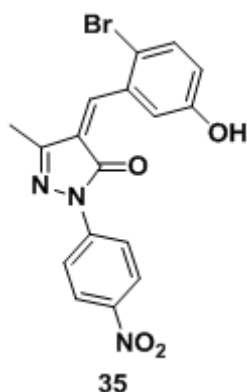


Compound **33** was obtained following the general procedures as an orange solid (120.0 mg, 80% yield). RP-HPLC $t_R = 20.4$ min, gradient condition: from 5% B to 100% B in 50 min, flow rate of 4 mL/min, $\lambda = 240$ nm. $^1\text{H NMR}$ (300 MHz, CDCl_3) δ 8.96 (t, $J = 2.0$ Hz, 1H), 8.21 (d, $J = 6.4$ Hz, 2H), 8.10 (ddt, $J = 22.3, 7.5, 2.0$ Hz, 2H), 7.61 (t, $J = 7.5$ Hz, 1H), 7.36 (d, $J = 1.0$ Hz, 1H), 7.08 – 7.03 (m, 1H), 6.78 (s, 1H), 2.30 (s, 3H).

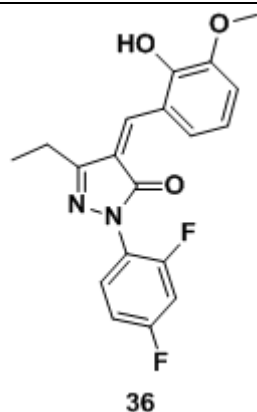
ESI-MS, calcd for $\text{C}_{17}\text{H}_{12}\text{N}_4\text{O}_6$ 368.3; found $m/z = 369.3$ $[\text{M} + \text{H}]^+$.



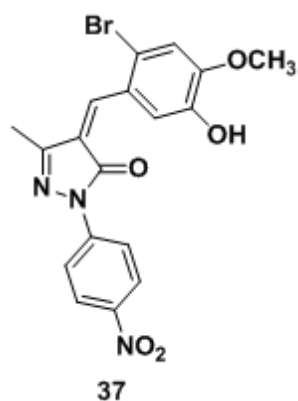
Compound **34** was obtained following the general procedures as an orange solid (130.0 mg, 68% yield). RP-HPLC $t_R = 21.8$ min, gradient condition: from 5% B to 100% B in 50 min, flow rate of 4 mL/min, $\lambda = 240$ nm. $^1\text{H NMR}$ (300 MHz, CDCl_3) δ 8.45 (d, $J = 7.5$ Hz, 1H), 8.38 (s, 1H), 8.25 (d, $J = 7.5$ Hz, 1H), 7.40 (d, $J = 1.0$ Hz, 1H), 6.96 (t, $J = 7.4$ Hz, 1H), 6.91 (ddd, $J = 7.5$, 2.1, 1.0 Hz, 1H), 6.83 (dd, $J = 7.3$, 2.2 Hz, 1H), 5.93 (s, 1H), 3.90 (s, 3H), 2.17 (q, $J = 8.0$ Hz, 2H), 1.04 (t, $J = 8.0$ Hz, 3H). ESI-MS, calcd for $\text{C}_{17}\text{H}_{16}\text{N}_4\text{O}_3$ 324.3; found $m/z = 325.3$ $[\text{M} + \text{H}]^+$.



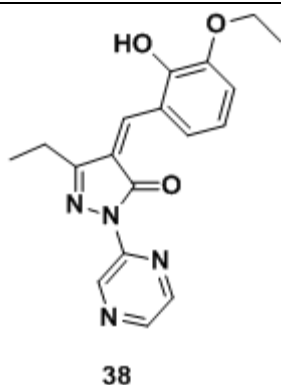
Compound **35** was obtained following the general procedures as an orange solid (130.0 mg, 65% yield). RP-HPLC $t_R = 20.4$ min, gradient condition: from 5% B to 100% B in 50 min, flow rate of 4 mL/min, $\lambda = 240$ nm. $^1\text{H NMR}$ (300 MHz, CDCl_3) δ 8.31 – 8.25 (m, 2H), 7.94 – 7.88 (m, 2H), 7.49 (d, $J = 0.9$ Hz, 1H), 7.44 (d, $J = 7.5$ Hz, 1H), 6.81 – 6.72 (m, 2H), 4.59 (s, 1H), 2.30 (s, 3H). ESI-MS, calcd for $\text{C}_{17}\text{H}_{12}\text{BrN}_3\text{O}_4$ 402.2; found $m/z = 402.2$ -404.2 $[\text{M} + \text{H}]^+$.



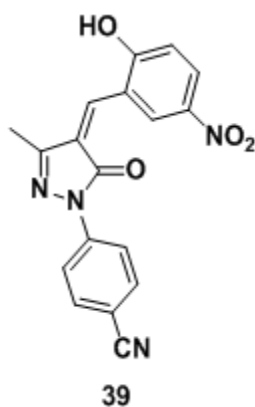
Compound **36** was obtained following the general procedures as an orange solid (130.0 mg, 70% yield). RP-HPLC $t_R = 21.4$ min, gradient condition: from 5% B to 100% B in 50 min, flow rate of 4 mL/min, $\lambda = 240$ nm. $^1\text{H NMR}$ (300 MHz, CDCl_3) δ 7.50 (dt, $J = 7.5, 5.7$ Hz, 1H), 7.40 (d, $J = 1.1$ Hz, 1H), 7.04 (td, $J = 8.9, 2.0$ Hz, 1H), 6.98 (d, $J = 7.4$ Hz, 1H), 6.96 – 6.86 (m, 2H), 6.83 (dd, $J = 7.4, 2.1$ Hz, 1H), 5.93 (s, 1H), 3.90 (s, 3H), 2.17 (q, $J = 8.0$ Hz, 2H), 1.05 (t, $J = 8.0$ Hz, 3H). ESI-MS, calcd for $\text{C}_{19}\text{H}_{16}\text{F}_2\text{N}_2\text{O}_3$ 358.3; found $m/z = 359.3$ $[\text{M} + \text{H}]^+$.



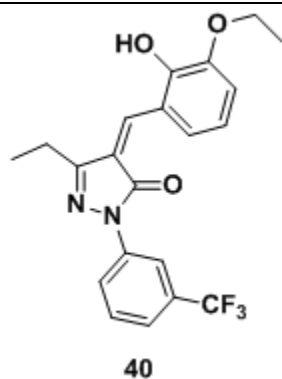
Compound **37** was obtained following the general procedures as an orange solid (110.0 mg, 60% yield). RP-HPLC $t_R = 25.4$ min, gradient condition: from 5% B to 100% B in 50 min, flow rate of 4 mL/min, $\lambda = 240$ nm. $^1\text{H NMR}$ (300 MHz, CDCl_3) δ 8.31 – 8.25 (m, 2H), 7.94 – 7.88 (m, 2H), 7.41 (d, $J = 0.9$ Hz, 1H), 7.02 (s, 1H), 6.72 (d, $J = 1.0$ Hz, 1H), 5.75 (s, 1H), 3.90 (s, 3H), 2.30 (s, 3H). ESI-MS, calcd for $\text{C}_{18}\text{H}_{14}\text{BrN}_3\text{O}_5$ 432.2; found $m/z = 432.2\text{--}434.2$ $[\text{M} + \text{H}]^+$.



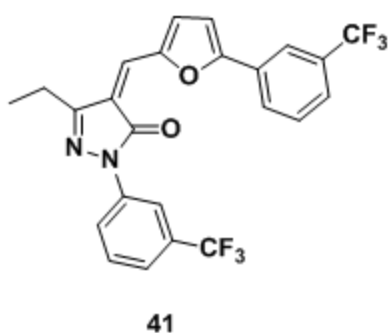
Compound **38** was obtained following the general procedures as a solid (130.0 mg, 70% yield). RP-HPLC $t_R = 21.4$ min, gradient condition: from 5% B to 100% B in 50 min, flow rate of 4 mL/min, $\lambda = 240$ nm. $^1\text{H NMR}$ (300 MHz, CDCl_3) δ 8.45 (d, $J = 7.5$ Hz, 1H), 8.38 (s, 1H), 8.25 (d, $J = 7.5$ Hz, 1H), 7.40 (d, $J = 1.1$ Hz, 1H), 6.97 (t, $J = 7.4$ Hz, 1H), 6.90 (ddd, $J = 7.5, 2.1, 1.0$ Hz, 1H), 6.83 (dd, $J = 7.4, 2.1$ Hz, 1H), 5.93 (s, 1H), 4.08 (q, $J = 8.0$ Hz, 2H), 2.17 (q, $J = 8.0$ Hz, 2H), 1.46 (t, $J = 8.0$ Hz, 3H), 1.04 (t, $J = 8.0$ Hz, 3H). ESI-MS, calcd for $\text{C}_{18}\text{H}_{18}\text{N}_4\text{O}_3$ 338.3; found $m/z = 339.3$ $[\text{M} + \text{H}]^+$.



Compound **39** was obtained following the general procedures as a solid (110.0 mg, 66% yield). RP-HPLC $t_R = 23.8$ min, gradient condition: from 5% B to 100% B in 50 min, flow rate of 4 mL/min, $\lambda = 240$ nm. $^1\text{H NMR}$ (300 MHz, CDCl_3) δ 8.24 – 8.16 (m, 2H), 8.03 – 7.96 (m, 2H), 7.84 – 7.78 (m, 2H), 7.36 (d, $J = 1.0$ Hz, 1H), 7.05 (d, $J = 7.4$ Hz, 1H), 6.78 (s, 1H), 2.30 (s, 3H). ESI-MS, calcd for $\text{C}_{18}\text{H}_{12}\text{N}_4\text{O}_4$ 348.3; found $m/z = 349.3$ $[\text{M} + \text{H}]^+$.



Compound **40** was obtained following the general procedures as a solid (120.0 mg, 76% yield). RP-HPLC $t_R = 26.8$ min, gradient condition: from 5% B to 100% B in 50 min, flow rate of 4 mL/min, $\lambda = 240$ nm. ^1H NMR (300 MHz, CDCl_3) δ 8.45 (dt, $J = 2.2, 1.2$ Hz, 1H), 7.85 (dt, $J = 7.0, 2.2$ Hz, 1H), 7.54 – 7.45 (m, 2H), 7.41 (d, $J = 0.9$ Hz, 1H), 6.97 (t, $J = 7.5$ Hz, 1H), 6.89 (ddd, $J = 7.5, 2.0, 1.0$ Hz, 1H), 6.83 (dd, $J = 7.4, 2.1$ Hz, 1H), 5.93 (s, 1H), 4.08 (q, $J = 8.0$ Hz, 2H), 2.17 (q, $J = 8.0$ Hz, 2H), 1.46 (t, $J = 8.0$ Hz, 3H), 1.05 (t, $J = 8.0$ Hz, 3H). ESI-MS, calcd for $\text{C}_{21}\text{H}_{19}\text{F}_3\text{N}_2\text{O}_3$ 404.3; found $m/z = 405.3$ $[\text{M} + \text{H}]^+$.



Compound **41** was obtained following the general procedures as a solid (132.0 mg, 80% yield). RP-HPLC $t_R = 28.9$ min, gradient condition: from 5% B to 100% B in 50 min, flow rate of 4 mL/min, $\lambda = 240$ nm. ^1H NMR (300 MHz, CDCl_3) δ 8.55 – 8.50 (m, 1H), 8.03 (dt, $J = 7.5, 2.0$ Hz, 1H), 7.91 – 7.83 (m, 2H), 7.70 (dt, $J = 7.7, 1.8$ Hz, 1H), 7.50 (dt, $J = 14.6, 7.4$ Hz, 3H), 7.29 (d, $J = 7.5$ Hz, 1H), 7.10 (d, $J = 7.5$ Hz, 1H), 6.17 (s, 1H), 2.17 (q, $J = 8.0$ Hz, 2H), 1.05 (t, $J = 8.0$ Hz, 3H). ESI-MS, calcd for $\text{C}_{24}\text{H}_{16}\text{F}_6\text{N}_2\text{O}_2$ 478.4; found $m/z = 479.4$ $[\text{M} + \text{H}]^+$.

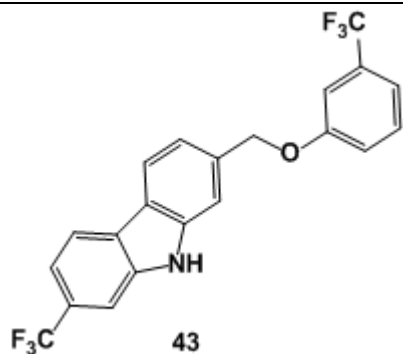
5.3 General procedure for the synthesis of carbazole compounds

5.3.1 General procedure for the preparation of 42a-42e

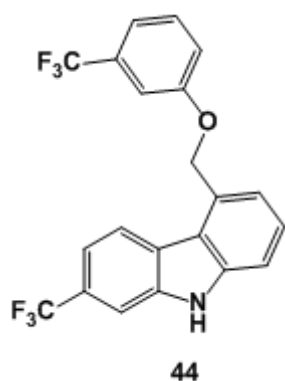
To a 25-mL flask was added a mixture of 1-bromo-2-nitro-4-(trifluoromethyl) benzene (0.18 mmol; 1 eq.), the appropriate phenylboronic acid (0.22 mmol; 1.2 eq.), K_2CO_3 (0.37 mmol; 2 eq.) and $Pd(PPh_3)_4$ (5% mmol). The flask was evacuated and backfilled with nitrogen three times. Degassed 1,4-dioxane (0.8 ml) and degassed water (0.4 ml) were added by means of an air-tight syringe. The reaction mixture was heated to reflux and stirred overnight under nitrogen atmosphere. After the solvent was removed under reduced pressure and the crude was taken up in diethyl ether. The precipitated was filtered through a Celite pad and washed with diethyl ether and concentrated *in vacuo* to give the desired products **42a-42e**, the products were used in the next step without further purification.

5.3.2 General procedure for synthesis of 43-47.

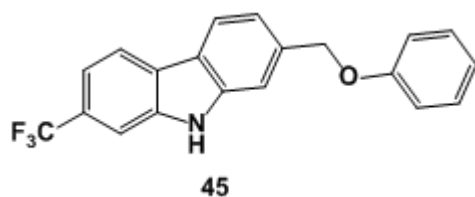
The nitro compounds **42a-42e** were suspended in triethyl phosphate (3 mL) in a tightly sealed 10 mL glass vial and was irradiated at a maximum irradiation power of 300 W for 15 min at a pre-selected temperature of 210 °C. After the reaction, the vial was cooled to 50 °C by gas jet cooling and the contents were transferred to a 50 mL flask with the help of EtOAc (10 mL). After cooling to r.t., the mixture was partitioned between H_2O and EtOAc (20 mL each) and the aqueous layer was further extracted with EtOAc (3×10 mL). The combined organic layers were dried over $NaSO_4$ and solvents were removed under reduced pressure the crude residue was purified by HPLC to give the desired products



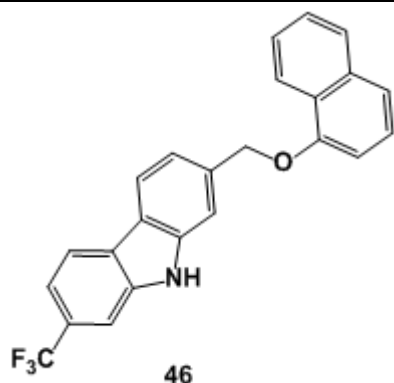
Compound **43** was obtained following the general procedures as a white solid (114.0 mg, 70% yield). RP-HPLC t_R = 35.9 min, gradient condition: from 5% B to 100% B in 50 min, flow rate of 4 mL/min, λ = 220 nm. ^1H NMR (500 MHz, CDCl_3) δ 8.03 (t, J = 7.4 Hz, 2H), 7.78 (d, J = 1.6 Hz, 1H), 7.71 (d, J = 1.4 Hz, 1H), 7.61 (s, 1H), 7.47 (dd, J = 7.5, 1.5 Hz, 1H), 7.38 – 7.30 (m, 2H), 7.23 (dq, J = 4.2, 2.0 Hz, 2H), 7.07 (dt, J = 7.5, 2.0 Hz, 1H), 5.11 (s, 2H).



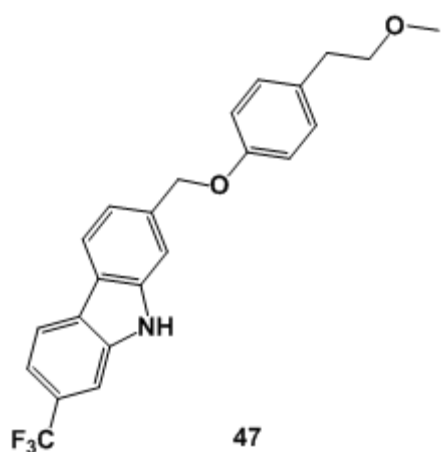
Compound **44** was obtained following the general procedures as a white solid (110.0 mg, 65% yield). RP-HPLC t_R = 34.9 min, gradient condition: from 5% B to 100% B in 50 min, flow rate of 4 mL/min, λ = 220 nm. ^1H NMR (500 MHz, CDCl_3) δ 7.95 (d, J = 7.5 Hz, 1H), 7.78 (d, J = 1.4 Hz, 1H), 7.63 – 7.56 (m, 2H), 7.42 (dd, J = 7.5, 1.5 Hz, 1H), 7.39 – 7.31 (m, 3H), 7.28 – 7.22 (m, 2H), 7.11 (dt, J = 7.3, 2.0 Hz, 1H), 5.12 (s, 2H).



Compound **45** was obtained following the general procedures as a white solid (122.0 mg, 75% yield). RP-HPLC t_R = 32.6 min, gradient condition: from 5% B to 100% B in 50 min, flow rate of 4 mL/min, λ = 220 nm. ^1H NMR (500 MHz, CDCl_3) δ 8.02 (dd, J = 7.5, 4.4 Hz, 2H), 7.78 (d, J = 1.6 Hz, 1H), 7.71 (d, J = 1.4 Hz, 1H), 7.61 (s, 1H), 7.47 (dd, J = 7.5, 1.5 Hz, 1H), 7.35 – 7.26 (m, 3H), 7.03 – 6.96 (m, 2H), 6.91 (tt, J = 7.5, 2.0 Hz, 1H), 5.11 (s, 2H).



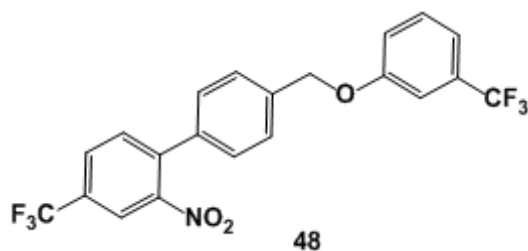
Compound **46** was obtained following the general procedures as a white solid (105.0 mg, 65% yield). RP-HPLC $t_R = 36.8$ min, gradient condition: from 5% B to 100% B in 50 min, flow rate of 4 mL/min, $\lambda = 220$ nm. $^1\text{H NMR}$ (500 MHz, CDCl_3) δ 8.34 (d, $J = 7.5$ Hz, 1H), 8.28 (dd, $J = 7.3, 1.6$ Hz, 1H), 8.15 (t, $J = 7.2$ Hz, 2H), 7.78 (dd, $J = 9.7, 1.6$ Hz, 3H), 7.66 (s, 1H), 7.54 – 7.38 (m, 4H), 7.34 (dd, $J = 7.5, 1.5$ Hz, 1H), 7.01 (dd, $J = 7.4, 1.4$ Hz, 1H), 5.11 (s, 2H).



Compound **47** was obtained following the general procedures as a white solid (95.0 mg, 70% yield). RP-HPLC $t_R = 39.2$ min, gradient condition: from 5% B to 100% B in 50 min, flow rate of 4 mL/min, $\lambda = 220$ nm. $^1\text{H NMR}$ (500 MHz, CDCl_3) δ 8.02 (t, $J = 7.1$ Hz, 2H), 7.78 (d, $J = 1.6$ Hz, 1H), 7.71 (d, $J = 1.5$ Hz, 1H), 7.60 (s, 1H), 7.47 (dd, $J = 7.5, 1.5$ Hz, 1H), 7.33 (dd, $J = 7.6, 1.5$ Hz, 1H), 7.15 (dt, $J = 7.6, 1.1$ Hz, 2H), 6.95 – 6.88 (m, 2H), 5.11 (s, 2H), 3.48 (t, $J = 7.5$ Hz, 2H), 3.23 (s, 3H), 2.73 (tt, $J = 7.5, 1.0$ Hz, 2H).

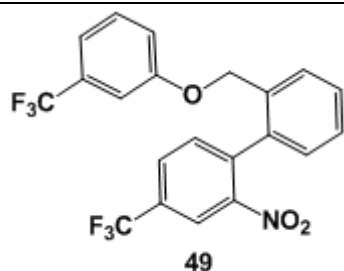
5.3.3 General procedure for the synthesis of biaryl compounds

To a 25-mL flask was added a mixture of aryl halide (i-iii, 0.18 mmol; 1 eq.), commercially available phenylboronic acid (A-L, 0.22 mmol; 1.2 eq.), K_2CO_3 (0.37 mmol; 2 eq.) and $Pd(PPh_3)_4$ (5% mmol). The flask was evacuated and backfilled with nitrogen three times. Degassed 1,4-dioxane (0.8 ml) and degassed water (0.4 ml) were added by means of an air-tight syringe. The reaction mixture was heated to reflux and stirred overnight under nitrogen atmosphere. After the solvent was removed under reduced pressure and the crude was taken up in diethyl ether. The precipitated was filtered through a Celite pad and washed with diethyl ether and concentrated *in vacuo*. The crude residue was purified by HPLC to give the pure products in good yields (70-90%) and high purity (>95%).



Compound 48 was obtained by following the general procedure as a yellow solid (90% yield). RP-HPLC $t_R = 31.5$ min, gradient condition: from 5% B to 40% B in

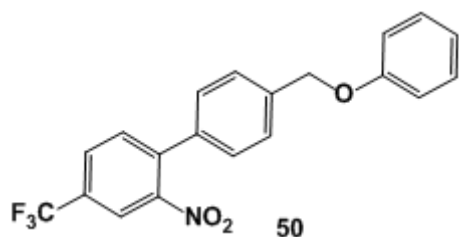
5 min, increased to 100% B in 40 min, $\lambda = 240$ nm. 1H NMR (300 MHz, $CDCl_3$) δ 8.17 (d, $J = 1.8$ Hz, 1H), 7.92 (dd, $J = 8.1, 1.8$ Hz, 1H), 7.64 (d, $J = 8.0$ Hz, 1H), 7.57 (d, $J = 8.2$ Hz, 2H), 7.45 (t, $J = 8.0$ Hz, 1H), 7.41 – 7.37 (m, 2H), 7.28 (d, $J = 7.1$ Hz, 2H), 7.21 – 7.16 (m, 1H), 5.18 (s, 2H).



Compound **49** was obtained by following the general procedure as a yellow solid (90% yield).

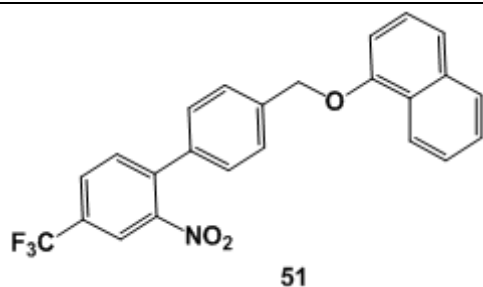
RP-HPLC t_R = 36.6 min, gradient condition: from 5% B to 40% B in 5 min, increased to 100% B in

50 min, λ = 240 nm. ^1H NMR (300 MHz, CDCl_3): δ = 8.29 (s, 1H), 7.87 (dd, J = 8.1, 1.8 Hz, 1H), 7.60 (dd, J = 7.8, 4.7 Hz, 2H), 7.52 (td, J = 7.6, 1.4 Hz, 1H), 7.47 (td, J = 7.6, 1.4 Hz, 1H), 7.35 (t, J = 8.0 Hz, 1H), 7.25 – 7.17 (m, 2H), 7.01 (t, J = 2.0 Hz, 1H), 6.96 (dd, J = 8.4, 2.5 Hz, 1H), 4.92 – 4.81 (m, 2H).



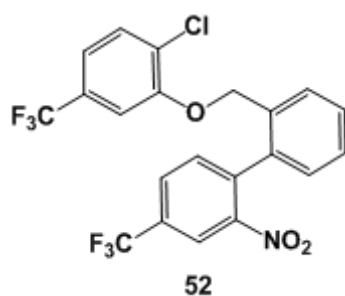
Compound **50** was obtained by following the general procedure as a yellow solid (90% yield). RP-HPLC t_R = 27.4 min, gradient condition: from 5% B

to 40% B in 5 min, increased to 100% B in 40 min, λ = 240 nm. ^1H NMR (300 MHz, CDCl_3) δ 8.17 (d, J = 1.9 Hz, 1H), 8.04 (dd, J = 7.7, 1.9 Hz, 1H), 7.94 (d, J = 7.5 Hz, 1H), 7.64 – 7.56 (m, 4H), 7.30 (t, J = 7.5 Hz, 2H), 6.99 – 6.87 (m, 3H), 5.05 (s, 2H).



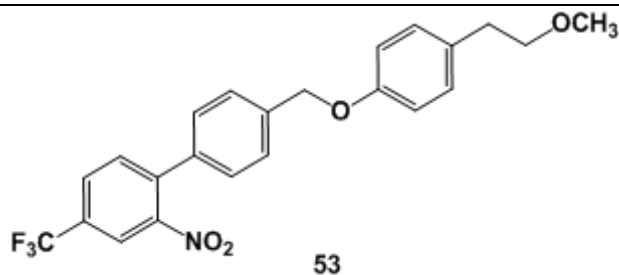
Compound **51** was obtained by following the general procedure as a yellow solid (90% yield). RP-HPLC t_R = 29.8 min, gradient condition: from

5% B to 40% B in 5 min, increased to 100% B in 40 min, λ = 240 nm. ^1H NMR (300 MHz, CDCl_3) δ 9.34 (t, J = 7.5 Hz, 1H), 8.27 (dd, J = 7.4, 1.5 Hz, 1H), 8.18 (t, J = 1.5 Hz, 1H), 8.08 – 8.02 (m, 1H), 7.95 (d, J = 7.5 Hz, 1H), 7.78 (dt, J = 7.4, 1.6 Hz, 1H), 7.67 (dd, J = 7.3, 1.3 Hz, 2H), 7.64 – 7.59 (m, 2H), 7.50 (td, J = 7.4, 1.6 Hz, 1H), 7.47 – 7.38 (m, 2H), 6.99 (dd, J = 7.5, 1.4 Hz, 1H), 5.11 (s, 2H).



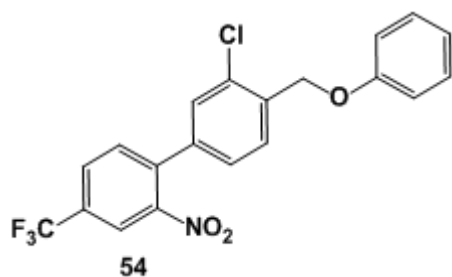
Compound **52** was obtained by following the general procedure as a yellow solid (90% yield). RP-HPLC t_R = 29.8 min, gradient condition: from 5% B to 40% B in 5 min, increased to 100% B in 40 min, λ = 240 nm. ^1H NMR (300

MHz, CDCl_3) δ 8.29 (d, J = 1.7 Hz, 1H), 8.14 – 8.08 (m, 1H), 7.95 (d, J = 7.5 Hz, 1H), 7.86 (dd, J = 7.4, 2.1 Hz, 1H), 7.59 – 7.50 (m, 2H), 7.50 – 7.42 (m, 2H), 7.30 – 7.24 (m, 1H), 6.81 (d, J = 1.8 Hz, 1H), 5.12 (d, J = 1.0 Hz, 2H).



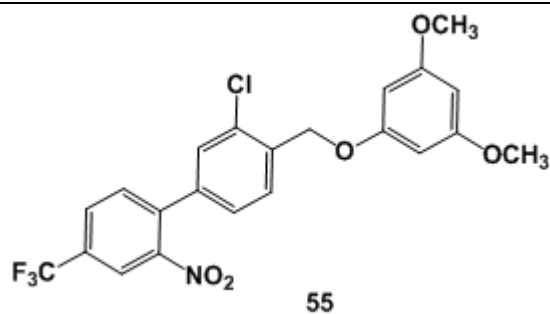
Compound **53** was obtained by following the general procedure as a yellow solid (75% yield). RP-HPLC t_R =

32.2 min, gradient condition: from 5% B to 40% B in 5 min, increased to 100% B in 40 min, λ = 240 nm. ^1H NMR (300 MHz, CDCl_3) δ 8.18 (dd, J = 1.9, 0.9 Hz, 1H), 8.08 – 8.02 (m, 1H), 7.94 (d, J = 7.4 Hz, 1H), 7.59 (s, 4H), 7.16 (dt, J = 7.6, 1.2 Hz, 2H), 6.90 – 6.83 (m, 2H), 5.05 (s, 2H), 3.48 (t, J = 4.3 Hz, 2H), 3.23 (s, 3H), 2.76 – 2.70 (m, 2H).



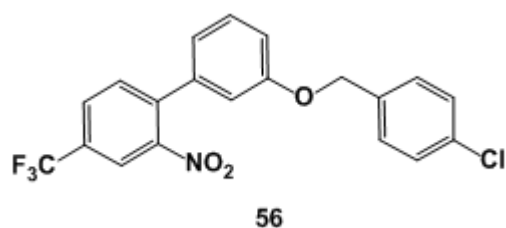
Compound **54** was obtained by following the general procedure as a yellow solid (85% yield). RP-HPLC t_R = 30.2 min, gradient condition: from 5% B to 40% B

in 5 min, increased to 100% B in 40 min, λ = 240 nm. ^1H NMR (300 MHz, CDCl_3) δ 8.23 – 8.19 (m, 1H), 8.06 (dd, J = 7.5, 1.9 Hz, 1H), 7.95 (d, J = 7.4 Hz, 1H), 7.66 – 7.58 (m, 2H), 7.41 (dd, J = 7.5, 2.0 Hz, 1H), 7.30 (t, J = 7.5 Hz, 2H), 7.01 – 6.95 (m, 2H), 6.91 (tt, J = 7.5, 2.1 Hz, 1H), 5.12 (d, J = 1.0 Hz, 2H).



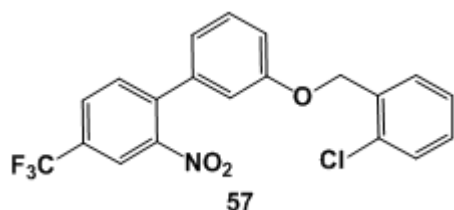
Compound **55** was obtained by following the general procedure as a yellow solid (77% yield). RP-HPLC $t_R = 30.2$ min, gradient condition: from 5% B to 40% B in 5 min, increased to 100% B in

40 min, $\lambda = 240$ nm. $^1\text{H NMR}$ (300 MHz, CDCl_3) δ 8.24 – 8.19 (m, 1H), 8.05 (dd, $J = 7.7, 1.9$ Hz, 1H), 7.94 (d, $J = 7.4$ Hz, 1H), 7.66 – 7.60 (m, 2H), 7.40 (dd, $J = 7.5, 2.0$ Hz, 1H), 6.14 (d, $J = 2.0$ Hz, 2H), 6.08 (t, $J = 2.0$ Hz, 1H), 5.12 (d, $J = 1.0$ Hz, 2H), 3.84 (s, 6H).



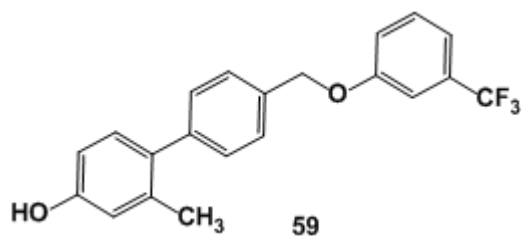
Compound **56** was obtained by following the general procedure as a yellow solid (77% yield). RP-HPLC $t_R = 31.5$ min, gradient condition: from 5% B to 40% B in 5 min, increased to 100% B in 40 min, $\lambda = 240$ nm. $^1\text{H NMR}$ (300 MHz, CDCl_3) δ

8.18 (d, $J = 1.8$ Hz, 1H), 8.03 (dd, $J = 7.5, 1.9$ Hz, 1H), 7.92 (d, $J = 7.5$ Hz, 1H), 7.43 – 7.36 (m, 5H), 7.23 (dd, $J = 6.6, 2.0$ Hz, 2H), 6.82 (dt, $J = 7.5, 2.0$ Hz, 1H), 5.05 (s, 2H).



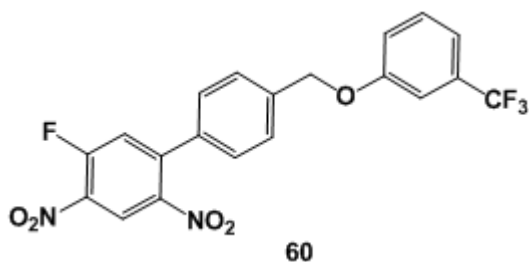
Compound **57** was obtained by following the general procedure as a yellow solid (79% yield). RP-HPLC t_R = 31.2 min, gradient condition: from 5% B to 40% B in 5 min, increased to 100%

B in 40 min, λ = 240 nm. $^1\text{H NMR}$ (300 MHz, CDCl_3) δ 8.19 – 8.14 (m, 1H), 8.01 (dt, J = 7.6, 1.5 Hz, 1H), 7.88 (d, J = 7.5 Hz, 1H), 7.48 – 7.43 (m, 2H), 7.43 – 7.36 (m, 1H), 7.31 – 7.20 (m, 3H), 7.16 (dt, J = 7.5, 2.0 Hz, 1H), 6.82 (dt, J = 7.5, 2.0 Hz, 1H), 5.12 (d, J = 0.9 Hz, 2H).



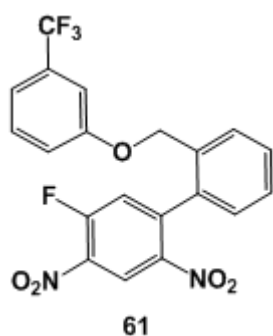
Compound **59** was obtained by following the general procedure as a yellow solid (70% yield). RP-HPLC t_R = 27.2 min, gradient condition: from 5% B to 40% B in

5 min, increased to 100% B in 40 min, λ = 240 nm. $^1\text{H NMR}$ (300 MHz, CDCl_3) δ 7.60 (dt, J = 7.4, 1.1 Hz, 2H), 7.57 – 7.51 (m, 2H), 7.37 – 7.28 (m, 2H), 7.25 – 7.17 (m, 2H), 7.03 (dt, J = 7.5, 2.0 Hz, 1H), 6.83 – 6.75 (m, 2H), 5.05 (d, J = 1.4 Hz, 2H), 2.30 (d, J = 1.1 Hz, 3H).

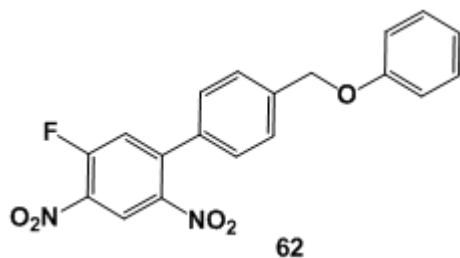


Compound **60** was obtained by following the general procedure as a white solid (85% yield). RP-HPLC t_R = 23.8 min, gradient condition: from 5% B to 40% B in 5 min, increased to 100% B in 40

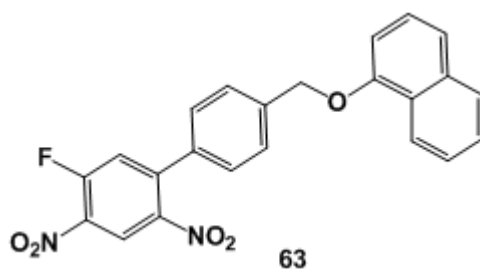
min, λ = 280 nm. $^1\text{H NMR}$ (300 MHz, CDCl_3): δ = 8.86 (d, J = 1.6 Hz, 1H), 7.58 (d, J = 8.1 Hz, 2H), 7.46 (t, J = 8.0 Hz, 1H), 7.40 – 7.37 (m, 2H), 7.27 (d, J = 3.6 Hz, 3H), 7.19 (dd, J = 8.4, 2.5 Hz, 1H), 5.20 (s, 2H).



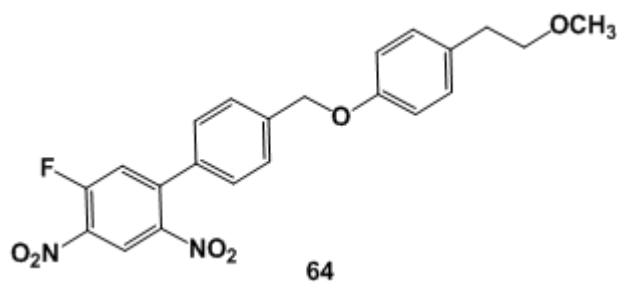
Compound **61** was obtained by following the general procedure as a white solid (90% yield). RP-HPLC t_R = 24.3 min, gradient condition: from 5% B to 40% B in 5 min, increased to 100% B in 40 min, λ = 280 nm. ^1H NMR (400 MHz, CDCl_3): δ = 8.95 (s, 1H), 7.64 – 7.57 (m, 1H), 7.57 – 7.46 (m, 2H), 7.37 (t, J = 8.0 Hz, 1H), 7.23 (tt, J = 3.4, 1.7 Hz, 3H), 7.05 – 6.94 (m, 2H), 4.95 – 4.81 (m, 2H).



Compound **62** was obtained by following the general procedure as an orange solid (70% yield). RP-HPLC t_R = 24.7 min, gradient condition: from 5% B to 40% B in 5 min, increased to 100% B in 40 min, λ = 280 nm. ^1H NMR (400 MHz, CDCl_3): δ = 8.78 (s, 1H), 7.51 – 7.42 (m, 3H), 7.42 – 7.36 (m, 1H), 7.31 – 7.27 (m, 3H), 7.24 (s, 1H), 7.12 – 7.06 (m, 2H), 5.15 (s, 2H).



Compound **63** was obtained by following the general procedure as a yellow solid (90% yield). RP-HPLC t_R = 36.5 min, gradient condition: from 5% B to 40% B in 5 min, increased to 100% B in 60 min, λ = 280 nm. ^1H NMR (400 MHz, CDCl_3): δ = 8.85 (s, 1H), 8.43 – 8.34 (m, 1H), 7.89 – 7.82 (m, 1H), 7.68 (d, J = 8.0 Hz, 2H), 7.60 – 7.47 (m, 3H), 7.47 – 7.36 (m, 3H), 7.28 (s, 1H), 6.94 (d, J = 7.6 Hz, 1H), 5.36 (s, 2H).

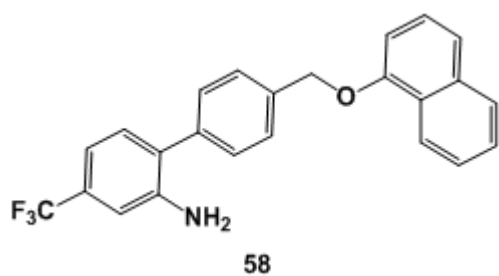


Compound **64** was obtained by following the general procedure as a yellow solid (90% yield). RP-HPLC t_R = 36.5 min, gradient condition: from 5% B to

40% B in 5 min, increased to 100% B in 60 min, λ = 280 nm. ^1H NMR (400 MHz, CDCl_3): δ = 8.85 (s, 1H), 7.57 (d, J = 8.1 Hz, 2H), 7.39 – 7.34 (m, 2H), 7.26 (s, 1H), 7.20 (d, J = 8.5 Hz, 2H), 6.98 – 6.94 (m, 2H), 5.14 (s, 2H), 3.62 (t, J = 7.1 Hz, 2H), 3.40 (s, 3H), 2.88 (t, J = 7.1 Hz, 2H).

5.3.3.1 Synthesis of 58

To 5 mL of a EtOH solution containing **51** (1.0 equiv) was added stannous chloride dehydrate (5.0 equiv) and the reaction mixture was refluxed for 18 h. The reaction mixture was evaporated and extracted with ethyl ether and NaOH solution. The resulted suspension was then filtered with Celite. The filter cake was washed with ethyl ether while the filtrate was extracted with ethyl ether. The organic layers were combined, dried over anhydrous Na_2SO_4 and concentrated under vacuum.



Compound **58** was obtained by following the general procedure as a yellow solid (65% yield). RP-HPLC t_R = 28.5 min, gradient condition: from 5% B to 40% B in 5 min, increased to 100% B in 60 min, λ =

240 nm. ^1H NMR (300 MHz, CDCl_3) δ 9.34 (t, J = 7.5 Hz, 1H), 8.30 (dd, J = 7.5, 1.5 Hz, 1H), 7.78 (dt, J = 7.5, 1.6 Hz, 1H), 7.70 – 7.59 (m, 4H), 7.50 (td, J = 7.4, 1.6 Hz, 1H), 7.47 – 7.38 (m, 2H), 7.22 – 7.17 (m, 2H), 7.14 (dd, J = 7.6, 2.0 Hz, 1H), 6.90 – 6.85 (m, 1H), 5.11 (s, 2H).

References

- [1] With cancer term refers to a group of more than 100 diseases in which cells begin to grow out of control. *International Journal of pharmaceutical compounding* (2008), **1**, 12.
- [2] G. Bergers and L.E. Benjamin, *Nature Reviews Cancer* (2003), **3**, 401-410.
- [3] Parkin DM, Bray F, Ferlay J, Pisani P. *CA Cancer J Clin* (2005), **55**, 74–108.
- [4] *Stewart, BW; Wild, CP, eds. (2014). "Cancer etiology". World Cancer Report 2014. World Health Organization. ISBN 9283204298.*
- [5] Bartkova J., Horčejšič Z., Koed K., Kraemer A., Tort F., Zieger K., Guldborg P., Sehested M., Nesland J.M., Lukas C., Ørntoft T., Lukas J., Bartek J. *Nature* (2005), **434**, 864-870.
- [6] Wyld L., Audisio R.A., Poston G.J. *Nature Reviews Clinical Oncology* (2015) **12**, 115–124.
- [7] Chabner B.A. and Roberts Jr T.G. *Nature Reviews Cancer* (2005), **5**, 65-72.
- [8] Papac, R. J. *Yale J. Biol. Med.* (2001) **74**, 391–398.
- [9] Osler W. *The principles and practice of medicine*. New York: D. Appleton and Company; 1893. p. 708.
- [10] Brested JH. *The Edwin Smith surgical papyrus*. Translated for The New York Historical Society. Chicago (IL): University of Chicago Press; 1930.

-
- [11] DeVita VT, Jr; Chu, E *Cancer Research*. (2008), 68 (21), 8643–86453.
- [12] Special Virus Cancer Program: Travails of a Biological Moonshot. *Science* (1971), Vol. **174**, Issue 4016, pp. 1306-1311. DOI: 10.1126/science.174.4016.1306
- [13] Fischinger P, DeVita VT. *Cancer Res* (1984), **44**, 4693–6.
- [14] Hanahan, D. & Weinberg, R. A. *Cell* (2000), **100**, 57–70.
- [15] G. Majno, I. Joris. *Cells, Tissues and Disease* (Oxford Univ. Press, 2004).
- [16] A. Scott, K.M. Khan, J.L. Cook, V. Duronio. What is “inflammation”? Are we ready to move beyond Celsus? *Brit. J. Sports Med.* (2004), **38**, 248– 249.
- [17] L. Frati, M. Russo. *Istituto dell’ enciclopedia -TRECCANI s.p.a* (2000)
- [18] A.B. Abbas, A.H. Lichtman. (2009). "Ch.2 Innate Immunity". In *Saunders (Elsevier). Basic Immunology. Functions and disorders of the immune system* (3rd ed.).
- [19] A.L. Graham, J.E. Allen, A.F. Read. *Annu. Rev. Ecol. Evol. Syst.* (2005), **36**, 373–93.
- [20] J. R. Vane. *J Physiol Pharmacol.* (2000), **51**, 573-586 and reference cited therein.
- [21] N.U. Horadagoda, K.M. Knox, H.A. Gibbs, S.W. Reid, A. Horadagoda, S.E. Edwards, P.D. Eckersall. *Veterinary Record* (1999), **144**, 437-441
- [22] M. Murakami, T. Hirano. *Front Immunol.* (2012), **3**, 323.

- [23] R. Tamblyn, L. Berkson, W. D. Dauphinee, D. Gayton, R. Grad, A. Huang, L. Isaac, P. McLeod, and L. Snell. *Ann Intern Med*, (1997), **127**, 429-438.
- [24] E.R. Rayburn, S.J. Ezell, R. Zhang. *Mol Cell Pharmacol*. (2009), **1(1)**, 29–43.
- [25] M.M. Wolfe, D.R. Lichtenstein, G. Singh. *N. Engl. J. Med*. (1999), **340**, 1888-1899.
- [26] P. Mehta, J.C. Mason. *Topical Reviews*. (2010), **6(5)**, 1-10.
- [27] D. Nikitovic, M. Tzardi, A. Berdiaki, A. Tsatsakis, G.N. Tzanakakis. *Front Immunol*. (2015), **6**, 169.
- [28] F. Balkwill, A. Mantovani. *Lancet* (2001), **357**, 539–545.
- [29] C. Porta, P. Larghi, M. Rimoldi, M.G. Totaro, P. Allavena, A. Mantovani, A. Sica. *Immunobiology* (2009), **214**, 761-77.
- [30] A. Mantovani, P. Allavena, A. Sica, F. Balkwill. *Nature* (2008), **454**, 436-444.
- [31] A. Mantovani. *Nature* (2009), **457**, 36-7.
- [32] A.M. De Marzo, E.A. Platz, S. Sutcliffe, J. Xu, H. Gronberg, C.G. Drake, Y. Nakai, W.B. Isaacs, W.G. Nelson. *Nat Rev Cancer* (2007), **7**, 256-69.
- [33] H. Yu, M. Kortylewski, D. Pardoll. *Nat Rev Immunol* (2007), **7**, 41- 51.
- [34] J. Rius, M. Guma, C. Schachtrup, K. Akassoglou, A.S. Zinkernagel, V. Nizet, R.S. Johnson, G.G. Haddad, M. Karin. *Nature* (2008), **453**, 807-11.
- [35] F. Balkwill. *Nature Rev. Cancer* (2004), **4**, 540–550.
- [36] F.H. Igney, P.H. Krammer. *J Leukoc Biol* (2002), **71**, 907-20.

- [37] B. Seliger. *BioDrugs* (2005), **19**, 347-54.
- [38] N. Arber, R.N. DuBois. *Curr. Gastroenterol. Rep.* (1999), **1(5)**, 441-8.
- [39] T. Lancaster, C. Silagy. *Dig Dis.* (1994), **12(3)**,170-6.
- [40] N. Arber. *Can. J. Gastroenterol.* (2000), **14(4)**, 299-307.
- [41] I. Mellman, G. Coukos, G. Dranoff. *Nature* (2011), **480**, 480-9.
- [42] B.B. Aggarwal, R.V. Vijayalekshmi, B. Sung. *Clin Cancer Res* (2009), **15**, 425-30.
- [43] Nicolaou K.C., *Angewandte Chemie International Edition* (2014), **53**, 9128-9140.
- [44] Burley, S. K.; Park, F. *Genome Biology* (2005), **6**, 330-330.
- [45] R.L. Elliott. *ACS Med. Chem. Lett.* (2012), **3**, 688 – 690.
- [46] David Taylor, The Pharmaceutical Industry and the Future of Drug Development, in *Pharmaceuticals in the Environment*, 2015, pp. 1-33 ISBN:978-1-78262-234-5
- [47] Newman D. J., Cragg G. M. *Journal of natural products* (2012), **75**, 311-335.
- [48] Laufer, S.; Holzgrabe, U.; Steinhilber, D. *Angewandte Chemie International Edition* (2013), **52**, 4072-4076.
- [49] Kassel, D. B. In *HPLC for Pharmaceutical Scientists*, John Wiley & Sons, Inc.: 2006; pp 533-575.
- [50] Hulme, C.; Akritopoulou-Zanze, I.; Dai, W.-M.; Beck, B.; Srivastava, S.; Wang, W.; Wang, K.; Czarna, A.; Holak, T.; Meireles, L.; Camacho, C.; Raghavan, B.; Day, B.; Dömling, A.; Qin, C.; Zhang, R.; Wang, Q.; Ren, J.; Tian, L.; Nikulnikov, M.; Krasavin, M.; Krasavin, M.; Parchinsky, V.; Shkavrov, S.; Bukhryakov, K.; Tsirulnikov, S.;

- Krasavin, M.; Bushkova, E.; Parchinsky, V.; Krasavin, M.; Kalinski, C.; Kysil, V.; Tsirolnikov, S.; Ivachtchenko, A.; Potapov, V.; Kysil, V.; Fetisova, N.; Nikitin, A.; Ivachtchenko, A.; Potapov, V.; Ilyn, A.; Fetisova, N.; Kravchenko, D.; Ivachtchenko, A.; Shilova, O.; Ilyin, A.; Ivachtchenko, A.; Shkirando, A.; Kysil, V.; Potapov, V.; Ivachtchenko, A.; Vaddula, B.; Kumar, D.; Sharad, S.; Dube, U.; Kapur, S. Multi-Component Reactions in Drug Discovery. *In MCR 2009*, Mironov, M. A., Ed. Springer New York: (2011); Vol. **699**, pp 75-106.
- [51] Kappe, C. O.; Dallinger, D. *Nat Rev Drug Discov* (2006), **5**, 51-63.
- [52] Wirth, T. *ChemSusChem* (2012), **5**, 215-216.
- [53] Wang W.X., Vinocur B., Shoseyov O., Altmanet A. *Acta Horti* (2001), **560**, 285–292.
- [54] Hartl, F. U. & Hayer-Hartl, M. *Nature Struct. Mol. Biol.* (2009), **16**, 574–581.
- [55] Saibil, H. *Nat Rev Mol Cell Biol* **2013**, 14, 630-42.
- [56] Jego G, Hazoumé A, Seigneuric R and Garrido C. *Cancer Lett* (2013), **332**, 275-285.
- [57] M. V. Powers and P. Workman. *FEBS Letters*, (2007), **581**, 19, pp. 3758–3769.
- [58] Xia Y, Rocchi P, Iovanna JL and Peng L. *Drug Discov Today* (2012), **17**, 35-43.
- [59] Joly AL, Wettstein G, Mignot G, Ghiringhelli F and Garrido C. *J Innate Immun* (2010), **2**, 238-247.
- [60] Johnson, J. L. *Biochimica et Biophysica Acta (BBA) - Molecular Cell Research* (2012), **1823**, 607-613.
- [61] Banerji U. *Clin Cancer Res* (2009), **15**, 9-14.

- [62] Fukuda A, Osawa T, Oda H, Tanaka T, Toyokuni S and Uchida K. *Biochem Biophys Res Commun* (1996), **219**, 76-81.
- [63] Boehm J, Orth T, Van Nguyen P and Soling HD. *Eur J Clin Invest* (1994), **24**, 248-257.
- [64] Whitesell, L.; Lindquist, S. L. *Nat Rev Cancer* (2005), **5**, 761-72.
- [65] Pratt WB. *Proc Soc Exp Biol Med* (1998), **217**, 420-434.
- [66] Hanahan D and Weinberg RA. *Cell* (2000), **100**, 57-70.
- [67] Holzbeierlein JM, Windsperger A and Vielhauer G. *Curr Oncol Rep* (2010), **12**, 95-101.
- [68] Amolins MW and Blagg BS. *Mini Rev Med Chem* (2009), **9**, 140-152.
- [69] Hanahan D and Weinberg RA. *Cell* (2011), **144**, 646-674.
- [70] Khong T and Spencer A. *Mol Cancer Ther* (2011), **10**, 1909-1917.
- [71] Neckers L. *Rends. Mol. Med.* (2002), **8**, 555-561.
- [72] Hartl FU, Bracher A and Hayer-Hartl M. *Nature* (2011), **475**, 324-332.
- [73] Prodromou, C.; Roe, S. M.; O'Brien, R.; Ladbury, J. E.; Piper, P. W.; Pearl, L. H. *Cell* (1997), **90**, 65-75.
- [74] Prodromou, C., Panaretou, B., Chohan, S., Siligardi, G., O'Brien, R., Ladbury, J. E., Roe, S. M., Piper, P. W., and Pearl, L. H. *EMBO J.* (2000), **19**, 4383-4392.
- [75] Ali, M. M., Roe, S. M., Vaughan, C. K., Meyer, P., Panaretou, B., Piper, P. W., Prodromou, C., and Pearl, L. H. *Nature* (2006), **440**, 1013-1017.
- [76] Hawle, P.; Siepmann, M.; Harst, A.; Siderius, M.; Reusch, H. P.; Obermann, W. M. *Mol Cell Biol* (2006), **26**, 8385-95.

- [77] Garnier, C.; Lafitte, D.; Tsvetkov, P. O.; Barbier, P.; Leclerc-Devin, J.; Millot, J. M.; Briand, C.; Makarov, A. A.; Catelli, M. G.; Peyrot, V. *J Biol Chem* (2002), **277**, 12208-14.
- [78] Soti, C.; Racz, A.; Csermely, P. *J Biol Chem* (2002), **277**, 7066-75.
- [79] Mickler, M., Hessling, M., Ratzke, C., Buchner, J., and Hugel, T. *Nat Struct Mol Biol* (2009), **16**, 281-286.
- [80] Soti, C.; Vermes, A.; Haystead, T. A.; Csermely, P. *Eur J Biochem* (2003), **270**, 2421-8
- [81] Scheufler, C., Brinker, A., Bourenkov, G., Pegoraro, S., Moroder, L., Bartunik, H., Hartl, F. U., and Moarefi, I. *Cell* (2000), **101**, 199-210.
- [82] Akerfelt M, Morimoto RI and Sistonen L. *Nat Rev Mol Cell Biol* (2010), **11**, 545-555.
- [83] A. Maloney, P. Workman, *Expert Opin. Biol. Ther.* (2002), **2**, 3– 24.
- [84] Taipale M, Jarosz DF and Lindquist S. *Nat Rev Mol Cell Biol* (2010), **11**, 515-528.
- [85] Normant E, Paez G and West KA. *Oncogene* (2011), **30**, 2581-2586.
- [86] Obermann, W. M., Sondermann, H., Russo, A. A., Pavletich, N. P., and Hartl, F. U. *J Cell Biol* (1998), **143**, 901-910.
- [87] Shiau, A. K., Harris, S. F., Southworth, D. R., and Agard, D. A. *Cell* (2006), **127**, 329-340.
- [88] Mickler, M., Hessling, M., Ratzke, C., Buchner, J., and Hugel, T. *Nat Struct Mol Biol* (2009), **16**, 281-286
- [89] Hessling, M., Richter, K., and Buchner, J. *Nat Struct Mol Biol* (2009), **16**, 287-293.

- [90] Panaretou, B. Siligardi G, Meyer P, Maloney A, Sullivan JK, Singh S, Millson SH, Clarke PA, Naaby-Hansen S, Stein R, Cramer R, Mollapour M, Workman P, Piper PW, Pearl LH, Prodromou C. *Mol Cell* (2002), **10**, 1307–1318.
- [91] MacLean, M. & Picard, D. *Cell Stress Chaperones* (2003), **8**, 114–119.
- [92] McLaughlin, S. H. Sobott F, Yao ZP, Zhang W, Nielsen PR, Grossmann JG, Laue ED, Robinson CV, Jackson SE. *J Mol Biol* (2006), **356**, 746–758.
- [93] Taldone T, Sun W, Chiosis G. *Bioorg Med Chem* (2009), **17**, 2225-2235.
- [94] Porter JR, Fritz CC, Depew KM. *Curr Opin Chem Biol* (2010), **14**, 412-420.
- [95] Jez J.M., Chen J.C.H., Rastelli G., Stroud R.M., Santi D.V. *Chem. Biol.* (2003), **10**, 361-368.
- [96] Z. Q. Yang, X. Geng, D. Solit, C. A. Pratilas, N. Rosen, S. J. Danishefsky, *J. Am. Chem. Soc.* (2004), **126**, 7881– 7889.
- [97] Y. Ikunia, N. Amishiro, M. Miyata, H. Narumi, H. Ogaea, T. Akiyama, Y. Shiotsu, S. Akinaga, C. Murakata, *J. Med. Chem.* (2003), **46**, 2534 – 2541.
- [98] E. Moulin, V. Zoete, S. Barluenga, M. Karplus, N. Winssinger, *J. Am. Chem. Soc.* (2005), **127**, 6999 –7004.
- [99] E. Moulin, S. Barluenga, N. Winssinger, *Org. Lett.* (2005), **7**, 5637 – 5639.
- [100] G. Chiosis, M. N. Timaul, B. Lucas, P. N. Munster, F. F. Zheng, L. Sepp- Lorenzino, N. A. Rosen, *Chem. Biol.* (2001), **8**, 289 –299.

- [101] G. Chiosis, B. Lucas, A. Shtil, H. Huevo, N. Rosen, *Bioorg. Med. Chem.* (2002), **10**, 3555–3564.
- [102] H. He, D. Zatorska, J. Kim, J. Aguirre, L. Llauger, Y. She, N. Wu, R. M. Immormino, D. T. Gewirth, G. Chiosis, *J. Med. Chem.* (2006), **49**, 381–390.
- [103] X. Barril, M. C. Beswick, A. Collier, M. J. Drysdale, B. W. Dymock, A. Fink, K. Grant, R. Howes, A. M. Jordan, A. Massey, A. Surgenor, J. Wayne, P. Workman, L. Wright, *Bioorg. Med. Chem. Lett.* (2006), **16**, 2543–2548.
- [104] X. Barril, P. Brough, M. Drysdale, R. E. Hubbard, A. Massey, A. Surgenor, L. Wright, *Bioorg. Med. Chem. Lett.* (2005), **15**, 5187–5191.
- [105] F. Dal Piaz, A. Vassallo, A. Temraz, R. Cotugno, M.A. Belisario, G. Bifulco, M.G. Chini, C. Pisano, N. De Tommasi and A. Braca. *J. Med. Chem.* (2013), **56**, 1583–1595.
- [106] R. C. Clevenger, B. S. J. Blagg, *Org. Lett.* (2004), **6**, 4459–4462.
- [107] G. Shen, B. S. J. Blagg, *Org. Lett.* (2005), **7**, 2157–2160.
- [108] M. Wang, G. Shen, B. S. J. Blagg, *Bioorg. Med. Chem. Lett.* (2006), **16(9)**, 2459–2462.
- [109] Jhaveri, K.; Taldone, T.; Modi, S.; Chiosis, G. *Biochimica et Biophysica Acta (BBA) - Molecular Cell Research* (2012), **1823**, 742–755.
- [110] J. R. McConnell and S. R. McAlpine, *Bioorg. Med. Chem. Lett.* (2013), **23**, 1923–1928.

- [111] Oki, Y.; Copeland, A.; Romaguera, J.; Fayad, L.; Fanale, M.; Faria Sde, C.; Medeiros, L. J.; Ivy, P.; Younes, A. *Leuk Lymphoma* (2012), **53**, 990-2.
- [112] Samarasinghe, B.; Wales, C. T. K.; Taylor, F. R.; Jacobs, A. T. *Biochemical Pharmacology* (2014), **87**, 445-455.
- [113] Bagatell, R.; Paine-Murrieta, G. D.; Taylor, C. W.; Pulcini, E. J.; Akinaga, S.; Benjamin, I. J.; Whitesell, L. *Clinical Cancer Research* (2000), **6**, 3312-3318.
- [114] Powers, M. V.; Workman, P. *FEBS Lett.* (2007), **581**, 3758-69.
- [115] Whitesell, L.; Bagatell, R.; Falsey, R. *Curr. Cancer Drug Targets* (2003), **3**, 349-358.
- [116] Shelton, S. N.; Shawgo, M. E.; Matthews, S. B.; Lu, Y.; Donnelly, A. C.; Szabla, K.; Tanol, M.; Vielhauer, G. A.; Rajewski, R. A.; Matts, R. L.; Blagg, B. S. J.; Robertson, J. D. *Mol. Pharmacol.* (2009), **76**, 1314-1322.
- [117] Eskew, J. D.; Sadikot, T.; Morales, P.; Duren, A.; Dunwiddie, I.; Swink, M.; Zhang, X.; Hembruff, S.; Donnelly, A.; Rajewski, R. A.; Blad, B.; Manjarrez, J. R.; Matts, R. L.; Holzbeierlein, J. M.; Vielhauer, G. A. *BMC Cancer* (2011), **11**, 468.
- [118] Zhao, H.; Donnelly, A. C.; Kusuma, B. R.; Brandt, G. E. L.; Brown, D.; Rajewski, R. A.; Vielhauer, G.; Holzbeierlein, J.; Cohen, M. S.; Blagg, B. S. *J. Med. Chem.* (2011), **54**, 3839.
- [119] Marcu, M. G., Chadli, A., Bouhouche, I., Catelli, M., and Neckers, L. *M. J. Biol. Chem.* (2000), **275**, 37181-37186.
- [120] Marcu, M. G., Schulte, T. W., and Neckers, L. *J. Natl. Cancer Inst.* (2000), **92**, 242-248.

- [121] Peyrat JF, Messaoudi S, Brion JD and Alami M. *Atlas Genet Cytogenet Oncol Haematol* (2011), **15**, 89-105.
- [122] Burlison JA and Blagg BS. *Org Lett* (2006), **8**, 4855-4858.
- [123] Shelton SN, Shawgo ME, Matthews SB. *Mol Pharmacol* (2009), **76**, 1314-1322.
- [124] Eskew JD, Sadikot T, Morales P. *BMC Cancer* (2011), **11**, 468.
- [125] C.M. Palermo, C.A. Westlake, T.A. Gasiewicz. *Biochemistry* (2005), **44**, 5041-5052.
- [126] D.B. Solit, A.D. Basso, A.B. Olshen, H.I. Scher, N. Rosen. *Cancer Res.* (2003), **63**, 2139-2144.
- [127] C. Soti, A. Racz, P.A. Csermely. *J. Biol. Chem.* (2002), **277**, 7066-7075.
- [128] Ardi, V. C.; Alexander, L. D.; Johnson, V. A.; McAlpine, S. R. *ACS Chem Biol* (2011), **6**, 1357-66.
- [129] Sellers, R. P.; Alexander, L. D.; Johnson, V. A.; Lin, C. C.; Savage, J.; Corral, R.; Moss, J.; Slugocki, T. S.; Singh, E. K.; Davis, M. R.; Ravula, S.; Spicer, J. E.; Oelrich, J. L.; Thornquist, A.; Pan, C. M.; McAlpine, S. R. *Bioorg Med Chem* (2010), **18**, 6822-56.
- [130] Cueto, M.; Jensen, P. R.; Fenical, W. *Phytochem.* (2000), **55** (3), 223-226.
- [131] M. Strocchia, S. Terracciano, M.G. Chini, A. Vassallo, M.C. Vaccaro, F. Dal Piaz, A. Leone, R. Riccio, I. Bruno and G. Bifulco. *Chem. Commun.*, (2015), **51**, 3850-3853.
- [132] Conde R, Belak ZR, Nair M, O'Carroll RF, Ovsenek N. *Biochem Cell Biol* (2009), **87**, 845-51.

- [133] Sreeramulu S, Gande SL, Gobel M, Schwalbe H. *Angew. Chem. Int.* (2009), **48**, 5853–5855.
- [134] Li, Y.; Karagoz, G. E.; Seo, Y. H.; Zhang, T.; Jiang, Y.; Yu, Y.; Duarte, A. M.; Schwartz, S. J.; Boelens, R.; Carroll, K.; Rudiger, S. G.; Sun, D. *J Nutr Biochem* (2012), **23**, 1617-26.
- [135] Yi F, Zhu P, Southall N, Inglese J, Austin CP, Zheng W, Regan L. *J. Biomol. Screen* (2009), **14**, 273–281.
- [136] Majno, G. & Joris, I. *Cells, Tissues and Disease* (Oxford Univ. Press, 2004)
- [137] Balkwill, F., Charles, K. A. & Mantovani, A. *Cancer Cell* (2005), **7**, 211–217.
- [138] A. Mantovani, P. Allavena, A. Sica, F. Balkwill. *Nature Insight* (2008), **454**, 436-444.
- [139] W.L. Smith, L.J. Marnett, D.L. DeWitt. *Pharmacol Ther* (1991), **49**, 153-79.
- [140] F.M. Johnson, P. Yang, R.A. Newman, N.J. Donato. *Journal of experimental therapeutics & oncology* (2004), **4(4)**, 317-25.
- [141] W.L. Smith, Y. Urade, P.L. Jakobsson. *Chemical Reviews* (2011), **111**, 5821-5865.
- [142] C.M. Hao, M.D. Breyer. *Kidney Int.* (2007), **71**, 1105-1115.
- [143] Y. Sugimoto, S. Narumiya. *J. Biol. Chem.* (2007), **282**, 11613-11617.
- [144] D.M. Aronoff, C. Canetti, M. Peter-Golden. *J. Immunol.* (2004), **173**, 559-565.

- [145] E. C.-J. A.C.P. de Oliveira, J. Langbein, L. Wendeburg, H.S. Bhatia, J.C.M. Schlachetzki, K. Biber, B.I. Fiebich. *J. Neuroinflammation* (2012), **9:2**.
- [146] M. Gosset, F. Berenbaum, A. Levy, A. Pigenet, S. Thirion, J.L. Saffar, C. Jacques. *Arthritis Res. Ther.* (2006), **8**, R135.
- [147] H.H. Chang, Z. Song, L. Wisner, T. Tripp, V. Gokhale, E.J. Meuillet. *Invest. New Drugs* (2012), **30**, 1865-1877.
- [148] J. Frasor, A.E. Weaver, M. Pradhan, K. Mehta. *Endocrinology* (2008), **149**, 6272-9.
- [149] W.E.T. Ackerman, T.L. Summerfield, D.D. Vandre, J.M. Robinson, D.A. Kniss. *Biol Reprod* (2008), **78**, 68-76.
- [150] O. Radmark, B. Samuelsson. *J. Intern. Med.* (2010), **268**, 5-14.
- [151] J. bauer, B. Waltenberger, S.M. Noha, D. Schuster, J.M. Rollinger, J. Boustie, M. Chollet, H. Stuppner, O. Werz. *ChemMedChem* (2012), **7**, 2077-2081.
- [152] X. Xue, Y.M. Shah. *Carcinogenesis* (2013), **34**, 163-169.
- [153] A. Banning, S. Florian, S. Deubel, S. Thalmann, K. Muller-Schmehl, G. Jacobasch, R. Brigelius-Flobe. *Antioxid. Redox Signaling* (2008), **10**, 1491-1500.
- [154] H.W. Wang, C.T. Hsueh, C.F. Lin, T.Y. Chou, W.H. Hsu, I.S. Wang, Y.C. Wu. *Ann. Surg. Oncol.* (2006), **13**, 1224-1234.
- [155] H. Itadani, H. Oshima, H. Kotani. *BMC Genomics* (2009), **10**, 615.
- [156] H. Oshima, M. Oshima. *Semin. Immunopathol.* (2013), **35**, 139-150.

- [157] F. Finetti, E. Terzuoli, A. Giachetti, R. Santi, D. Villari, H. Hanaka, O. Radmark, M. Ziche, S. Donnini. *Endocr. Relat. Cancer* (2015), **22**, 665-678.
- [158] M. Nakanishi, D.C. Montrose, P. Clark, P.R. Nambiar, G.S. Belinsky, K.P. Claffey, D. Xu, D.W. Rosenberg. *Cancer Res.* (2008), **68**, 3251-3259.
- [159] M. Nakanishi, A. Menoret, T. Tanaka, S. Miyamoto, D.C. Montrose, A.T. Vella, D.W. Rosenberg. *Cancer Prev. Res.* (2011), **4**, 1198-1208.
- [160] K. Larsson, P.J. Jakobsson. *Prostaglandins Other Lipid Mediators.* (2015), **120**, 161-165.
- [161] F. Finetti, E. Terzuoli, E. Bocci, I. Coletta, L. Polenzani, G. Mangano, M.A. Alisi, N. Cazzolla, A. Giachetti, M. Ziche, S. Donnini. *PLoS One* (2012), **7**, e40576.
- [162] P.J. Jakobsson, S. Thorén, R. Morgenstern, B. Samuelsson. *Proceedings of the National Academy of Sciences* (1999), **96**, 7220-7225.
- [163] P.J. Jakobsson, R. Morgenstern, J. Mancini, A. Ford-Hutchinson, B. Persson. *Protein Sci* (1999), **8**, 689-92.
- [164] P.J. Jakobsson, J.A. Mancini, A.W. Ford-Hutchinson. *J Biol Chem* (1996), **271**, 22203-10.
- [165] P.J. Jakobsson, J.A. Mancini, D. Riendeau, A.W. Ford-Hutchinson. *J Biol Chem* (1997), **272**, 22934-9.
- [166] D. Martinez Molina, S. Eshaghi, P. Nordlund. *Curr. Opin. Struct. Biol.* (2008), **18**, 442-449.

- [167] T. Sjögren, J. Nord, M. Ek, P. Johansson, G. Liu, S. Geschwindner. *Proceedings of the National Academy of Sciences* (2013), **110**, 3806-3811.
- [168] A. Hamza, M. Tong, M.D. AbdulHameed, J.Liu, A.C. Goren, H.H. Tai, C.G. Zhan. *J. Phys. Chem. B.* (2010), **114**, 5605-5616.
- [169] S.C. Pawelzik, N.R. Uda, L. Spahiu, C. Jegerschold, P. Stenberg, H. Hebert, R. Morgenstern, J. Jakobsson. *J. Biol. Chem.* (2010), **285**, 29254-29261.
- [170] L. Xing, R.G. Kurumbail, R.B. frazier, M.S. Davies, H.Fujiwara, R.A. Weinberg, J.K. Gierse, N. Caspers, J.S. Carter, J.J. McDonald, W.M. Moore, M.L. Vazques. *J. Couput.-Aided Mol. Des.* (2009), **23**, 13-24.
- [171] S. Ahmad, D. Niegowski, A. Wetterholm, J.Z. Haeggstrom, R. Morgenstern, A. Rinaldo-Matthis. *Biochemistry* (2013), **52**, 1755-1764.
- [172] G. Corso, I. Coletta, R. Ombrato. *J. Chem. Inf. Model.* (2013), **53**, 1804-1817.
- [173] S. He, L. Lai. *J. Chem. Inf. Model.* (2011), **51**, 3254-3261.
- [174] C.L. Li, T.T. chang, M.F. Sun, H.Y. chen, F.J. Tsai, M. Fisher, C.Y.C. Chen, C.L. Lee, W.C. Fang, Y.H. Wong. *Mol. Simul.* (2011), **37**, 226-236.
- [175] S. He, Y. Wu, D. Yu, L. Lai. *Bionchem. J.* (2011), **440**, 13-21.
- [176] E.B. Prage, S.C. Pawelzik, L.S. Busenlehner, K. Kim, R. Morgenstern, P.J. Jakobsson, R.N. Armstrong. *Biochemistry* (2011), **50**, 7684-7693.
- [177] P. Paragi-Vedanthi, M. Doble. *BMC Bioinf.* (2010), **11 Suppl 1**, 851.
- [178] Saha, S.; Engstrom, L.; Mackerlova, L.; Jakobsson, P. J.; Blomqvist, A. *Am J Physiol Regul Integr Comp Physiol* (2005), **288**, R1100-7.

- [179] Wang, M.; Song, W. L.; Cheng, Y.; Fitzgerald, G. A. *J Intern Med* (2008), **263**, 500-5.
- [180] Nakanishi, M.; Gokhale, V.; Meuillet, E. J.; Rosenberg, D. W. *Biochimie* (2010), **92**, 660-664.
- [181] Koeberle, A.; Werz, O. *Biochem. Pharmacol.* (2015), **98**, 1-5.
- [182] Koeberle, A.; Werz, O. *Curr. Med. Chem.* (2009), **16**, 4274-4296.
- [183] Korotkova, M.; Jakobsson, P. J. *Toxicol.* (2014), **114**, 64-69.
- [184] Norberg, J. K.; Sells, E.; Chang, H. H.; Alla, S. R.; Zhang, S.; Meuillet, E. J. *Pharm. Pat. Anal.* (2013), **2**, 265-288.
- [185] Pellicano, R. *Minerva Gastroenterol Dietol* (2014), **60**, 255-61.
- [186] Flower, R. J. *Nature Reviews Drug Discovery* (2003), **2** (3), 179-91.
- [187] Salinas, G; Rangasetty, U. C.; Uretsky, B. F.; Birnbaum, Y. *Journal of Cardiovascular Pharmacology and Therapeutics.* (2007), **12** (2), 98-111.
- [188] McGettigan, P.; Henry, D. *Jama* (2006), **296**, 1633-44.
- [189] H.H. Chang, E.J. Meuillet. *Future Med Chem* (2011), **3**, 1909-34.
- [190] J.K. Norberg, E. Sells, H.H. Chang, S.R. Alla, S. Zhang, E.J. Meuillet. *Pharm Pat Anal* (2013), **2**, 265-88.
- [191] D. Xu, S.E. Rowland, P. Clark, A. Giroux, B. Cote, S. Guiral, M. Salem, Y. Ducharme, R.W. Friesen, N. Methot, J. Mancini, L. Audoly, D. Riendeau. *J Pharmacol Exp Ther* (2008), **326**, 754-63.
- [192] S.C. Pawelzik, N.R. Uda, L. Spahiu, C. Jegerschöld, P. Stenberg, H. Hebert, R. Morgenstern, P.-J. Jakobsson. *J Biol Chem* (2010), **285** (38), 29254-61.

- [193] J. Bauer, A. Koeberle, F. Dehm, F. Pollastro, G. Appendino, H. Northoff, A. Rossi, L. Sautebin, O. Werz. *Biochem. Pharmacol.* (2011), **81**, 259-268.
- [194] A. Minassi, L. Cicione, A. Koeberle, J. Bauer, S. Laufer, O. Werz, G. Appendino. *Eur. J. Org. Chem.* (2012), **2012**, 772-779.
- [195] J. Bauer, S. Kuehnl, J.M. Rollinger, O. Scherer, H. Northoff, H. Stuppner, O. Werz, A. Koeberle. *J. Pharmacol. Exp. Ther.* (2012), **342**, 169-176.
- [196] A. Koeberle, A. Rossi, J. Bauer, F. Dehm, L. Verotta, H. Northoff, L. Sautebin, O. Werz. *Front. Pharmacol.* (2011), **2**, 7.
- [197] A. Koeberle, H. Northoff, O. Werz. *Mol. Cancer Ther.* (2009), **8**, 2348-2355.
- [198] M. Verhoff, S. Seitz, M. Paul, S.M. Noha, J. Jauch, D. Schuster, O. Werz. *J. Nat. Prod.* (2014), **77**, 1445-1451.
- [199] M. Hämäläinen, R. Nieminen, M.Z. Asmawi, P. Vuorela, H. Vapaatalo, E. Moilanen. *Planta Med.* (2011), **77**, 1504-1511.
- [200] K.C. Chen, M.F. Sun, S.C. Yang, S.S. Chang, H.Y. Chen, F.J. Tsai, C.Y. Chen. *Chem. Biol. Drug Des.* (2011), **78**, 679-688.
- [201] Y. Li, S. Yin, D. Nie, S. Xie, L. Ma, X. Wang, Y. Wu, J. Xiao. *Int. J. Hematol.* (2011), **94**, 472-478.
- [202] J. Wang, D. Limburg, J. Carter, G. Mbalaviele, J. Gierse, M. Vazques. *Bioorg. Med. Chem. Lett.* (2010), **20**, 1604-1609.
- [203] R. De Simone, I. Bruno, R. Riccio, K. Stadler, J. Bauer, A.M. Schaible, S. Laufer, O. Werz. *Bioorg. Med. Chem.* (2012), **20**, 5012-5016.

- [204] F. Rorsch, I. Wobst, H. Zettl, M. Schubert-Zsilavec, S. Grosch, G. Geisslinger, G. Schneider, E. Proschak. *J. Med. Chem.* (2010), **53**, 911-915.
- [205] N. Kablaoui, S. Patel, J. Shao, D. Demian, K. Hoffmaster, F. Berlioz, M.L. Vazques, W.M. Moore, R.A. Nugent. *Bioorg. Med. Chem. Lett.* (2013), **23**, 907-911.
- [206] B. Cote, L. Boulet, C. Brideau, D. Claveau, D. Ethier, R. Frenette, M. Gagnon, A. Giroux, J. Guay, S. Guiral, J. Mancini, E. Martins, F. Masse, N. Methot, D. Riendeau, J. Rubin, D. Xu, H. Yu, Y. Ducharme, R.W. Friesen. *Bioorg Med Chem Lett* (2007), **17**, 6816-20.
- [207] T. Shiro, K. Kakiguchi, H. Takahashi, H. Nagata, M. Tobe. *Bioorg. Med. Chgem.* (2013), **21**, 2868-2878.
- [208] A. Wiegard, W. Hanekamp, K. Griessbach, J. Fabian, M. Lehr. *Eur. J. Med. Chem.* (2012), **48**, 153-163.
- [209] T.Y.H. Wu, H. Juteau, Y. Ducharme, R.W. Friesen, S. Guiral, L. Dufresne, H. Poirier, M. Salem, D. Riendeau, J. Mancini, C. Brideau. *Bioorganic & Medicinal Chemistry Letters* (2010), **20**, 6978-6982.
- [210] S. He, C. Li, Y. Liu, L. Lai. *J. Med. Chem.* (2013), **56**, 3296-309.
- [211] R. De Simone, M.G. Chini, I. Bruno, R. Riccio, D. Mueller, O. Werz, G. Bifulco. *J. Med. Chem.* (2011), **54**, 1565-1575.
- [212] S. Terracciano, G. Lauro, M. Strocchia, K. Fischer, O. Werz, R. Riccio, I. Bruno, G. Bifulco. *ACS Med. Chem. Lett.* (2015), **6**, 187-191.
- [213] K. Deckmann, F. Rorsch, G. Geisslinger, S. Grosch. *Cell. Signaling* (2012), **24**, 460-467.
- [214] T. Hanke, F. Dehm, S. liening, S.D. Popella, J. Maczewsky, M. Pillong, J. Kunze, C. Weinigel, D. Barz, A. Kaiser, M. Wurglics, M.

- Lammerhofer, G. Schneidern, L. Sautebin, M. Schubert-Zsilavec, O. Werz. *J. Med. Chem.* (2013), **56**, 9031-9044.
- [215] M. Elkady, R. Niess, A.M. Schaible, J. Bauer, S. Luderer, G. Ambrosi, O. Werz, A. Laufer. *J. Med. Chem.* (2012), **55**, 8958- 8962.
- [216] C. Greiner, H. Zettl, A. Koeberle, C. Pergola, H. Northoff, M. Schubert-Zsilavec, O. Werz. *Bioorg. Med. Chem.* (2011), **19**, 3394-3401.
- [217] B. Waltenberger, K. Wiechmann, J. Bauer, P. Markt, S.M. Noha, G. Wolber, J.M. Rollinger, O. Werz, D. Schuster, H. Stuppner. *J. Med. Chem.* (2011), **54**, 3163-3174.
- [218] A. Koerberle, F. Pollastro, H. Northoff, O. Werz. *Br. J. Pharmacol.* (2009), **156**, 952-961.
- [219] G.B. Arhancet, D.P. Walker, S. Metz, Y.M. Fobian, S.E. Heasley, J.S. Carter, J.R. Springer, D.E. Jones, M.J. Hayes, A.F. Shaffer, G.M. Jerome, M.T. Baratta, B. Zweifel, W.M. Moore, J.L. Masferrer, M.L. Vazquez. *Bioorganic & Medicinal Chemistry Letters* (2013), **23**, 1114-1119.
- [220] M. Hieke, C. Greiner, M. Dittrich, F. Reisen, G. Schneider, M. Schubert- Zsilavec, O. Werz. *J Med Chem* (2011), **54**, 4490-507.
- [221] D. Xu, S.E. Rowland, P. Clark, A. Giroux, B. Cote, S. Guiral, M. Salem, Y. Ducharme, R.W. Friesen, N. Methot, J. Mancini, L. Audoly, D. Riendeau. *J Pharmacol Exp Ther* (2008), **326**, 754-63.
- [222] J.G. Luz, S. Anthonysamy, S.L. Kuklish, B. Condon, M.R. Lee, D. Allison, X.P. Yu, S. Chandrasekhar, R. Backer, A. Zhang, M. Russell, S.S. Chang, A. Harvey, A.V. Sloan, M.J. Fisher. *J. Med. Chem.* (2015), **58**, 4727-4737.

- [223] C.O. Kappe. *Eur J Med Chem* (2000), **35**, 1043-52.
- [224] A.K. Tewari, V.P. Singh, P. Yadav, G. Gupta, A. Singh, R.K. Goel, P. Shinde, C.G. Mohan. *Bioorganic Chemistry* (2014), **56**, 8–15.
- [225] L.S. Tsutsumi, D. Gündisch, D. Sun. *Current Topics in Medicinal Chemistry* (2016), **16(11)**, 1290-1313.
- [226] R. M. Rao, G. N. Reddy, J. Sreeramulu. *Der Pharma Chemica* (2011), **3 (5)**, 301-309.
- [227] P. Biginelli. *Ber. Dtsch. Chem. Ges.* (1891), **24**, 1317–1319.
- [228] F. Bigi, S. Carloni, B. Frullanti, R. Maggi, G. Sartori. *Tetrahedron Letters* (1999), **40**, 3465-3468.
- [229] T. Jin, S. Zhang, T. Li. *Synthetic Communications* (2002), **32**, 1847-1851
- [230] J.H. Clark, D.J. Macquarrie, J. Sherwood. *Chem. Eur. J.* (2013), **19**, 5174–5182
- [231] C.O. Kappe. *Acc. Chem. Res.* (2000), **33**, 879-888.
- [232] Y. Zhu, Y. Pan, S. Huang. *Synthetic Communications* (2004), **34**, 3167-3174.
- [233] Y. Ma, C. Qian, L. Wang, M. Yang. *J. Org Chem* (2000), **65**, 3864-8.
- [234] A.S. Paraskar, G.K. Dewkar, A. Sudalai. *Tetrahedron Letters* (2003), **44**, 3305-3308.
- [235] S.K. De, R.A. Gibbs. *Synthesis* (2005), **2005**, 1748-1750.
- [236] C.O. Kappe. *Bioorganic & Medicinal Chemistry Letters* (2000), **10**, 49-51.
- [237] B. Ahmed, R.A. Khan, Habibullah; M. Keshari. *Tetrahedron Letters* (2009), **50**, 2889-2892.

- [238] A. Dondoni, A. Massi. *Tetrahedron Letters* (2001), **42**, 7975-7978.
- [239] F. Dong, L. Jun, Z. Xinli, Y. Zhiwen, L. Zuliang. *Journal of Molecular Catalysis A: Chemical* (2007), **274**, 208-211.
- [240] M.M. Heravi, S. Asadi, B.M. Lashkariani. *Mol Divers* (2013), **17**, 389-407.
- [241] A. Stadler, C.O. Kappe. *J. Comb. Chem.* (2001), **3**, 624-30.
- [242] C.O. Kappe, A. Stadler. *Methods Enzymol.* (2003), **369**, 197-223.
- [243] L. Pisani, H. Prokopcová, J.M. Kremsner, C.O. Kappe. *Journal of Combinatorial Chemistry* (2007), **9**, 415-421.
- [244] S.V. Ryabukhin, A.S. Plaskon, E.N. Ostapchuk, D.M. Volochnyuk, A.A. Tolmachev. *Synthesis* (2007), **2007**, 417-427.
- [245] J.I.G. Cadogan, M. Cameron-Wood. *Proc. Chem. Soc.* (1962), **361**.
- [246] J.I.G. Cadogan. *In Organophosphorus Reagents in Organic Synthesis Ed.; Academic: London, (1979); Chapter 6.*
- [247] N. Miyaura, T. Yanagi, A. Suzuki. *Synth. Commun.* (1981), **11**, 513.
- [248] A. Suzuki. *J. Organomet. Chem.* (2002), **653**, 83-90
- [249] A. Gadakh, C. Pandit, S.S. Rindhe, B. Karale. *International Journal of Chemistry* (2010), **2**, 206-212.
- [250] S. Soga, S. Akinaga, Y. Shiotsu. *Curr Pharm Des* (2013), **19**, 366-76.
- [251] Y. Oki, A. Copeland, J. Romaguera, L. Fayad, M. Fanale, C. Faria Sde, L.J. Medeiros, P. Ivy, A. Younes. *Leuk Lymphoma* (2012), **53**, 990-2.
- [252] E.I Heath, D.W. Hillman, U. Vaishampayan, S. Sheng, F. Sarkar, F. Harper, M. Gaskins, H.C. Pitot, W. Tan, S.P.; Ivy, R. Pili, M.A. Carducci, G.A. Liu. *Clinical cancer research : an official journal of the American Association for Cancer Research* (2008), **14**, 7940-7946.

- [253] P.G. Richardson, A.Z. Badros, S. Jagannath, S. Tarantolo, J.L. Wolf, M. Albitar, D. Berman, M. Messina, K.C. Anderson, K. C. *Br J Haematol* (2010), **150**, 428-37.
- [254] M.V. Powers, P.A. Clarke, P. Workman. *Cell Cycle* (2009), **8**, 518–526.
- [255] R. Bagatell, G.D. Paine-Murrieta, C.W. Taylor, E.J. Pulcini, S. Akinaga, I.J. Benjamin, L. Whitesell. *Clinical Cancer Research* (2000), **6**, 3312-3318.
- [256] B. Samarasinghe, C.T.K. Wales, F.R. Taylor, A.T. Jacobs. *Biochemical Pharmacology* (2014), **87**, 445-455.
- [257] P.K. Sorger. *Cell* (1991), **65**, 363-366.
- [258] R.I. Morimoto. *Genes Dev* (1998), **12**, 3788–3796.
- [259] C. Wu. *Annu Rev Cell Dev Biol* (1995), **11**, 441–69.
- [260] Y. Shi, D.D. Mosser, R.I. Morimoto. *Genes Dev* (1998), **12**, 654-66.
- [261] J. Anckar, L. Sistonen. *Annu Rev Biochem* (2011), **80**, 1089–1115.
- [262] I. Shamovsky, E. Nudler. *Cell. Mol. Life Sci.* (2008), **65(6)**, 855–861.
- [263] W. Xia, R. Voellmy. *J Biol Chem* (1997), **272**, 4094-102.
- [264] Y. Wang, S.R. McAlpine. *Chem Commun (Camb)* (2015), **51**, 1410-3.
- [265] R. Conde, Z.R. Belak, M. Nair, R.F. O'Carroll, N. Ovsenek. *Biochem Cell Biol* (2009), **87**, 845-51
- [266] S.N. Shelton, M.E. Shawgo, S.B. Matthews, Y. Lu, A.C. Donnelly, K. Szabla, M. Tanol, G.A. Vielhauer, R.A. Rajewski, R.L. Matts, B.S. Blagg, J.D. Robertson. *Mol Pharmacol* (2009), **76**, 1314-22
- [267] M.A. Cooper. *Anal Bioanal Chem* (2003), **377**, 834-42

- [268] A. Vassallo, M.C. Vaccaro, N. De Tommasi, F. Dal Piaz, A. Leone. *PloS One* (2013), **8**, e74266.
- [269] W. Guo, P. Reigan, D. Siegel, J. Zirrolli, D. Gustafson, D. Ross. *Cancer Res.* (2005), **65**, 10006-10015.
- [270] L. Sedlackova, M. Spacek, E. Holler, Z. Imryskova, I. Hromadnikova. *Tumour Biol.* (2011), **32**, 33-44.
- [271] Induced Fit Docking, protocol 2015-2, Glide version 6.4, Prime version 3.7, Schrödinger, LLC, New York, NY, **2015**.
- [272] M. M. U. Ali, S. M. Roe, C. K. Vaughan, P. Meyer, B. Panaretou, P. W. Piper, C. Prodromou, L. H. Pearl, *Nature* (2006), **440**, 1013-1017.
- [273] C. C. Lee, T. W. Lin, T. P. Ko, A. H. Wang. *PLoS One* (2011), **6**, e19961
- [274] H. Prokopcova, C.O. Kappe. *Angew Chem Int Ed Engl* (2009), **48**, 2276-86.
- [275] N. Arshad, J. Hashim, C.O. Kappe. *J. Org. Chem.* (2009), **74**, 5118-5121.
- [276] H. Prokopcovà, C.O. Kappe. *Adv. Synth. Catal* (2007), **349**, 448-452.
- [277] L.S. Liebeskind, J. Srogl. *Organic Letters* (2002), **4**, 979-981.
- [278] H. Yang, H. Li, R. Wittenberg, M. Egi, W. Huang, L.D. Liebeskind. *J Am Chem Soc* (2007), **129**, 1132-40.
- [279] Y. Yu, L.S. Liebeskind. *The Journal of Organic Chemistry* (2004), **69**, 3554-3557.
- [280] A. Innitzer. *Synlett* (2005), **2005**, 2405-2406.
- [281] A. Lengar, C.O. Kappe. *Organic Letters* (2004), **6**, 771-774.

- [282] I. Nicoletti, G. Migliorati, M.C. Pagliacci, F. Grignani, C.A. Riccardi. *J Immunol Methods* (1991), **139**, 271-9.
- [283] L. Mayor-Lopez, E. Tristante, M. Carballo-Santana, E. Carrasco-Garcia, S. Grasso, P. Garcia-Morales, M. Saceda, J. Lujan, J. Garcia-Solano, F. Carballo, C. de Torre and I. Martinez-Lacaci. *Transl. Oncol.* (2014), **7**, 590.
- [284] A. Vassallo, M.C. Vaccaro, N. De Tommasi, F. Dal Piaz, A. Leone. *PLoS One* (2013), **8**, e74266.
- [285] F. Dal Piaz, A. Vassallo, A. Temraz, R. Cotugno, M.A. Belisario, G. Bifulco, M.G. Chini, C. Pisano, N. De Tommasi, A. Braca. *J Med Chem* (2013), **56**, 1583-95.
- [286] B. G. Yun, W. Huang, N. Leach, S. D. Hartson and R. L. Matts, *Biochemistry* (2004), **43**, 8217.
- [287] M. G. Marcu, A. Chadli, I. Bouhouche, M. Catelli and L. M. Neckers, *J. Biol. Chem.* (2000), **275**, 37181.
- [288] R. K. Allan, D. Mok, B. K. Ward and T. Ratajczak, *J. Biol. Chem.* (2006), **281**, 7161.
- [289] W. Sherman, T. Day, M. P. Jacobson, R. A. Friesner and R. Farid, *J. Med. Chem.* (2006), **49**, 534.
- [290] S. Terracciano, A. Foglia, M. G. Chini, M. C. Vaccaro, A. Russo, M. Strocchia, F. Dal Piaz, C. Saturnino, R. Riccio, G. Bifulco and I. Bruno, *RSC Adv.* (2016), **6**, 82330.
- [291] Maestro, version 10.2, Schrödinger, LLC, New York, NY, **2015**.
- [292] *J.K. Buer. Inflammopharmacology.* (2014), **22** (5), 263–7.
- [293] D. Wang, R.N. Dubois. *Prostaglandins and cancer* (2006) *Gut* **55**, 115-122.

- [294] S. Rakoff-Nahoum. *Yale J. Biol. Med.* (2006), **79**, 123-130.
- [295] K.D. Rainsford. *Am. J. Med.* (1999), **107**, 27S-35S.
- [296] P. McGettigan, D. Henry. *JAMA* (2006), **296**, 1633-1644.
- [297] Y. Cheng, M. Wang, Y. Yu, J. Lawson, C.D. Funk, G.A. Fitzgerald. *J. Clin. Invest.* (2006), **116**, 1391-1399.
- [298] J. W. Hoftiezer, J. C. O'Laughlin, K. J. Ivey. *Gut* (1982), **23(8)**, 692-697.
- [299] P. Leclerc, S.C. Pawelzik, H. Idborg, L. Spahiu, C. Larsson, P. Stenberg, M. Korotkova, P.J. Jakobsson. *Prostaglandins & Other Lipid Mediators* (2013), **102-103**, 1-12.
- [300] Botta, A., Sirignano, E., Popolo, A., Saturnino, C., Terracciano, S., Foglia, A., Sinicropi, M.S., Longo, P., e Di Micco, S., *Mol. Inform.* (2015), **34**, 2-11.
- [301] P. Gupta, J.K. Gupta, A.K. Halve. *IJPSR*, (2015) **6(6)**, 2291-2310.
- [302] Y. Hu, P. Wei, H. Zhou, P.K. Ouyang, Z.C. Chen. *Chin. Chem. Lett.* (2006), **17**, 299.
- [303] H. Sheibani, M. Babaie. *Synth. Commun.* (2010), **40**, 257.
- [304] A. Saini, J.S. Sandhu, R.S. Bhatti. *J Indian Chem Soc.* (2007), **84**, 1239.
- [305] J. Sun, C.G. Yan, Y. Han. *Synth. Commun.* (2001), **31**, 151.
- [306] D. Li, L. Song, S. Song, S. Zhu. *J. Fluorine Chem.* (2007), **128**, 952.
- [307] D. M. Khidre, H. M. Abou-Yousef, M. Refat, H. Mahran. *Phosphorus, Sulfur, and Silicon and the Related Elements.* (2002), **177**, 647-658.
- [308] J.K.R. Thomas, L.T. Jian. *Am. Chem. Soc.* (2001), **123**, 9404.
- [309] J.F. Morin, M. Leclerc. *Macromolecules* (2002), **35**, 8413; and references cited therein.

- [310] N.D. McClenaghan, R. Passalacqua, F. Loiseau, S. Campagna, B. Verheyde, A. Hameurlaine, W. Dehaen. *J. Am. Chem. Soc.* (2003), **125**, 5356.
- [311] H.J. Knölker, K.R. Reddy. *Chem. Rev.* (2002), **102**, 4303.
- [312] F.A. Neugebauer, H. Fischer. *Chem. Ber.* (1972), **105**, 2686.
- [313] N.V. Moskalev. *Khim. Geterotsikl. Soedin.* (1990), **2**, 187.
- [314] Z. Zhu, J.S. Moore. *J. Org. Chem.* (2000), **65**, 116.
- [315] Z. Zhu, J.S. Moore. *Macromolecules* (2000), **33**, 801.
- [316] P. Appukkuttan, E. Van der Eycken, W. Dehaen. *SYNLETT* (2005), **1**, 0127–0133.
- [317] G.I.J. Cadogan, M. Carmen-Wood. *Proc. Chem. Soc.* (1962), **361**.
- [318] G.I.J. Cadogan, M. Carmen-Wood, R.K. Makie, R.J.G.J. Searle J. *Chem. Soc.* (1965), **4831**.
- [319] G.I.J. Cadogan. *Organophosphorus Reagents in Organic Synthesis*; Academic Press Inc.: London, (1979), **279**.
- [320] A. Lew, P.O. Krutzik, M.E. Hart, A.R. Chamberlin. *J. Comb. Chem.* (2002), **2**, 95.
- [321] C.O. Kappe. *Curr. Opin. Chem. Biol.* (2002), **6**, 314.
- [322] P. Lidström, J. Westman, A. Lewis. *Comb. Chem. High Throughput Screening* (2002), **5**, 441.
- [323] N. Miyaura, K. Yamada, A. Suzuki. *Tetrahedron Lett.* (1979), **20**, 3437–3440.
- [324] N. Miyaura. *Top. Curr. Chem.* (2002), **219**, 11–59.

- [325] A. S. J. K. Gillie. *Journal of American Chemical Society* (1980), **102**, 4933-4941.
- [326] R. F. Heck. *Palladium Reagents in Organic Syntheses*, **1985**.
- [327] E. Negishi. *Wiley-Interscience: New York, NY, USA*, (2002).
- [328] A. Suzuki. *J. Organomet. Chem.* (2002), **653**, 83–90.